#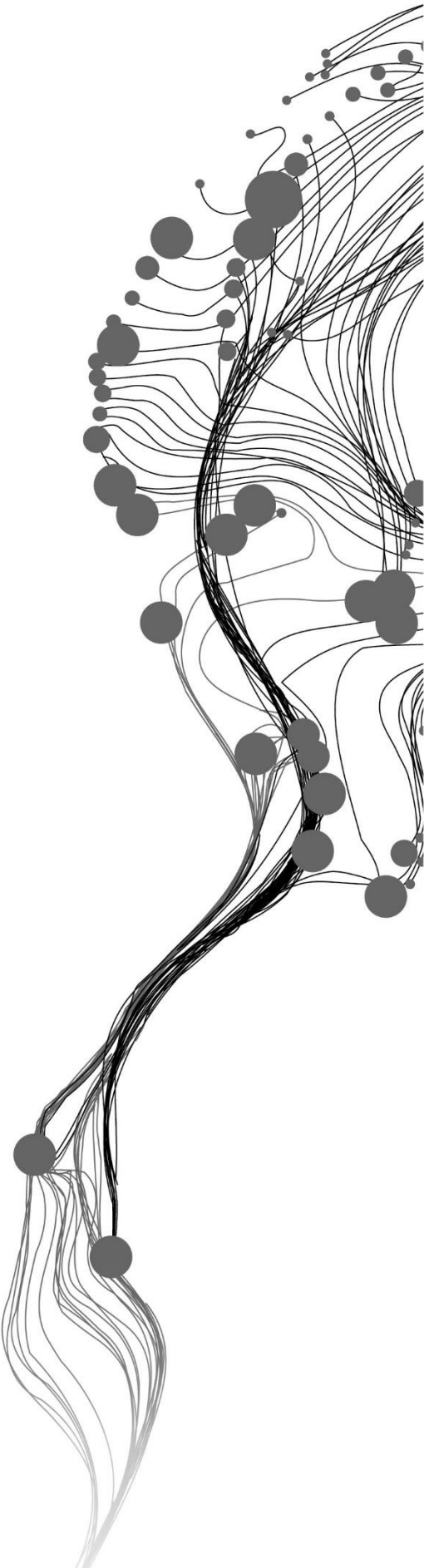 SENSITIVITY ANALYSIS OF SOILGRIDS250M DATA FOR SOIL EROSION MODELLING: A CASE STUDY OF BAN DAN NA KHAM WATERSHED, THAILAND

CHIKE ONYEKA MADUEKE
FEBRUARY 2019

SUPERVISORS:

Dr. D.P.K. Shrestha
Dr. P. Nyktas

SENSITIVITY ANALYSIS OF SOILGRIDS250M DATA FOR SOIL EROSION MODELLING: A CASE STUDY OF BAN DAN NA KHAM WATERSHED, THAILAND

CHIKE ONYEKA MADUEKE
Enschede, The Netherlands
February 2019

ABSTRACT

The prevention and control of soil erosion requires the use of state-of-the-art erosion prediction models. Nevertheless, the models require extensive input of detailed spatial and temporal data. Some of these data are not readily available in many developing countries, particularly detailed soil data. Moreover, conventional methods of soil data acquisition are expensive, subjective and time-consuming, buttressing the need for cheaper, systematic and readily-available data. SoilGrids250m could potentially fill the data gap. In this study, the sensitivity of SoilGrid250m data for erosion modelling was assessed. Point-based comparison of SoilGrids250m and field-based soil data show that except for clay, all the other parameters of the two datasets were significantly different. On the other hand, a comparison of area-based averages of hillslope units show that, apart from silt, at $P>0.01$ all other parameters of the two datasets are not significantly different. Similarly, for point-based assessment, all the Revised Morgan-Morgan-Finney (RMMF) model outputs generated from the datasets were significantly different. As was the case when the input soil data were assessed, the area-based model output comparison show that besides soil loss, all the output of the RMMF modelling process were not significantly different. This implies that depending on the scale of operation or the extent of detail required, SoilGrids250m data can be a very valuable alternative to soil survey data. When detailed on-site data are required, SoilGrids250m may not be a very good alternative because the point-based assessments show that both datasets are different. Nevertheless, in the absence of field data, especially when adequate funds and time are not available, SoilGrids250m can be used to generate the detachment by raindrops and runoff, total detachment, runoff, runoff transport capacity, sediment deposition and soil loss. Afterwards, using the models generated in this study, the expected values for field-based data for any target site in Northern Thailand can be predicted. Finally, the results show that soil loss was lowest in forests (below the soil loss tolerance limit of 11 ton/ha/annum) and highest on arable lands (consistently above 11 ton/ha/annum). Arable farming may consequently be discouraged on steep slopes. On moderate and gentle slopes, implementation of soil conservation strategies should be enforced as a prerequisite to sustainable arable farming.

KEYWORDS: Sensitivity Analysis, SoilGrids250m, Soil Survey, Soil Erosion Modelling, Revised Morgan-Morgan-Finney Model (RMMF), Runoff, Soil Detachment, Sediment Deposition, Soil Loss.

ACKNOWLEDGEMENTS

To my parents,
Mr. Famachi E.O. Madueke and Mrs. Caro R.N. Madueke.
Thank you for believing in me, even when there was nothing to believe.

TABLE OF CONTENTS

LIST OF FIGURES

LIST OF TABLES

1.   INTRODUCTION

1.1.   Background and Justification

Globally, soil erosion has been identified as one of the most destructive and severe forms of land degradation (FAO & ITPS, 2015; Melaku et al., 2018). This is more so, as the impacts of soil erosion are not limited to the on-site loss of topsoil, nutrients, organic matter, crop residues, soil quality and growing plants. The off-site impacts, leading to the inundation of downhill farms by eroded soils, silting in of drainage channels and reservoirs, water pollution and the degradation aquatic habitat, may even be more critical. Soil erosion consequently poses a threat to the sustainability of a nation's economic, social and environmental systems. The situation is made more precarious by the expectation that climate change will aggravate the current state of land degradation (Starkloff & Stolte, 2014; Deelstra, 2015; Li & Fang, 2016; Giang et al., 2017; Wang et al., 2018).

The all-encompassing negative impacts of soil erosion necessitate the need for sustainable land management that takes erosion control and prevention into consideration. Various preventive and control measures exist, but the successful implementation of these measures and the attendant land use planning requires a prior understanding of the spatio-temporal dynamics of soil degradation in a region. As a consequence, proper land use planning at the watershed scale requires the use of state-of-the-art erosion prediction models (De Vente et al., 2013). Many soil erosion prediction models are currently in existence (Hajigholizadeh et al., 2018). These models may either be data-driven or process-driven, but they are generally grouped into event-based, daily and annual models, depending on the temporal resolution of the required rainfall data.

Event-based models focus on the relatively short duration, high intensity rainfall and runoff events that account for the bulk of the soil erosion that take place on an annual basis. Numerous event-based models are currently in existence, some of which are the Limburg Soil Erosion Model [LISEM] (De Roo et al., 1996), the Areal Nonpoint Source Watershed Environment Response Simulation [ANSWERS] (Beasley et al., 1980), the Kinematic Runoff and Erosion Model [KINEROS] (Woolhiser et al., 1990) and the European Soil Erosion Model [EUROSEM] (Morgan et al., 1998). According to Hajigholizadeh et al. (2018), all of these models are catchment-based, generate a wide range of hydrological outputs, and require event-based rainfall data. It is, however, noteworthy that not all event-based models require detailed short duration rainfall data. LandscApe ProcesS modelling at mUlti-dimensions and Scales [LAPSUS] (Schoorl et al., 2000; Sonneveld et al., 2010), unlike most other event-based models, considers the total rainfall of one year as a single rainfall event. This is hinged on the fact that, while other event-based models are designed for the assessment of the degree of land degradation caused by a single rainfall event, LAPSUS was designed for the assessment of how the landscape has evolved over a long period of time. As such, the kind of information required, determines, to a large extent, the temporal resolution of the required rainfall data, and consequently, the kind of model adopted.

The inherent processes of a typical event-based model like LISEM, are divided into the hydrological and the sediment cycle (De Roo et al., 1996; Jetten, 2018). The hydrological cycle encompasses such processes as rainfall, interception, storage, kinematic wave, flooding and coupling of flow; while the sediment cycle, on the other hand, is made up of such processes as splash detachment, flow detachment, deposition, sediment transport, sediment diffusion and sediment load (Jetten, 2018a). In line with the contention of Starkloff & Stolte (2014), these models are consequently essential to the understanding of the underlying processes behind rainfall, interception, splash, runoff, surface storage, erosion and deposition; providing us with the insight on how to effectively combat the negative impacts of extreme weather events.

Furthermore, as Hajigholizadeh et al. (2018) asserted, event-based hydrological models are appropriate for regions with strongly seasonal rainfall, where the bulk of the soil erosion would be associated with high intensity rainfall events. This is in line with the findings of other researchers who assessed the relationship between rainfall intensity and the magnitude of erosion that take place within a watershed (Baartman et al., 2012; Alexakis et al., 2013; Clutario et al., 2014; Mohamadi & Kavian, 2015; Wang et al., 2016). Moreover, Baartman et al. (2012) and Shrestha & Jetten (2018) concluded that the best estimate of annual soil erosion should be the sum of all the event-based erosion estimate for the year. Theoretically, this may be feasible, but it is easier and more realistic to compute annual soil loss as the sum of the daily soil loss that took place in a single year.

More so, the event-based models need a lot of data because, in addition to simulating particle detachment, transportation and deposition during an event in detail, it is required that the catchment needs to be initialized to simulate the circumstances before the rainfall event (Shrestha & Jetten, 2018). The situation is made dire by the fact that the detailed, high temporal and spatial resolution rainfall data required for event-based rainfall-runoff modelling is not available in most developing countries. In the absence of the appropriate data, daily rainfall-runoff modelling for erosion estimates is a good approximation of event-based model outputs on a daily basis (Shrestha & Jetten, 2018). Rainfall data is, however, not the only input data required to run an erosion model. The models require detailed input of soil, climate, land cover and topographic data, most of which are not readily accessible. These data, according to Näschen et al. (2018), are rarely available in many developing countries, constituting a major drawback to the use of physically-based models. Similarly, Avwunudiogba & Hudson (2014) contended that the less stringent data requirements and ease of implementation of lumped parameter annual hydrologic models make them the preferred choice in humid tropical mountainous environment.

Indeed, annual soil erosion models are less data-intensive, consequently making them more amenable to use in many developing countries, where scarcity of good quality, high resolution data is a major issue. Annual models are based on the average annual rainfall, and as such, according to Hajigholizadeh et al. (2018), may not be appropriate for regions with strongly seasonal rainfall events. This is a major challenge, but when projections are required on the spatial extent of land degradation, as well as the impacts on policy decisions relating to different land uses, annual hydrological models are still quite useful. In spite of that, the available models have many limitations.

Most annual lumped parameter models, like Universal Soil Loss Equation [USLE] (Wischmeier & Smith, 1978; Renard et al., 1991) and Soil Loss Estimator Model for Southern Africa [SLEMSA] (Stocking, 1981) are incapable of quantifying sediment deposition and runoff (Avwunudiogba & Hudson, 2014). This limits the range of applicability of these models in landscape, catchment and watershed management. Revised Morgan-Morgan-Finney (RMMF) Model, unlike these models, can be used to estimate a wide range of hydrological processes like sediment detachment by runoff and raindrops, total sediment detachment, runoff, runoff transport capacity, sediment deposition and soil loss (Morgan, 2001). This makes it a veritable tool for land resources management as it effectively combines relatively low data needs with the generation of outputs with a wide range of usefulness.

Despite the relatively low data requirements of the RMMF model, it still requires input of soil, climate, land cover and topographic data. Nonetheless, while land cover and topographic data can be generated from satellite imageries and digital elevation models (DEM) respectively, accessibility of soil data is more problematic. This makes the acquisition of sound soil information critical and inevitable (Schuler et al., 2006), underscoring the need for up-to-date location-specific soil information. Conventional soil surveys are however, expensive, subjective and time-consuming (Moonjun, 2007; Schuler et al., 2006), buttressing the need for cheaper, systematic and readily-available soil data. Recently a freely available SoilGrids data (https://soilgrids.org/) became available at 250m spatial resolution. It is "a globally consistent, data-driven

system that predicts soil properties and classes using global covariates and globally fitted models" (ISRIC, 2017), which could be a potential alternative to soil survey data, especially in an area where detailed data is lacking. The functional value of SoilGrids250m for erosion modelling is, however, still relatively unknown, especially in the tropical region. This study consequently aims to assess the functional value of SoilGrids250m for soil erosion modelling.

1.2. Research Problem

1.2.1. Comparative Analysis of Available Soil Data Sources

Soil data – i.e., soil texture, soil detachability, cohesion, bulk density, saturated hydraulic conductivity (ksat), porosity, field capacity and wilting point – constitutes a major proportion of the RMMF model inputs. Some of these data are not usually recorded in soil survey reports. The unavailable soil data need to be generated from their readily available counterparts using pedotransfer functions. The texture-based method of Saxton et al. (1986) has been widely applied, and now exists as a software, SPAW (Saxton & Rawls, 2006). These hydrologic soil properties can be generated from both soil survey and SoilGrids250m data. It is noteworthy that the SoilGrids250m data may differ considerably from soil survey data in terms of mapping methodology, soil properties represented, information about soil attributes, number and nature of soil classes represented and alignment of soil units to the soil-landscape model. There is consequently the need for a comparative analysis of the nature and characteristics of data from both sources.

1.2.2. Functional Value of SoilGrids250m Data for Soil Erosion Modelling

SoilGrids250m data has not been used widely for soil erosion modelling. It has however been applied by Hunink et al. (2015) and Sarkar & Mishra (2018) in soil erosion vulnerability mapping in Tanzania and India respectively. Similarly, Shrestha (2018) used SoilGrids250m data as input in the course of assessing the impacts of extreme rainfall on annual soil loss. Nevertheless, in all of these cases, the focus was not on the assessment of the value of SoilGrids250m data for erosion modelling. The researchers used the data as though it was a perfect substitute for conventional soil survey data. This may produce misleading results as the predictive value of both data sources are supposedly different. As such, there is the need to assess the functional value of SoilGrids250m data for soil erosion assessment at the catchment scale, vis-à-vis field-generated data.

1.3. Research Objectives and Questions

The major objective of this study is to determine the functional value of SoilGrids250m data for soil erosion modelling in the Ban Dan Na Kham Watershed of Northern Thailand. In order to achieve this objective, the following sub-objectives and related research questions were investigated:

1. To conduct a comparative analysis of SoilGrids250m and field-based soil data
▪   What are the characteristic features of soils within the study area?
▪   What are the similarities between SoilGirds250m data and field-generated soil data?
2. To assess the functional value of SoilGrids250m for soil erosion modelling
▪   What is the predicted annual erosion using the different soil data sources?
▪   How does the outputs of the two soil data sources compare to each other?
3. To assess the sensitivity of the RMMF model outputs to the different input parameters
▪   Which soil parameters are the RMMF model outputs most sensitive to?
▪   Which land cover parameters are the RMMF model outputs most sensitive to?
4. To assess the spatial vulnerability of the watershed to soil erosion
▪   Which land cover types are more prone to erosion?
▪   Which geomorphologic units are more prone to erosion?

2. METHODOLOGY

2.1. Study Area

2.1.1. Location of the Study Area

This study was carried out at the Ban Dan Na Kham Watershed located in Mueang District, Uttaradit Province, Thailand. It is located within Latitudes 17o40'N – 17o55'N, and Longitudes 99o50'E – 100o20'E. It covers an area of approximately 86.91 km², with altitude ranging from 60 to 753m above sea level. It is about 489 km away from Bangkok and 123 km from Phitsanulok. It is accessible by road and by train to Phitsanulok, Bangkok and other neighbouring cities. The location map of the study area is shown in Figure 2-1.
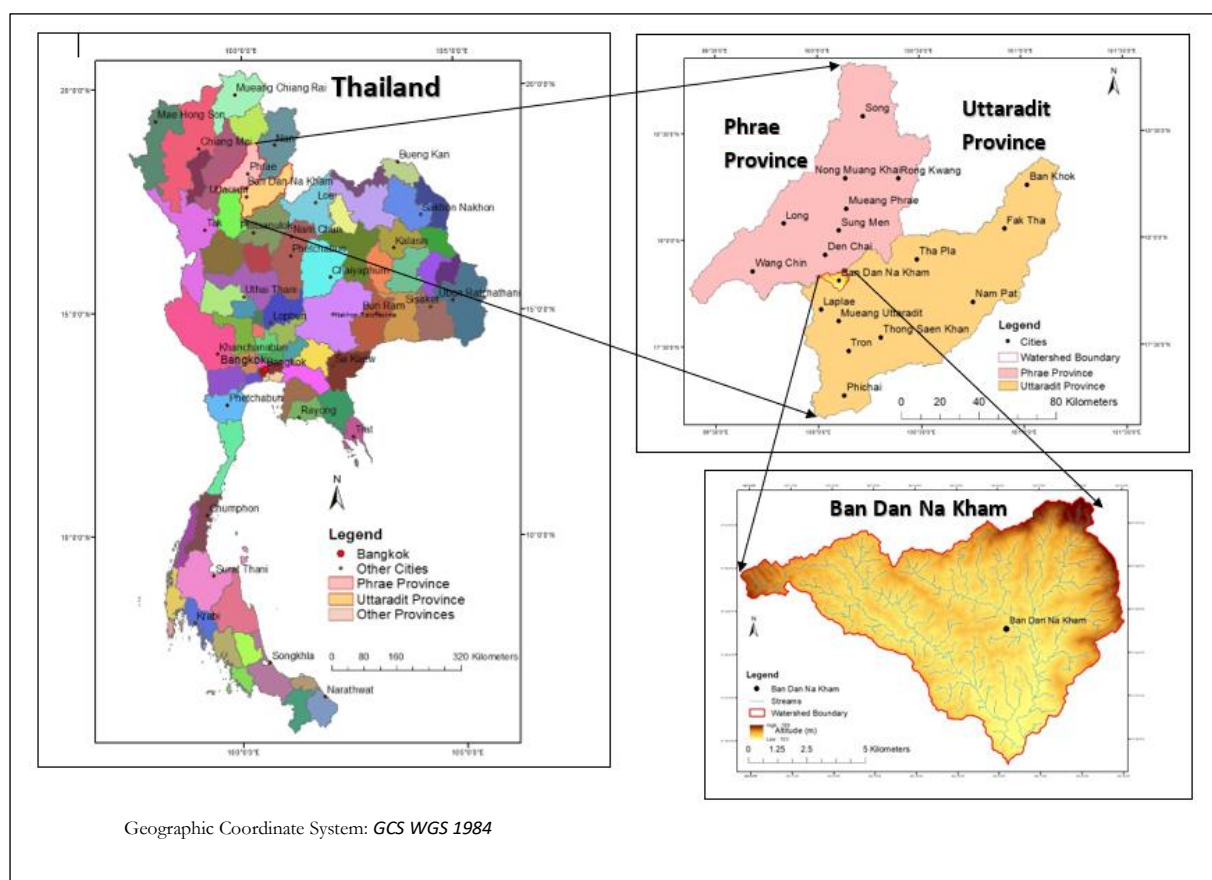
Figure 2-1: Study area – Ban Dan Na Kham watershed

2.1.2. Topography and Hydrology

The region is located in the Northern Continental Highlands (Scholten & Siriphant, 1973). It is hilly and mountainous; is the source of several rivers and streams, and it is located within the vicinity of the Nan River. The hills are north-south oriented, are parallel from west to east, and are intersected by several valleys. The southern fringe is dominated by high terraces and fans of old alluvium and colluvium. The landscape is essentially an undulating terrain.

2.1.3. Geology and Soils

There are three groups of soils in the study area, viz. soils of hills and mountains, soils of the higher terraces and low plateaus, and soils of alluvial plains and lower terraces (Figure 2-2). Nevertheless, due to the very

coarse scale (1: 2,500,000) of the soil map (Figure 2-2), the only soil unit that falls within the watershed is the reddish-yellow podzolic soils on steep lands formed from acid to intermediate rocks (Figure 2-2). The soil units within the area, as summarized in the map produced by Moormann and Rojanasoontan in 1967 and stored in the European digital archive on soil maps (EuDASM) (Panagos et al., 2011), are outlined below.

a. *Soils of Hills and Mountains:* The soils are divided into four classes:

- Red-yellow podzolic soils, mostly on hilly terrain, formed on materials from acid and intermediate rocks (Class 16)

- Red-yellow podzolic soils and reddish-brown lateritic soils found on steep land rich in intermediate basic rocks (Class 20).

- Mainly red-yellow podzolic soils formed on steep lands rich in acid to intermediate rocks (Class 21)

- Shallow undifferentiated soils on lava plateaus and volcanoes (Class 23)

b. *Soils of the Higher Terraces and Low Plateaus:* The soils are divided into two classes:

- Gray podzolic soils on old alluvium (Class 14)

- Red-yellow podzolic soils on old alluvium (Class15)

c. *Soils of Alluvial Plains and Lower Terraces:* The soils are divided into three classes:

- Alluvial soils on recent fresh water alluvium (Class 2)

- Low humic gley soils on semi-recent and old alluvium (Class 7)

- Low humic gley soils and gray or reddish yellow podzolic soils on old alluvium (Class 9)
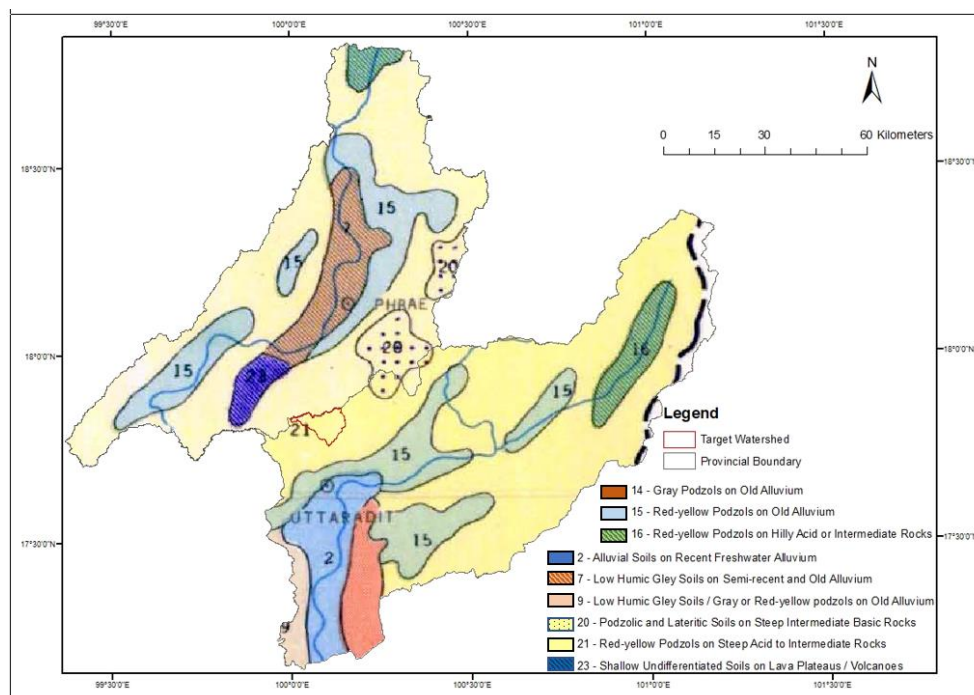
Geographic Coordinate System: *GCS WGS 1984*
(Source: General Soil Condition of Thailand by produced by Moormann and Rojanasoontan in 1967 and stored in the EuDASM Archive (Panagos et al., 2011)
Figure 2-2: Soil map of the study area

2.1.4.   Climate

Ban Dan Na Kham Watershed is located in the humid tropics, under the influence of the north-eastern and south-western Monsoons. It has three seasons: dry (Winter), hot (Summer, with gradually increasing rainfall and thunderstorms) and rainy seasons. Over 90 % of the annual rains fall within the rainy season, which lasts for about 5 months (mid-May to mid-October), with most of the rains coming in August and

September. Monsoon rains are unpredictable, so rainfall varies considerably within and between years, but generally ranges from 1,200 to 1,600 mm per annum. Cloud cover is usually least from November to March. Temperatures generally range from 18℃ in winter to 37℃ in summer. The maximum temperature is usually about 40℃. The temperature decreases at the onset of the rains (mid-May), during which, it is generally below 40℃. Humidity is generally high, ranging from 63 to 81%.

2.2. Data Collection and Preparation

The data requirements for running the Revised MMF annual erosion model and generating the relevant outputs are shown in Appendix 2-1. Some of the instrument that were used during this study are the GPS receiver, data sheets, soil auger, soil sample rings, field knife, hammer, measuring tape, squeezing bottle and shear vane apparatus. The software that were used in this study include ArcGIS, SNAP Desktop, Erdas Imagine, PCRaster, SPAW, Google Earth, SPSS, Microsoft Excel and Microsoft Word.

2.2.1. Watershed Delineation and Design of Sampling Scheme

In order to delineate the watershed, flow direction was computed using the SRTM DEM of the Ban Dan Na Kham region of Thailand. Based on the flow direction, an appropriate outlet point was defined. All the surrounding areas on higher elevation contributing runoff to the defined point were then delineated as part of the watershed.

The soil sampling scheme was designed using elevation profiles in Google Earth (Figure 2-5). It was predefined such that samples were taken from the various hillslope positions – Summit, Shoulder, Back Slope, Foot Slope and Toe Slope (Figure 2-3) – throughout the watershed. Accessibility of the site and its ability to also serve as a land cover sample site was taken into consideration prior to its selection. As such, the sampling scheme was not random, it was purposive.
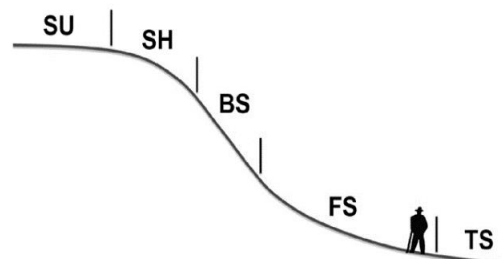
(Source: Miller & Schaetzl (2015))
[SU= Summit, SH = Shoulder, BS = Back Slope, FS = Foot Slope, TS = Toe Slope]
Figure 2-3: Hillslope model

2.2.2. Field Data Collection

Samples were taken at some of the pre-defined locations. However, due to the high altitudes, steep slopes and inaccessibility of some of the pre-defined sample sites, the sampling scheme was readapted in the field to suit the peculiarities of the terrain. Figure 2-4 shows a map of the watershed, as well as the proposed and the updated sample sites. Nevertheless, the accuracy of field-generated hillslope classes may have been reduced by the obstruction of field view by tall trees. Furthermore, given the fact that the field of view was relatively small and inadequate, compared to the spectral profile of Google Earth, on-site hillslope classification may be encumbered. As such, after the fieldwork, the hillslopes were checked again with the elevation profile of Google Earth (Figure 2-5). Where there appeared to be a major disagreement between the field and the Google Earth hillslope classes, it was re-checked with a flow accumulation data generated from the SRTM DEM.

A total number of 48 samples were collected from the various hillslope positions of the watershed. Prior to soil sample collection, the sites were described using site description forms (Appendix 2-2). The geographic coordinates (Easting (m), Northing (m) and altitude (m)) were measured using the Germin GPS. The predominant vegetation, the average plant height (m), the land use, the landform and the hillslope position were recorded. The canopy cover (%) was then estimated using the densiometer. Afterwards, the soil depth (m), shear strength (Kpa) and soil colour were determined using the soil auger, the shear vane apparatus and the Munsell Colour Chart respectively. Disturbed samples were taken with a spade, while undisturbed soil samples for hydraulic conductivity (mm/hr) and bulk density (Mg/m³) were taken using steel soil sample rings at a depth of 5cm below the surface. The rings were subsequently sealed with plastic corks. Figure 2-6 shows the researcher assessing the shear strength on a sloping terrain, while Figure 2-7 shows the researchers assessing soil depth with a soil auger and collecting soil samples with a spade. Figure 2-8 shows the researchers assessing the canopy cover with a densiometer and the soil depth with a soil auger. In Figure 2-9, one of the researchers was collecting soil samples with sample rings while the other one was assessing shear strength with a shear vane apparatus.
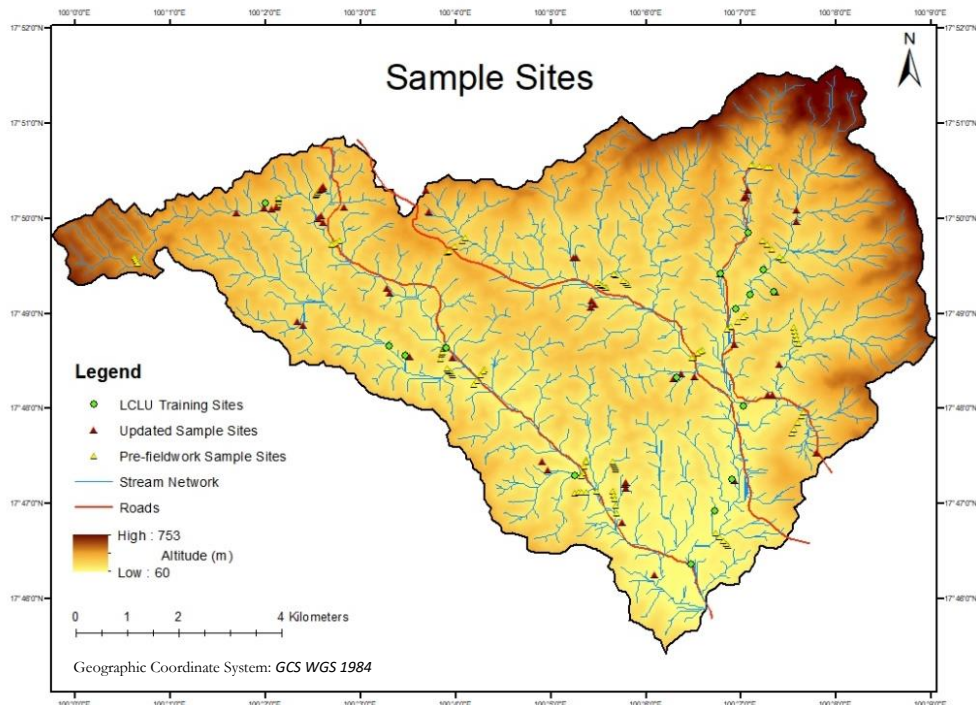
Figure 2-4: Map of the watershed, showing the soil and land cover sample sites
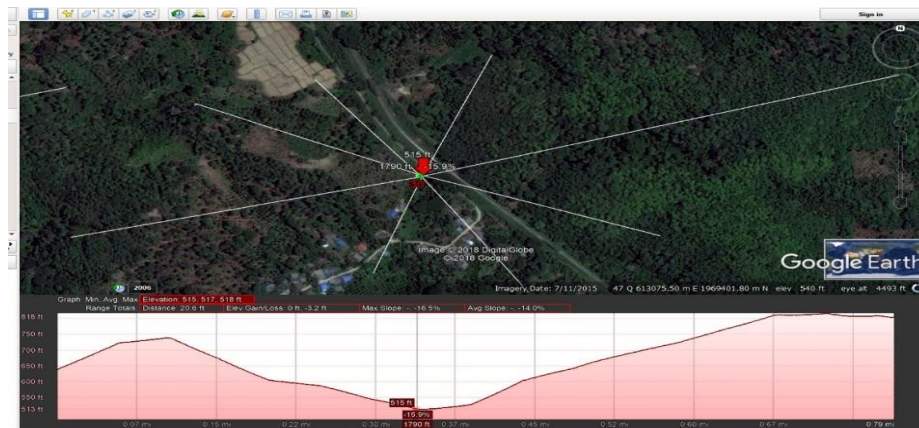
Figure 2-5: Rechecking a field-defined sample site with Google Earth elevation profile

Figure 2-6: Assessment of shear strength on a sloping terrain

Figure 2-7: Sample collection with a spade and assessment of soil depth with a soil auger

Figure 2-8: Assessment of canopy cover with a densiometer and soil depth with a soil auger

Figure 2-9: Sample collection with sample rings and shear strength assessment of level land

2.2.3. Soil Analysis

The 48 soil samples collected in the field were analysed at the Civil Engineering Laboratory of the Naresuan University in Phitsanulok, Thailand. The undisturbed samples were tested for saturated hydraulic conductivity, bulk density and porosity. The disturbed samples were tested for particle size distribution, soil texture and organic matter content. Figure 2-10 shows the soil samples in metal cans while Figure 2-11 shows the researchers preparing the soil samples for analysis.

(a) ***Particle Size Distribution:*** The particle size distribution was assessed using the hydrometer method, as described in the Soil Survey and Laboratory Manual (Soil Survey Staff, 2014). The soil samples were air-dried and passed through a 2mm sieve. 40g of the sample was weighed into a glass beaker to which 100ml of distilled water and 100ml of Calgon (5% sodium hexametaphosphate) solution were added. It was then left overnight, after which it was passed into a dispersing cup and stirred for 5 minutes with a mechanical mixer. The mixture was transferred into a 1000ml sedimentation cylinder, which was then filled to the 1000ml mark. Another sedimentation cylinder containing 100ml Calgon and distilled water, but no soil, was also prepared. The soil solution was stirred for 30 seconds. The temperature of both solutions were recorded, and the hydrometer readings taken at 30 seconds, 60 seconds, 3 minutes, 10 minutes, 30 minutes, 60 minutes, 90 minutes, 120 minutes and 1440 minutes. 10g of the soils were subsequently oven-dried at 105°C, and then, reweighed. The proportion of sand, silt and clay in the soil were then computed as suggested by Gee & Bauder (1986) and described by Soil Survey Staff (2014). Using the proportions, the soil texture was determined with the textural triangle. Figure 2-12 shows the sedimentation cylinders and beakers containing soil samples already treated with sodium hexametaphosphate.

Figure 2-10: Soil samples ready to be processed for further analysis

Figure 2-11: Sample preparation for laboratory analysis

Figure 2-12: Sedimentation cylinders and beakers containing treated soil samples

Figure 2-13: Assessment of saturated hydraulic conductivity with makeshift permeameter

(b) **Bulk Density:** The soil samples in the core rings were weighed and placed in the oven for 24 hours (or until it achieves a constant weight) at 110ºC (Soil Survey Staff, 2014). The weight and volume of the empty cylinders were subsequently determined. Bulk density was then computed in as the ratio of oven-dry soil weight to the volume of the soil.

(c) **Porosity:** Soil porosity, which is the proportion of the soil occupied by air and water, was determined using bulk density and particle density (2.65 Mg/m³). It was computed as:

$$Porosity = \left(1 - \frac{Bulk\ Density}{Particle\ Density}\right) x\ 100\ \dots\dots\dots\dots\dots\dots\dots\dots\dots Eq.1$$

(d) **Saturated Hydraulic Conductivity:** Saturated hydraulic conductivity (Ksat) was determined using the constant head method of Klute & Dirksen (1986). It is usually determined with the aid of a laboratory permeameter. However, due to the lack of the permeameter, an alternative was designed (Figure 2-13) using the same operating principles. The plastic corks of the soils in the sample cores were removed, and the bottom sealed off with a permeable fabric. The rings containing the samples were then placed on elevated platforms in a water bath. The bath was filled with water, up to 2/3 the height of the cylinders. The samples were left overnight (or until fully saturated). The rings were then elongated with the aid of transparent, waterproof sellotapes. The hydraulic conductivity apparatus was subsequently set up as shown in Figure 2-13. The height of water above the soil column was noted. The volume of water that passed through the soil column at a pre-selected time interval was recorded until it becomes constant. The hydraulic conductivity was finally calculated using the formula:

$$Ksat = \frac{V * L}{A * t * h}\ \dots\dots\dots\dots\dots\dots\dots\dots\dots\dots\dots\dots\dots\dots\dots\dots\dots Eq.2$$

Where V = volume of water flowing through the sample (cm³), L = length of the soil sample (cm), A = cross-section surface of the sample (cm²), t = time taken for water (V) to flow through the soil column (hr), *and* h = height of water above the soil surface in the sample cylinder (cm).

(e) **Soil Organic Matter:** Organic matter was estimated through the direct method of loss on ignition as reported by Dor & Banin (1989). 5g of soil was weighed into a crucible and left overnight in an oven set at a temperature of 105°C. It was then cooled to room temperature in a desiccator for 20 minutes, after which it was reweighed and transferred to a furnace. The temperature of the furnace was raised to 400°C. The sample was left in the furnace for 8 hours. It was then removed, and again cooled to room temperature in a desiccator, before being reweighed. The organic matter was expressed as a percentage of the weight loss between oven-drying and furnace ignition to the weight after oven-drying.

2.3. Comparative Analysis of SoilGrids250m and Field Data

Soil data was generated from two sources, viz. SoilGrids250m and field sampling. The 5cm layer of the SoilGrids250m data for the study area was downloaded from https://soilgrids.org/. Bulk density, organic carbon, clay, sand, silt and gravel data were available in this repository for 7 soil depth intervals (ISRIC, 2017). The field samples were collected from various hillslope positions (Figure 2-3). These were, however, point data that need to be extrapolated for the entire watershed. Several hillslope algorithms were considered as potential tools for the delineation of the soil units. These include the digital hillslope classification described by Miller & Schaetzl (2015), the r.geomorphon algorithm in GRASS GIS based on the works of Jasiewicz & Stepinski (2013), the TPI (topographic position index) slope and landform classification implemented by Miller (2014), but based on the works of Deumlich et al. (2010) and the supervised hillslope classification which was based on an overview of the field-generated data.

2.3.1. Generation of Physiographic Map for Representing Soil Variation

Several hillslope delineation algorithms were considered in the course of this study. Each of these are briefly discussed below.

1. **Digital Classification of Hillslope Positions:** This was based on the work of Miller & Schaetzl (2015). They used 3m resolution LiDAR DEMs to generate slope gradient, profile curvature and relative elevation at a neighbourhood scale of 9m, 63m and 135m respectively. The adopted neighbourhoods were in line with the analysis scale that soil scientists use while analysing hillslope positions (Miller, 2014). In this study, to mimic the resolution of the LiDAR DEM, the SRTM DEM was resampled to 3m using cubic convolution. Slope gradient, profile curvature and relative elevations were then calculated using the appropriate neighbourhood scales. The slope gradient map was classified into high, medium and low; profile curvature was classified into positive and negative; while relative elevation was classified into high and low. The hillslope was then delineated using the decision tree algorithm (Figure 2-14) implemented in the relief analysis toolbox by Miller (2014). The output generated from the model was then compared with the field-generated hillslope units to determine to what extent they align.
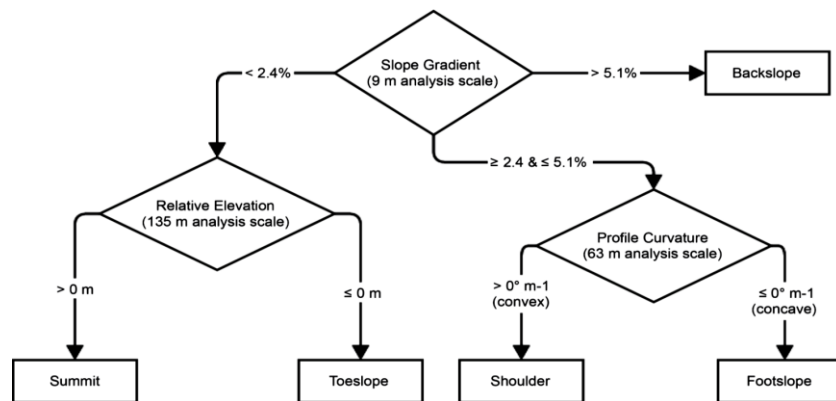
Source: Miller & Schaetzl (2015)

Figure 2-14: Decision tree for generating the digital hillslope positions

2. **Geomorphic Unit Delineation Using r.geomorphon in GRASS GIS:** The geomorphon classifies hillslopes using pattern recognition, rather than differential geometry (Jasiewicz & Stepinski, 2013). It creates a pattern by comparing a target pixel with the pixel values of the 8 neighbouring pixels along the line of sight of the 8 principal directions. This creates a tuple of negatives, positives and zeros, indicating pixels with lower, higher and equal values respectively. The output however depends on the search radius and the flatness threshold. The search radius refers to the distance or the number of cells around the target cell on which the calculation is based, while the flatness threshold relates to degree of flatness of the area under observation. According to Veselsky et al. (2015), as the flatness threshold increases, the spatial extent of plains automatically increases at the expense of other landforms. In this way, the model creates 498 unique patterns for every cell. Nevertheless, out of all of these, only 10 patterns represent the possible morphological terrain types of a standard landscape, referred to as geomorhons (Figure 2-15). In this study, an outer radius of 45m was adopted since it was not meant to be less than the resolution of the DEM. Given the mountainous nature of the terrain, the pre-programmed flatness threshold of 1 and an inner search radius of 0 were used for the generation of the geomorphic units. The generated units were then compared with the field-generated hillslope units to determine to what extent they align.
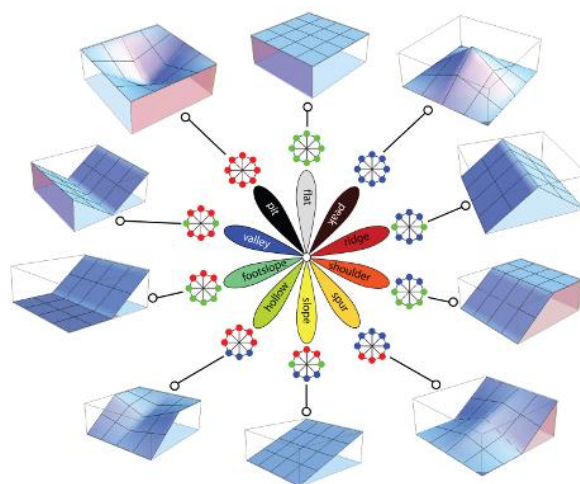
Source: Jasiewicz & Stepinski (2013)
Figure 2-15: Landscape patterns represented as geomorphons

3. **TPI Slope and Landform Classification:** The TPI (topographic position index) Slope and Landform Classes were calculated using the Relief Analysis toolbox developed by Miller (2014). The underlying theory behind the functionality of the computations were based on the works of Deumlich et al. (2010). They contended that using the TPI slope and landform analysis, information can be combined at both the local and regional scale, enabling the establishment of relationships that can help in the delineation of the spatial extent and distribution of soils. The TPI compares the elevation of each grid cell in a DEM with the mean elevation of a neighbourhood defined by circles of arbitrary radius.

In this study the 30m SRTM DEM was used to generate TPI and slope maps, adopting the 25m, 125m and 500m neighbourhood settings used by Deumlich et al. (2010). They were then used as inputs for the calculation of the TPI Landform and TPI Slope Position Classes. Furthermore, the DEMs were resampled to 5m resolution to mimic the resolution of the airborne laser scanning-derived DEM used by Deumlich et al. (2010). The process was repeated and the output recalculated. The outputs were then compared with the field-generated hillslope units to determine to what extent they align.

4. **Supervised Hillslope Delineation:** This was based on an overview of the field-generated data. Slope gradient, elevation, profile curvature and flow accumulation were calculated for each of the soil sample sites. Box plots were then made showing the minimum, the median, the maximum and the outliers of all these parameters on each of the sampled hillslope position. Using the spread of these data as inputs, Table 2-1 was generated. Raster maps of each of these parameters were then stacked as layers and used for image segmentation in eCognition. Altitude was rated 0.5 while the other 3 parameters were each rated 1. The ratings determined the degree of contribution of each raster in the segmentation process through which a vector file was generated. Altitude received a lower rating because, unlike the three other variables, a specific altitude cannot be attributed to a particular hillslope position. In fact, across the landscape, some foot slopes even had higher elevation than some summits. As such, while altitude still plays a key role in the hillslope delineation process, it was not as critically important as the other parameters. The vector file was then spatially queried in accordance with the decision rule in Table 2-1, to generate the supervised hillslope classification. The generated output was then compared with the field-generated hillslope units to determine to what extent they align.

Table 2-1: Decision rule for hillslope classification based on field data

	Summit	Shoulder	Back Slope	Foot Slope	Toe Slope	Valley SB	Valley Bottom SB	Streams
Slope Gradient	V. Gentle - Gentle	V. Gentle - Moderate	Gentle - Steep	V. Gentle - Gentle	V. Gentle - Gentle			
Profile Curvature	Convex - Even	M. Convex - Even	Convex - Concave	Convex - V. M. Convex - Concave				
Flow Accumulation	Very Low	Very Low	Low - Moderate	Low - Moderate	Moderate	High	Very High	E. High
Altitude	Very High > 180 m	High > 150 m	Medium > 120 m					

NOTE:							
Slope Gradient	V. Gentle 0.0 - 5.0	Gentle 5.0 - 15.0	Moderate 15 - 23	Steep > 23			
Profile Curvature	V. Convex < -1	Convex -1 - -0.5	M. Convex -0.5 - -0.05	Even -0.05 - 0.05	M. Concave 0.05 - 0.5	Concave 0.5 - 1	V. Concave >1
Altitude	Low 0 - 150	Medium 150 - 250	High > 250				
Flow Accumulation	Very Low 0 - 2	Low 2 - 10	Moderate 10 - 50	High 50 - 250	Very High 250 - 6000	E. High > 6000	

SB = Stream Beds, V. Concave = Very Concave, V. Gentle = Very Gentle, M. Concave = Moderately Concave, V. Convex = Very Convex M. Convex = Moderately Convex, E. High = Extremely High

2.3.2. Comparative Analysis of Field and SoilGrids250m Data

The hydrologic data were generated for the field data using Saxton et al. (1986) pedotransfer functions, which has been updated and transformed into the SPAW (Soil-Plant-Air-Water) computer model (Saxton & Rawls, 2006). For the SoilGrids250m data, a model developed by Jetten (2018), also based on the pedotransfer functions of Saxton et al. (1986), was used to generate the hydrologic properties (model codes are shown in Appendix 2-3). The data used to generate the hydrologic outputs were soil texture, sand, clay, gravel and organic matter content. The outputs that were generated include wilting point, field capacity, porosity and saturated hydraulic conductivity.

The nature and characteristics of both data sources were assessed visually and statistically. To get an overview the range, the median and the outliers of the soil characteristics under different land uses and hillslope units, box plots were generated for each soil characteristic.

Furthermore, the SoilGrids250m cell values corresponding to the field sample sites data points were expected were extracted. Similarly, the average of the SoilGrids250m values corresponding to each of the

delineated hillslope units were also calculated. Box plots were then generated for the SoilGrids250m and field data to visually show how they compare to each other. Regression graphs were also generated to determine the kind of relationship that exists between the two datasets.

To determine to what extent the data sources are similar, the Euclidean Distance between the two data sources was computed using the formula:

$$ED = \sqrt{\sum_{i=1}^{n}(xi - yi)^2} \dots\dots\dots\dots\dots\dots\dots\dots\dots\dots\dots\dots\dots\dots\dots\dots Eq.3$$

Where ED = Euclidean Distance, n = number of variables, i = point variable (soil characteristic), x = SoilGrid250m data and y = Field Data.

To determine whether there is a statistically significant difference between the 2 sets of data some preliminary tests were conducted to determine which statistical methods are more appropriate for the assessment. Skewness and kurtosis z-values, and Shapiro-Wilk test p-value were calculated to determine whether the data were normal. The data were considered to be normal if the Shapiro-Wilk test p-value is greater than 0.05 and the skewness and kurtosis z-values are within the range of -1.96 to +1.96. Levene's Test was conducted to determine whether the variance of the two data sources are homogenous. According to Martin & Bridgmon (2012) the variances are not significantly different when the computed p-value is greater than 0.05; but when it is less than that, they can be considered to be significantly different. In accordance with the assertion of Dytham (2011), t-test was calculated if the data was continuous, approximately normally distributed and had homogenous variance. If these conditions were not met, Wilkoxon Signed Rank Test was conducted.

2.4. Generation of Other RMMF Model Inputs

Besides the soil data, the RMMF model also requires land cover, terrain and rainfall data. The processes through which these data were generated, are outlined in this section.

2.4.1. Land Cover Classification

A land cover map of the study area was generated prior to the fieldwork using unsupervised classification of Sentinel 2 imagery in Erdas Imagine. This guided the location of soil / land cover sample sites within each unit. The 48 sites which were described in the course of soil sample collection also doubled as land cover training / validation sites. 16 additional sites were sampled specifically for land cover classification / validation, amounting to a total of 64 sites. 150 validation points were subsequently generated from Google Earth (30 per land cover types) for accuracy assessment purposes.

Sentinel 2 multispectral satellite imagery of the study area acquired on November 6, 2018, was downloaded and pre-processed for atmospheric, aerosol, terrain and cirrus correction in SNAP using the Sen2Cor algorithm. After pre-processing the image, the 64 land cover training samples were used to estimate the mean and variance of the pixel values of each land cover class, enabling the determination of the appropriate range of pixel values that belong to each land cover class. Using the Maximum Likelihood approach, the statistical probability of each grid cell belonging to a land cover class was computed. The grid cells were subsequently allocated to the land cover class to which they most likely belong.

The accuracy of the classification was assessed using the 150 sample sites generated from Google Earth. The land cover class type of each of the sample point was compared with Google Earth / field-generated land cover class for that points. This enabled the calculation of the percent accuracy of each land cover class, both individually and collectively.

Land cover related parameters that were measured in the field, like plant height (PH), canopy cover (CC) and surface cover (SC), were built into the Land Use Table that was subsequently associated with the land cover map in PCRaster. Other secondary parameters that were also built into the table are the ratio of actual to potential evapotranspiration (Morgan, 2005), crop management factor ($C = 1 – CC$), rainfall interception by vegetation ($A = $ Rainy Days $*$ Smax $/$ Annual Rainfall), leaf area index ($LAI = \ln(1 – CC) / -0.4$), maximum plant canopy storage ("Smax1 $= 0.935 + 0.498*LAI - 0.00575$ for field crops" or "Smax2 $= 1.46*LAI**0.56$ for trees") and effective hydrological depth (Morgan, 2001). Using the lookupscalar command in PCRaster, individual maps were generated for each parameter based on the land cover map.

2.4.2. Rainfall Data

The cumulative annual rainfall (1,380mm) and number of rainy days (117) were generated from data acquired from the Royal Meteorology Department of Thailand through the Civil Engineering Department of Naresuan University, Phitsanulok, Thailand (Appendix 2-5 and Figure 2-16). The lowest rainfall for the period under review was recorded in March 2018 (3.6mm), while the maximum rainfall was recorded in August 2018 (301mm).

Month	Rainfal (mm)	Days
Oct-17	133.3	13
Nov-17	5.2	4
Dec-17	25.2	3
Jan-18	7	2
Feb-18	12.3	1
Mar-18	3.6	3
Apr-18	72.7	10
May-18	280.4	18
Jun-18	200.5	15
Jul-18	148	19
Aug-18	301	16
Sep-18	191.1	13
Total	1380.3	117
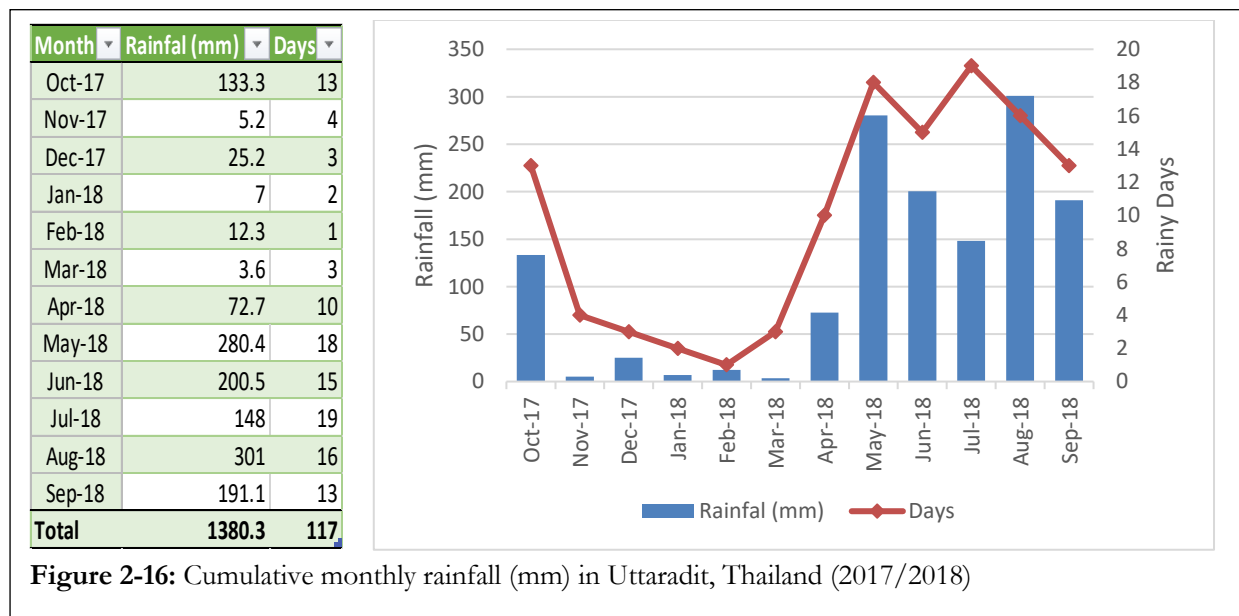
Figure 2-16: Cumulative monthly rainfall (mm) in Uttaradit, Thailand (2017/2018)

2.4.3. Topographic Data

The 30m resolution SRTM DEM was resampled to 15m because other model inputs like the land cover map, had 15m spatial resolution. The resampling consequently ensured that the grid cells of all the model inputs are well aligned, enabling easy and effective manipulation of model inputs to generate the appropriate model outputs. Afterwards the slope was computed from the DEM. Finally, the local drainage direction (LDD) was produced to depict the flow of water from a grid cell to its neighbours, based on the understanding that water flows in the direction of least resistance, which may also be synonymous with the direction of steepest slope.

2.5. Erosion Modelling

The runoff and erosion assessment was based on the RMMF erosion modelling methodology reported by Morgan (2001). The model separates soil erosion into the water phase and the sediment phase. The water phase determines the erosive energy of rainfall and runoff volume, while the sediment phase determines to a great extent, the particle detachment by rainfall and runoff, as well as the transport capacity of the runoff.

According to Morgan (2001), particle detachment and runoff transport capacity play a crucial role in the determination of soil erosion, as the lower of the two variables is representative of the erosion rate.

2.5.1. The RMMF Erosion Modelling Process

1. **Rainfall Energy Estimation:** Effective rainfall (ER; mm) was considered to be affected by annual rainfall (R; mm) and the proportion of the rainfall that reaches the ground (A) after some of the rainfall has been intercepted by plant canopy cover (CC; %). And usually, A is a value that ranges from 0 to 1.

$$ER = R * A \dots\dots\dots\dots\dots\dots\dots\dots\dots\dots\dots\dots\dots\dots\dots\dots Eq.\,4$$

Furthermore, Effective Rainfall (ER; mm) is a product of both leaf drainage (LD; mm) and direct Throughfall (DT; mm) of rainfall.

$$ER = LD + DT \dots\dots\dots\dots\dots\dots\dots\dots\dots\dots\dots\dots\dots\dots Eq.\,5$$

The split in the effective rainfall (ER; mm) is a direct function of canopy cover (CC; %)

$$LD = ER * CC \dots\dots\dots\dots\dots\dots\dots\dots\dots\dots\dots\dots\dots\dots\dots..\dots\dots Eq.\,6$$

$$DT = ER - LD \dots\dots\dots\dots\dots\dots\dots\dots\dots\dots\dots\dots\dots\dots\dots\dots Eq.\,7$$

The kinetic energy (KE(DT); J/m²) of throughfall is a function of rainfall intensity (I; mm/h)

$$KE(DT) = DT(11.9 + 8.7logI) \dots\dots\dots\dots\dots\dots\dots\dots\dots\dots\dots\dots\dots Eq.\,8$$

Similarly, kinetic energy of leaf drainage (KE(LD), J/m²) is dependent on plant height (PH; m)

$$KE(LD) = (15.8 * PH0.5) - 5.87 \dots\dots\dots\dots\dots\dots\dots\dots\dots\dots\dots\dots\dots Eq.\,9$$

It is noteworthy that if the results of the computation of the kinetic energy of the rainfall is negative, it is assumed to be equal to zero.

2. **Estimating Runoff:** Runoff (Q; mm) occurs when daily rainfall exceeds soil moisture storage capacity (Rc; mm). It is expressed as:

$$Q = R\, e^{\frac{-Rc}{Ro}} \dots\dots\dots\dots\dots\dots\dots\dots\dots\dots\dots\dots\dots\dots\dots\dots\dots\dots Eq.\,10$$

Where Q = Annual Runoff (mm), R = Annual Rainfall (mm), R_o = Mean Rain per Rainy Day (mm), Rc = Soil Moisture Storage Capacity (mm) and R_n = Number of Rainy Days per annum

$$Ro = \frac{R}{R_n} \dots\dots\dots\dots\dots\dots\dots\dots\dots\dots\dots\dots\dots\dots\dots\dots\dots\dots Eq.\,11$$

Soil moisture storage capacity (Rc; mm), on its part, was dependent on moisture content at field capacity (MS; %, w/w), bulk density (BD; Mg/m³) and on the ratio of Actual to Potential Evapotranspiration (E_t/E_o)

$$Rc = 1000MS * BD * EHD(Et / Eo) \dots\dots\dots\dots\dots\dots\dots\dots\dots\dots\dots\dots Eq.\,12$$

Where Rc = Soil Moisture Storage Capacity (mm), MS = Soil Moisture Content at Field Capacity (%, w/w), BD = Bulk Density (Mg/m³), EHD = Effective Hydrological Depth (m) and Et/Eo = Ratio of Actual to Potential Evapotranspiration

It is noteworthy that according to Morgan (2001) effective hydrologic depth (EHD) indicates the depth of soil within which the moisture storage capacity controls the generation of runoff. It is a function of plant cover, which influences rooting depth and root density; and is also sometimes a function of effective soil depth.

Nevertheless, according to Morgan (2001), all the runoff within a grid are generated in the grid. Shrestha et al. (2014) was however, of the opinion that the total runoff in a grid is the sum of the runoff generated within the grid and the runoff flowing into the grid from surrounding grids located on higher terrain. This is quite logical because runoff is not stagnant, it flows from place to place; the implication being that it flows from one grid to another as it moves towards the outlet. Shrestha et al. (2014) incorporated this into the erosion modelling process by using flow accumulation over a gridded

landscape to quantify the runoff. The flow direction was first defined in terms of the direction of the steepest slope, after which, local drainage direction network was generated. The total area contributing runoff was subsequently calculated for each grid cell.

3. **Particle Detachment by Raindrop Impact:** Particle detachment by raindrop impact (F; kg/m²) was a function of soil detachability (K; g/J) and kinetic energy of rainfall (KE)

$$F = K * KE * 10^{-3} \dots \dots \dots \dots \dots \dots \dots \dots \dots \dots \dots \dots \dots \dots \dots Eq.\,13$$

4. **Soil Particle Detachment by Runoff:** In addition to detachment by raindrop impact (F; kg/m²), soil particles were also considered to be detachable by runoff (H; kg/m²). Detachment by runoff (H; kg/m²) is a function of the resistance of the soil (Z), runoff (Q; mm), slope steepness (S; º) and ground cover (GC; %)

$$H = ZQ1.5 sinS(1 - GC) * 10^{-3} \dots \dots \dots \dots \dots \dots \dots \dots \dots \dots \dots \dots Eq.\,14$$

However, the underlying assumption is that soil particle detachment occurs when soil protection by ground cover is not available. Also, the resistance of the soil (Z) was considered to be a function of soil cohesion (COH; kPa) as measured on saturated soils with a shear vane apparatus.

$$Z = \frac{1}{0.5 * COH} \dots \dots \dots \dots \dots \dots \dots \dots \dots \dots \dots \dots \dots \dots \dots \dots \dots Eq.\,15$$

5. **Transport Capacity of Runoff:** Transport Capacity of Runoff (TC; kg/m²) was a function of Runoff (Q; mm), Crop or Plant Cover Factor (C) – taken as the product of C and P factors in USLE – and Slope Angle (S; º)

$$TC = CQ^2 sinS * 10^{-3} \dots \dots \dots \dots \dots \dots \dots \dots \dots \dots \dots \dots \dots \dots \dots \dots Eq.\,16$$

6. **Estimating Soil Erosion:** The summation of the estimated soil particle detachment by runoff and raindrop impact amounted to the total annual soil detachment. This was then compared with the annual runoff transport capacity. The lesser of the two values was considered to be equal to the annual soil erosion rate.

7. **Running the RMMF Model:** The model was run twice, each time with a different soil data source. The outputs generated were then assessed statistically to determine the degree of similarity between the outputs generated from the two data sources. The complete scripts for running the model is shown in Appendix 2-4.

2.5.2. Comparative Assessment of SoilGrids250m and Field-based Outputs

The difference between the values of the erosional processes generated from SoilGrids250m data and field-based soil data were calculated. The magnitude of the residual value after one image has been subtracted from its counterpart is a measure of the similarity of the two sets of output.

Furthermore, 120 random points were generated from the hillslope map using stratified random sampling. 30 points were generated for each hillslope unit. The grid values corresponding to the random points were then extracted from both sets of model outputs. The average estimate for each hillslope unit was also calculated. Two sets of comparative assessment were then performed.

First, the two sets of outputs were compared point-by-point, based on the 120 random points. The field-based output was plotted against the corresponding SoilGrids250m output to determine whether they are correlated. To determine to what extent the outputs were similar, the Euclidean Distance was calculated. To determine whether there is a statistically significant difference between the two sets of outputs, T-Test or Wilkoxon Signed Rank Test was calculated. In both cases, according to Dytham (2011), if the calculated p-value is less than 0.05, then there is a significant difference between the data sources.

Subsequently, hillslope unit-based averages of the two sets of outputs were compared in the same way. This was meant to determine whether the parcel-based averages are similar, even when the point-based data are dissimilar.

2.5.3.   Assessment of the Sensitivity of the Model Parameters

The model was run with the field-based data, starting with an arbitrary baseline setting for all parameters (Table 2-2). Subsequently, the value of one parameter was increased in steps of 20%, while the other parameters were held constant. The same process was repeated for all the constituent soil, land cover and rainfall parameters of the RMMF model.

The overall averages of all the erosion-related outputs of the RMMF model were then generated. The impact, in percentage, of each parametric increase on the erosional processes were calculated. This enabled the determination of the parameters for which a minimal change resulted in the greatest change in the predicted erosional processes.

Table 2-2: Baseline settings for sensitivity analysis of model parameters

	Land Use Type	Code	Et/Eo	C (0-1)	EHD (m)	A (0-1)	CC (0-1)	SC (0-1)	PH (m)
Land Cover	Arable Land	1	0.30	0.45	0.12	0.16	0.25	0.16	1.42
	Orchards	2	0.37	0.33	0.18	0.20	0.34	0.50	10.60
	Forests	3	0.47	0.05	0.20	0.50	0.47	0.41	19.88
	Built-up	4	0.20	0.04	0.10	0.10	0.20	0.10	2.00
	Teak Plantation	5	0.45	0.08	0.20	0.47	0.46	0.26	20.35
	Soil Units	**Code**	**MS (0-1)**		**K (g/J)**		**COH (Kpa)**		**EHD (m)**
Soil Properties	Back Slope	1	0.32		0.80		5.10		0.12
	Foot Slope	2	0.31		0.80		4.81		0.18
	Streams	3	0.20		0.50		2.00		0.20
	Summit/Shoulder	4	0.36		0.70		4.48		0.10
	Valley Floor	5	0.31		0.80		4.44		0.20
Rainfall	Rainfall Amount (mm)					1380			
	Rainy Days					117			

Et/Eo = Ratio of Actual to Potential Evapotranspiration, C = Crop Management Factor (0-1), A = Rainfall Interception by Vegetation (0-1), CC = Canopy Cover (0-1), SC = Surface Cover (0-1), PH = Plant Height (m), EHD = Effective Hydrologic Depth (m), MS = Field Capacity (0-1), K = Soil Erodibility (g/J), COH = Cohesion = Shear Strength (Kpa)

2.5.4.   Assessment of the Spatial Extent of Soil Erosion within the Different Land Cover and Slope Units of the Watershed

To determine the relationship between the steepness of the slope and the erosional processes within the watershed, the slope map was demarcated into 3 units. The units were classified as gentle slope (< 8°), moderate slope (8 – 30°) and steep slope (>30°). Furthermore, in order to determine the integrated impact of slope and land cover on soil erosion in the watershed, the slope unit and land cover maps were overlaid to generate a single land cover-slope map.

The mean values of the different erosional processes taking place in the watershed were calculated from the field-based outputs for both the slope units, the land cover types, the hillslope classes and the land cover-slope units. To enable the graphical depiction of the spatial dynamics of the erosional processes occurring within the watershed, the results were presented in bar charts and tables.

2.6.   Flowchart

The flowchart of methods, outlining the relationships between the adopted methods and the input data is shown in Figure 2-17.
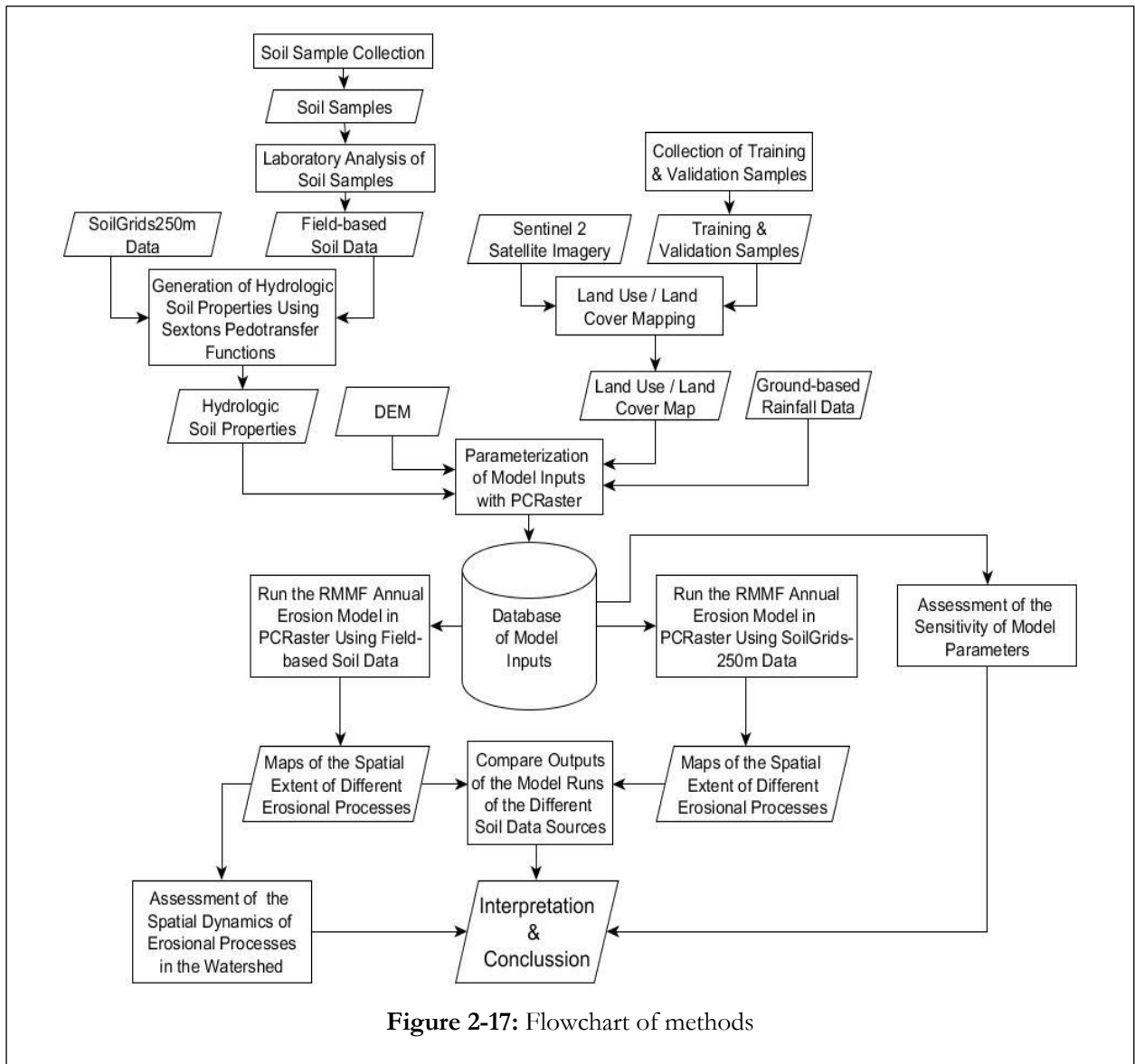
Figure 2-17: Flowchart of methods

3.   RESULTS AND DISCUSSION

3.1.   Acquisition and Comparative Analysis of Soil Data

The first research question of this study focussed on the determination of the characteristic features of the soils of the study area. Nevertheless, before this could be done, physiographic map units were generated for the study area. The range of the SoilGrid250m data values downloaded for the watershed were discussed in section 3.1.1. In section 3.1.2 the findings from the various hillslope assessments conducted prior to arriving at the final map units were discussed. Subsequently, the variation in soil properties across the landscape were discussed in section 3.1.3.

3.1.1.   SoilGrids250m Data for the Watershed

The maximum, minimum and mean values of different soil properties from SoilGrids250m across the hillslope positions of the study area are shown in Table 3-1. While some of data were downloaded directly from the World Soil Information (ISRIC) directory (gravel, sand, silt, clay, bulk density and organic carbon), others were generated through the use of Saxton et al. (1986) pedotransfer functions.

Gravel (14 to 43 %), sand (36 to 50 %), silt (24 to 37 %), clay (20 to 32 %), field capacity (26 to 33 %) and wilting point (13 to 20 %) were relatively uniform across the study area. Mean bulk density was marginally higher in the valley, but generally ranges from 1.47 to 1.90 Mg/m³. Similarly, soil porosity (46 to 56 %) was also marginally lower on the valley. The higher bulk density and lower soil porosity may be attributed to the predominant arable land use of the valleys, which lead to soil compaction. This may also account for the relatively lower hydraulic conductivity in the valley. Nevertheless, hydraulic conductivity generally ranges from 9.77 mm/hr to 58.62 mm/hr. Organic matter ranges from 0.9 to 3.20 %, but the mean value was much lower on the valley. This may also be attributed to the arable land use as Haynes et al. (2003) pointed out that agricultural activities tend to reduce soil organic matter and microbial biomass.

In tandem with the findings of this study, Herrmann et al. (2007) reported sand, silt, clay, porosity and organic matter values of 38%, 21%, 41%, 58% and 4.13% respectively for soils of Northern Thailand. Sand, silt and porosity were within the vicinity of the range of values reported for the SoilGrids250m data. On the other hand, clay and organic matter were about 28% higher than the maximum values of 32% (clay) and 3.2% (organic matter) reported for SoilGrids250m. The difference may be attributed the fact that the SoilGrids250m was the product of global soil modelling using machine learning while the data reported by Herrmann et al. (2007) were generated from the analysis of soil data collected from the field.

Table 3-1: Variability of soil properties from SoilGrids250m across different hillslope positions

SN	Parameter	Summit			Back Slope			Valley		
		Min.	Max.	Mean	Min.	Max.	Mean	Min.	Max.	Mean
1.	Gravel (%)	14	43	27	16	43	27	14	43	26
2.	Sand (%)	36	50	41	36	50	41	36	50	41
3.	Silt (%)	24	37	33	24	37	33	24	37	32
4.	Clay (%)	20	32	26	20	31	26	20	32	27
5.	Bulk Density (Mg/m³)	1.47	1.90	1.65	1.46	1.90	1.65	1.47	1.90	1.66
6.	Soil Porosity (%)	46	56	52	46	56	52	46	56	51
7.	Ksat (mm/hr)	10.39	58.62	22.94	9.83	58.62	23.09	9.77	43.37	20.24
8.	Field Capacity (%)	26	33	30	26	33	30	26	33	30
9.	Wilting Point (%)	13	20	17	13	20	17	13	20	17
10.	Organic Matter (%)	0.95	3.20	1.85	0.95	3.20	1.87	0.90	3.20	1.67

3.1.2. Generation of Physiographic Map for Representing Soil Variation

Table 3-2 shows the confusion matrix defining the degree of accuracy of field observations of hillslope units when compared to the hillslopes generated after the field observations were updated with the Google Earth elevation profile. The accuracy of the field observation, relative to the post-fieldwork assessment, is 65 %. This seems like a conservative proportion, as the accuracy of on-site assessment was expected to supersede that of remotely-sensed information. This may, however, not always be the case as the obstruction of view by tall trees and other structures and the reduced field of view may sometimes becloud the judgement of the researcher, especially when the terrain is frequently undulating. Furthermore, there is usually no clear boundary that can be seen in the field to depict the beginning of one class and the end of another. This may explain why 19 % of the sites were placed in classes just adjacent to the appropriate class, while only the remaining 17 % were placed further away.

The hillslope unit with the least accuracy was the Shoulder, where 0 % accuracy was recorded. This is in line with the fact, as noted in the field, that the Shoulder was usually not wide enough to be distinguishable from the Summit. Consequently, all the field-generated Shoulders were eventually classified as part of the Summit. On the other hand, the unit with the highest accuracy was the Back Slope. This may also be attributed to the fact that, as noted in the field, the Back Slope was usually very extensive and easy to distinguish. It consequently has an accuracy as high as 86%.

Table 3-2: Accuracy assessment of field-generated hillslope units

		Post-Fieldwork					Total	Accuracy (%)
		Summit	Shoulder	Back Slope	Foot Slope	Toe Slope		
Field	**Summit**	4	2	1	3		10	40
	Shoulder			3	1	1	5	0
	Back Slope			12	2		14	86
	Foot Slope				7	2	9	78
	Toe Slope			2		8	10	80
	Total	4	2	18	13	11	48	**65**

In order to extrapolate the point-based field data to the entire watershed, the digital delineation of hillslope positions (Miller & Schaetzl, 2015), the r.geomorphon algorithm in Grass GIS (Jasiewicz & Stepinski, 2013), the TPI slope and landform algorithm (Deumlich et al., 2010) and the supervised hillslope delineation were assessed to determine the most adequate for the study.

1. Digital Delineation of Hillslope Positions

Figure 3-1 shows a map of the hillslope as delineated with the method highlighted in Miller & Schaetzl (2015). It is noteworthy that the dominant landscape position is the Back Slope. This may be the case because in the course the fieldwork, it was noted that the Back Slope was quite extensive, relative to the other hillslope positions. However, instead of the 5 hillslope units that should have been delineated, only 3 were delineated; the Shoulder and the Foot Slope were not delineated. This is in line with the findings during the fieldwork that the shoulder and the foot slopes are quite narrow, and not easily distinguishable from the adjacent hillslope positions. Similarly, Miller & Schaetzl (2015) reported that the hillslope positions with the lowest accuracy were the Shoulder and the Foot Slope. As such, as seen in Table 3-3 much of the Shoulder and the Foot Slope were delineated as part of the Back Slope. Overall, 100%, 55% and 25% of the Back Slope, the Toe Slope and the Summit respectively, were delineated accurately. 46% of other hillslope positions were, however, also delineated as part of the Back Slope.

The overall accuracy of the classification delineation was 52%. Irrespective of the fact that none of the Shoulders and the Foot Slopes were delineated, the accuracy was still comparable to the 62% accuracy reported by Miller & Schaetzl (2015). Nevertheless, even though the accuracy of the delineation was relatively high, it was hinged more on the accuracy of Back Slope predictions, which was also grossly inaccurate because a large proportion of other hillslope positions were wrongly classified as part of the unit.

The poor performance of the delineation may be attributed to the coarse resolution of the DEM used. Miller & Schaetzl (2015) used a 3m resolution LiDAR DEM, which was able to generate all the 5 hillslope units. The required detail for running the model was not available in the 30m SRTM DEM that was used in this study. Resampling the DEM to 3m enabled the running of the model, but it could not generate information that was not originally present in the parent DEM.
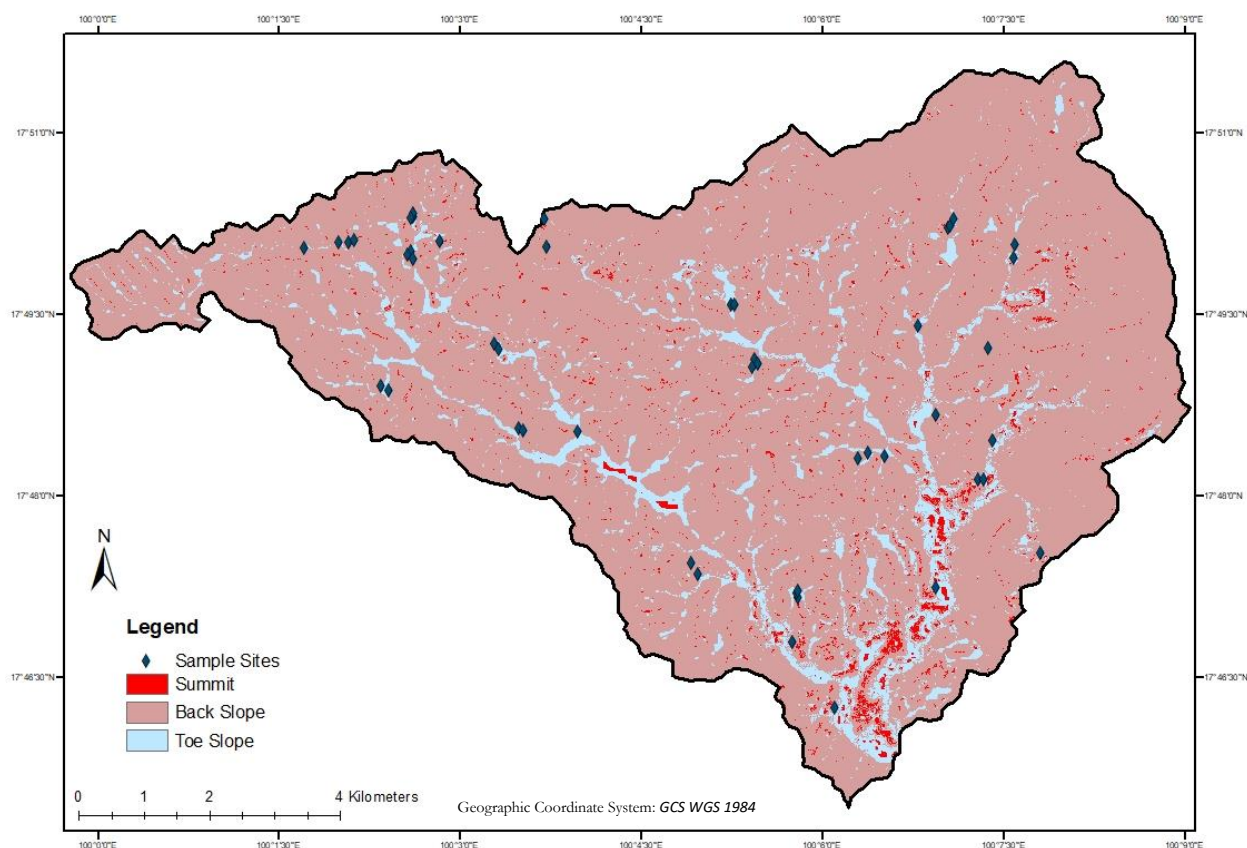
Figure 3-1: Digital hillslope positions

Table 3-3: Accuracy assessment of digital hillslope position delineation

		Hillslope Delineation						
		Summit	Shoulder	Back Slope	Foot Slope	Toe Slope	Total	Accuracy (%)
	Summit	1		3			4	25
Field	**Shoulder**			2			2	0
	Back Slope			18			18	100
	Foot Slope			10		3	13	0
	Toe Slope			5		6	11	55
	Total	1	0	38	0	9	48	52

2. Delineation of Geomorphic Units

Figure 3-2 shows a map of the geomorphic units of the study area, as delineated with the r.geomorphon in Grass GIS. The map shows that out of the 10 geomorphic units delineated in the study area, the most prominent were the Slope class – which is also synonymous with the back slope – and the Flats. To make them comparable to field observations, some of the slope classes were merged due to their similarity, e.g. Summit, Ridge and Spur; Hollow, Valley and Depression, etc. These may not be perfect matches, but they were merged to facilitated ease of comparison.

75%, 33% and 100% of the Summit, Back Slope and Toe Slope respectively, were predicted accurately (Table 3-4). None of the Shoulder and the Foot Slope were correctly predicted. The delineation of the shoulder as part of the Summit, and the Foot Slope as part of the Toe Slope may be attributed to the fact that at the 30m resolution of the SRTM DEM, those units are not easy to separate, as was also evident during the fieldwork. Furthermore, unlike the digital hillslope position algorithm, the r.geomorphon was apparently unable to predict most of the Back Slope, which had 33% accuracy. This may not necessarily be the case as some of the Spurs and Hollows / Depressions that were classified as part of the Summit and Toe Slope respectively, may have been located on the Back Slope.

The overall accuracy was 41.67%. Kramm et al. (2017) reported an accuracy of 39% for 30m SRTM DEM and 70% for 5m Pléiades Stereo Image, implying that a higher resolution DEM data will yield more accurately delineated geomorphic units. Irrespective of an accuracy of about 42%, it is still a valuable tool. Moreover, the generated geomorphic units were quite distinct from the five hillslope positions to which they were compared. If these units were delineated prior to the fieldwork, soil samples may have been collected from each of the delineated units, and the accuracy may have been much higher.
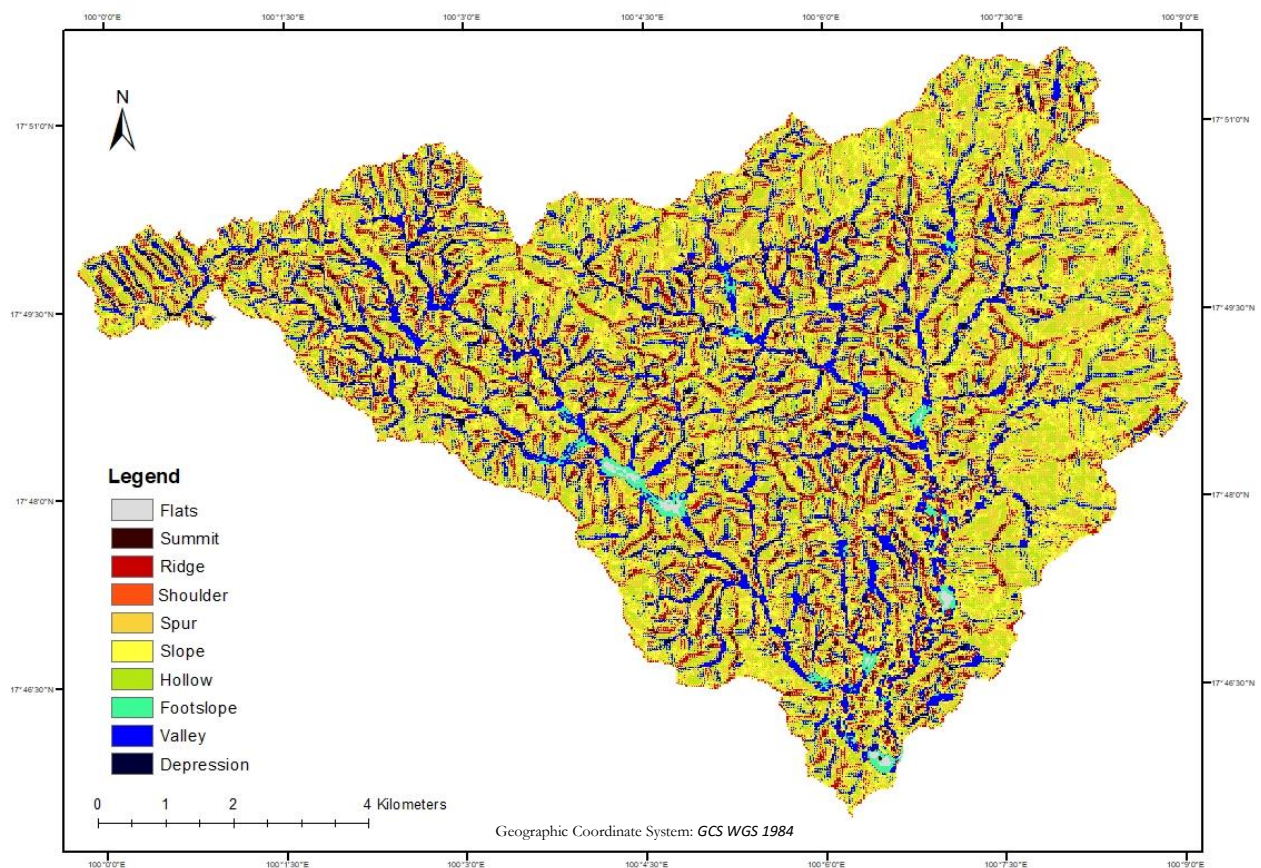
Figure 3-2: Geomorphic units

Table 3-4: Accuracy assessment of geomorphic units

		Geomorphic Units					Total	Accuracy (%)
		Summit	Shoulder	Back Slope	Foot Slope	Toe Slope		
Field	**Summit**	3				1	4	75
	Shoulder	2					2	0
	Back Slope	4		6		8	18	33
	Foot Slope	4		2		7	13	0
	Toe Slope					11	11	100
	Total	13	0	8	0	27	48	41.67

3. Delineation of TPI Slope Units

Figure 3-3 shows a map of the TPI slope units. The map indicates that the dominant hillslope units are Summit/Top/Ridge and the Depressions. Expectedly, as shown in Table 3-5, the Summit and the Toe Slope were over-predicted, as other hillslope units were delineated as part of both units. The overall accuracy of the delineated hillslope units was 35%. Kramm et al. (2017) reported an accuracy of 41%. The higher accuracy may be attributed to the fact that they compared the delineated classes with field assessment of the same nomenclature. This result shows that the TPI slope algorithm was mainly able to separate lowland from upland areas. This is in line with the assertion of Weiss (2001) that the classification enables the delineation of mountains, ridgelines and valleys.
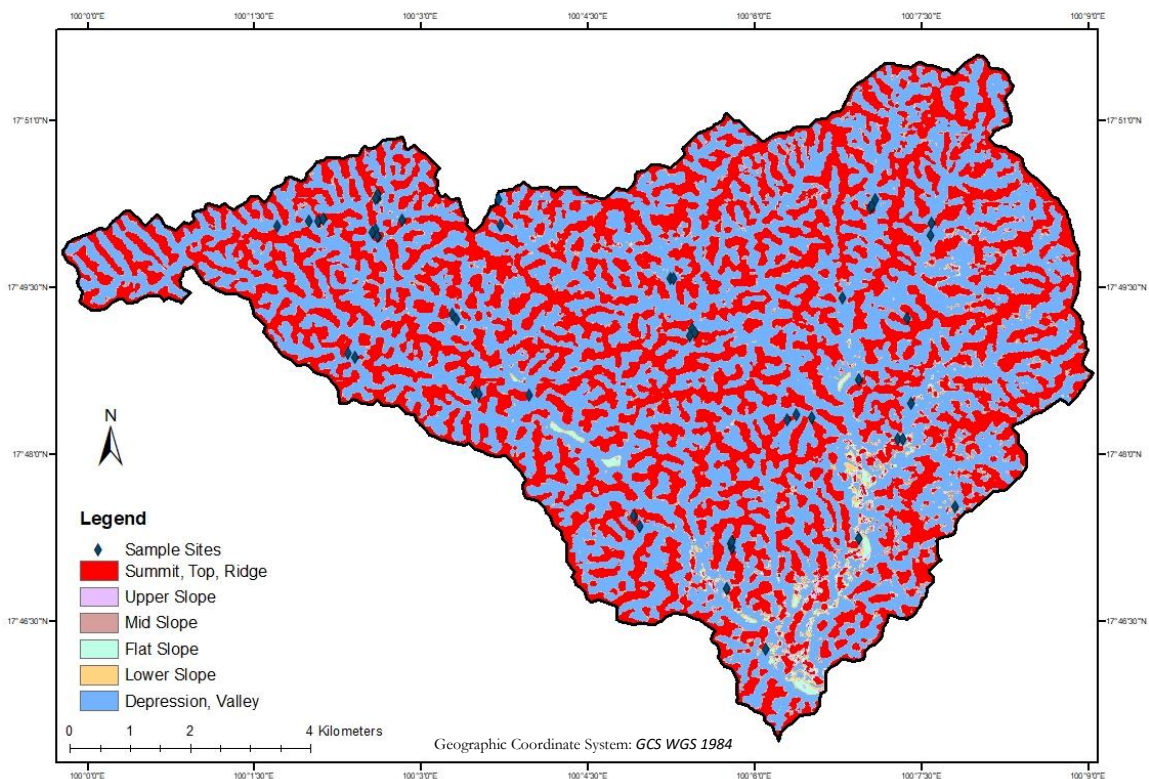
Figure 3-3: TPI slope units

Table 3-5: Accuracy assessment of TPI slope units

		TPI Slope Units					Total	Accuracy (%)
		Summit	Shoulder	Back Slope	Foot Slope	Toe Slope		
Field	**Summit**	4					4	100
	Shoulder	2					2	0
	Back Slope	5		1	3	9	18	6
	Foot Slope		1	1	1	10	13	8
	Toe Slope					11	11	100
	Total	11	1	2	4	30	48	35

4.   Delineation of TPI Landform Units

Figure 3-4 shows a map delineating the watershed into its constituent TPI Landforms. It shows that the landscape was delineated into 10 landform units. Nevertheless, at first glance, with respect to delineating the hillslope according to field observations, the map units seemed meaningless because virtually the entire area was classified into small depressions, larger depressions and culmination area. Small and large depressions may be correlated to Toe Slope, while culmination area does not seem to belong to any of the hillslope units (Table 3-6). By implication, 88% of the sample sites were classified as Toe Slope (small depressions, larger depressions, hollows and flats), while 10.42% was classified as Culmination Area, giving an overall accuracy of 25.58%. However, on closer observation, it was realized that 75% of the Summit and 50% of the Shoulder were classified as Culmination Area. It consequently became apparent that the landform units may be very useful in separating the Summit and Shoulder from other landscape units. Nevertheless, the Culmination Area seemed to be more extensive than the Summit/Shoulder should have been; besides, no site was delineated as Top / Shoulder or Local Elevation in Lowlands.

To explore the possibilities further, the SRTM DEM was resampled from 30m to 5m, to reflect the 5m resolution of the airborne laser-derived 5m DEM used by Deumlich et al. (2010) in the course of assessing the functionality of the algorithm. This finer resolution was able to separate the Top/Shoulder class from the Culmination Area, as the 75% of the Summit that was classified as Culmination Area became classified as a Top/Shoulder surrounded by the Culmination Area (Table 3-7). As such, even though the algorithm was still only able to separate the landscape into upland (culmination area) and lowland areas, it was able to isolate the summit within the culmination area. In addition to that, some Summit and Shoulders were still delineated as part of the Culmination Area.

The ability of the model to isolate the Top/Shoulder from the Culmination Area may be attributed to the interaction of the of the pixel values of the grid cells and the neighbourhood defined by the circle of arbitrary radius. Figure 3-5 shows a schematic DEM with 30m grid cells. These grid cells were subsequently resampled to 5 by 6m grid cells. Given an arbitrary radius of 25m, when the pixel value of the central 30m grid was compared to the average pixel value of the neighbourhood defined by the 25m radius, only one coarse value was generated for the entire grid. On the other hand, when the pixel value of each of the numbered 5 by 6m grid cells is compared with the average pixel values of the same neighbourhood size, the same calculation is repeated 30 times. Based on the impact of the neighbourhood average on each of these fine grid cells, it was able to isolate terrains that the larger grid cells could not isolate. This is in tandem with the assertion of Weiss (2001) and Jenness (2006) that topographic position index is scale-dependent.
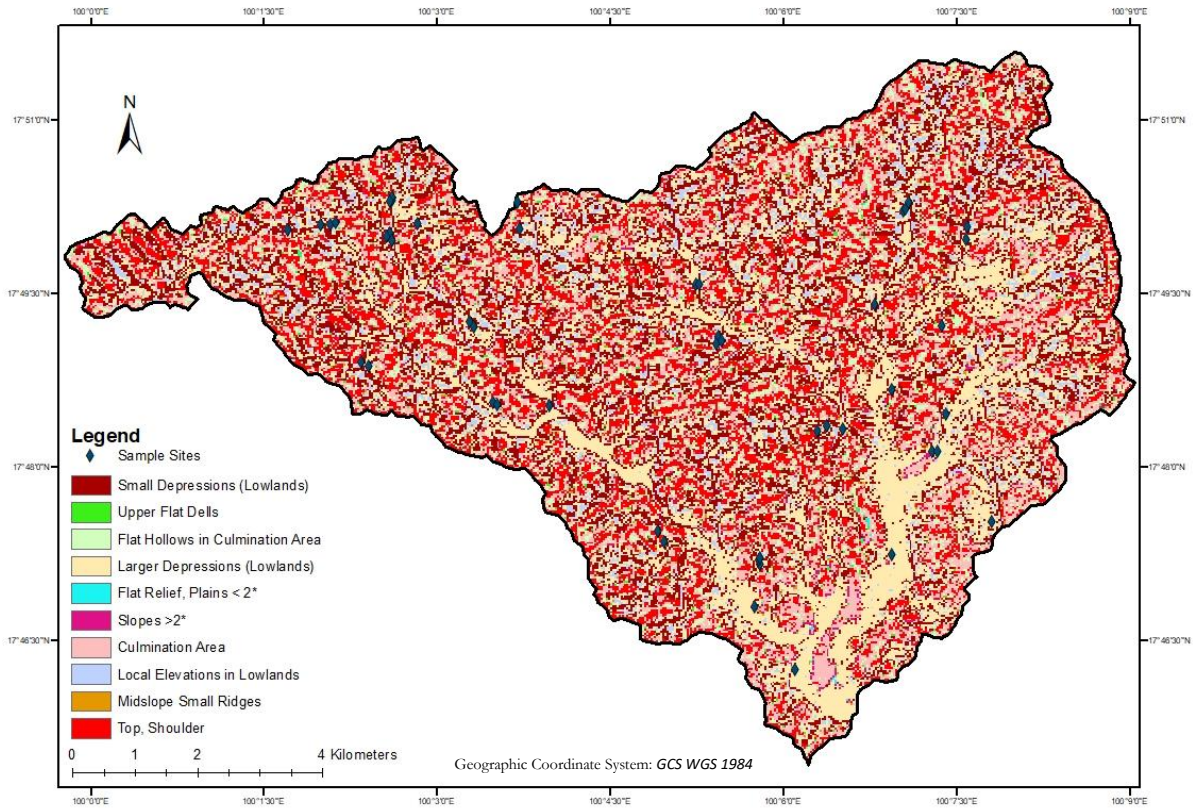
Figure 3-4: TPI landform units

Table 3-6: Accuracy assessment of TPI landform units using a 30m DEM

		TPI Landform (30m DEM)						Accuracy (%)	Cul. Area
		Summit	Shoulder	Back Slope	Foot Slope	Toe Slope	Total		
Field	**Summit**					1	1	0	3
	Shoulder					1	1	0	1
	Back Slope			1		17	18	5.56	1
	Foot Slope					13	13	0	
	Toe Slope					10	10	100	
	Total	0	0	1	0	42	43	25.58	5

Table 3-7: Accuracy assessment of TPI landform units using a 5m DEM

		TPI Landform @ 5m						Accuracy (%)	Cul. Area
		Summit	Shoulder	Back Slope	Foot Slope	Toe Slope	Total		
	Summit	3					3	100	1
	Shoulder					1	1	0	1
Field	**Back Slope**	2				14	16	0	1
	Foot Slope					13	13	0	
	Toe Slope					11	11	100	1
	Total	5	0	0	0	39	44	31.818	
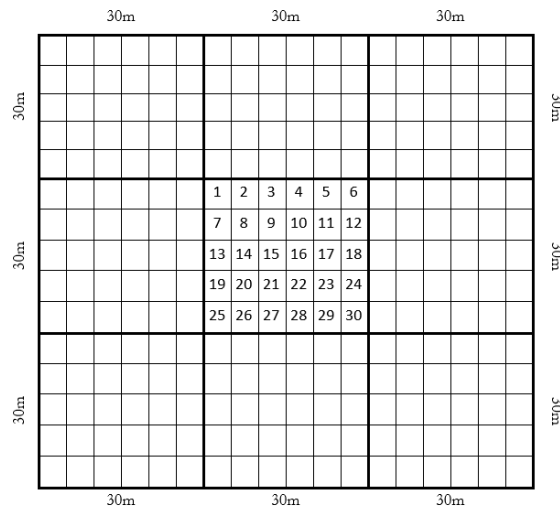
Figure 3-5: Grid cells showing the interactive effects of cell size and arbitrary radius on the generation of the TPI landform

5.   Supervised Hillslope Delineation

Flow accumulation (Figure 3-6a), elevation (Figure 3-6b), profile curvature (Figure 3-6c) and slope (Figure 3-6d) data were generated for each of the sample sites. The data was explored to get an overview of their respective ranges for each hillslope position. Figure 3-6a shows that flow accumulation was generally low for the study area, except for the Toe Slope where it was relatively high, with an outlier as high as 449. The unit originally had outliers as high as 4,548, which were deleted and classified as part of the stream beds. Nevertheless, the Toe Slope still had the highest flow accumulation, ranging from 3.5 to 449. This may be attributed the fact that Toe Slopes are ideally the lowest points on the landscape, relative to other hillslope positions. As such, all the runoff generated in the higher altitudes end up in the Toe Slope. As a consequence, cells with very high flow accumulation are either on the Toe Slope or on the stream beds.

Generally, elevation was least on the Toe Slope, with a median value of 169m, even though the lowest elevation was recorded on the Foot Slope (112m) (Figure 3-6b). This was an expected outcome because the Toe Slopes and the Foot Slopes are adjacent and are located at the bottom of the landscape. The range of elevations did not however seem to show a specific pattern related to hillslope. For instance, the summits, just like other position, can be found on higher as well as lower terrains. More so, the site with the highest elevation was located on the back slope. This was attributed to the heterogeneity of the landscape. If the study area had been located on a single hillslope, then we would have had a sequence of elevations that align with the different positions of the landscape. This was, however, not the case, as we had numerous high and low hillslopes within study area. The median values were, however, higher for the summit and shoulder, decreasing afterwards from the Back Slope through the Foot Slope to the Toe Slope. This is in line with the findings of Miller & Schaetzl (2015), who reported high relative elevation for Summit and Shoulder, medium elevation for Back Slope and low elevation for Foot Slope and Toe Slope.

The Back Slope has the widest range of curvature values, ranging from -1.244 to 1.380 (Figure 3-6c). This implies that the Back Slope has regions that are concave (positive), regions that are convex (negative) and regions that are even (zero). The shoulder and the Summit generally had negative values, implying that they are convex. The Foot Slope and Toe Slope were mostly positive (concave), with median values close to zero (even). On the other hand, Miller & Schaetzl (2015), reported linear profile curvature for Summit, Back Slope and Toe Slope, concave curvature for the Foot Slope and convex curvature for the Shoulder. With regards to the curvature of the Shoulder and the Foot Slope, both studies were in agreement. The marginal disagreement with respect to other hillslope positions may be attributed to the heterogeneity of the Ban Dan Na Kham watershed.

The Back Slope had the steepest slope (27°) and the widest range of slope values (5 – 27°) (Figure 3-6d). On the other hand, the Shoulder has the least median slope values (4°), though the Summit and the Toe Slope values were also low. This was also in line with the findings of Miller & Schaetzl (2015) , who reported that the Back Slope had high slopes, the Summit and Toe Slope had low slopes, while the Shoulder and Foot Slope had medium slopes. The fact that the Shoulder of the study area had relatively low slopes may be attributed to the peculiarities of the terrain as noted during the fieldwork, with particular reference to the relative narrowness of the Shoulder, which made it difficult to separate it from the Summit.
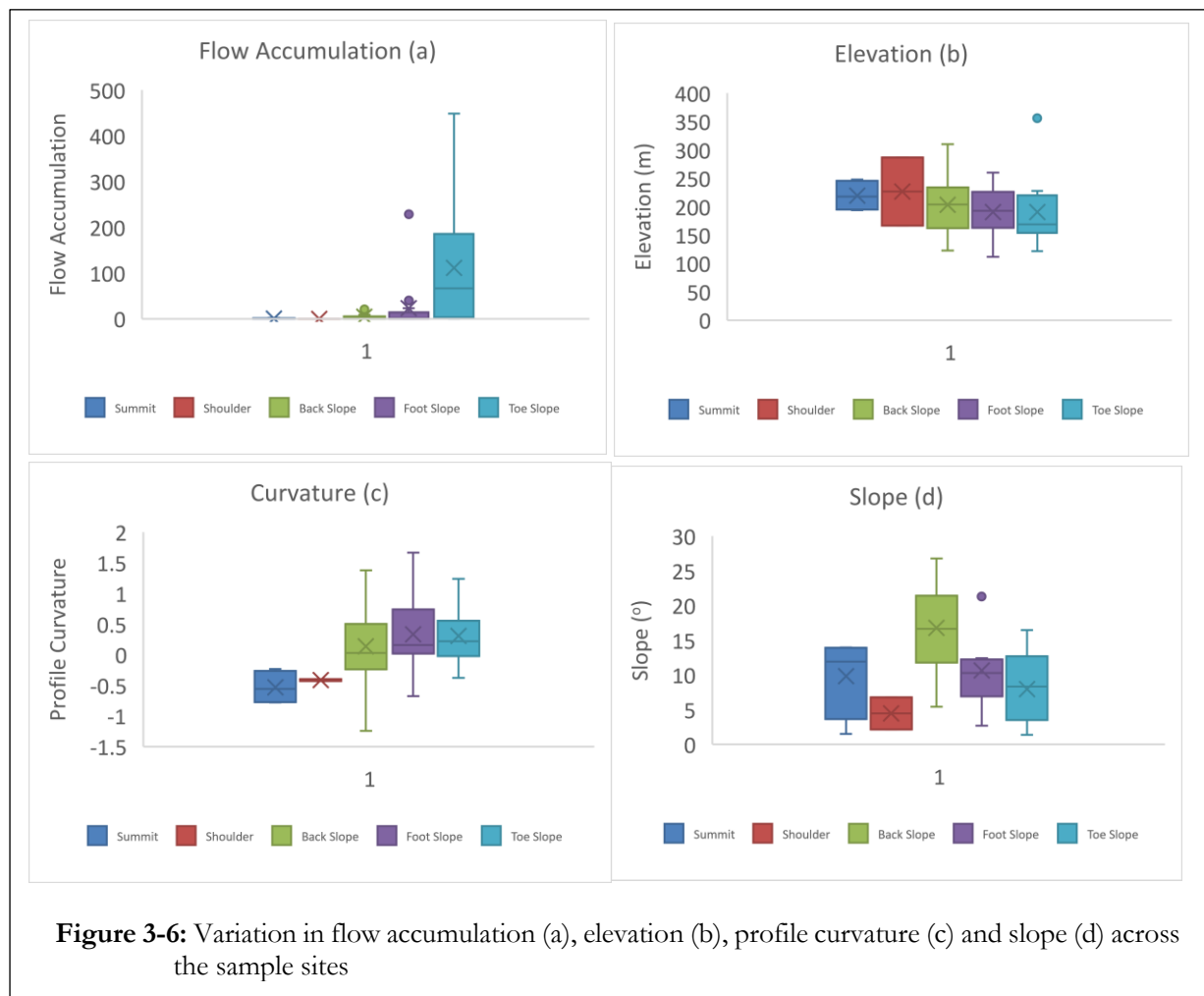
Figure 3-6: Variation in flow accumulation (a), elevation (b), profile curvature (c) and slope (d) across the sample sites

These values were used to generate the decision rules (Table 2-1) which enabled the classification of the Supervised Hillslopes in ArcMap using the vector file generated in eCognition through the segmentation of slope, profile curvature, flow accumulation and elevation raster maps. The constituent units of the generated map are the Back Slope, Foot Slope, High Stream Beds, Low Stream Beds, Shoulder, Streams, Summit and Toe Slope. It is however noteworthy that none of the sampled Shoulder or Summit sites were correctly delineated (Table 3-8). While 50% of the Back Slope, 54% of the Foot Slope and 55% of the Toe Slope were correctly delineated, the overall accuracy was 46%. Furthermore, 38% of the units were placed in positions just adjacent to the appropriate unit, while only about 16% were delineated in units farther away from the appropriate one. The relatively low performance may be attributed to the heterogeneity of the terrain. The placement of 38% in units just adjacent to the appropriate ones is also an indication the model efficiency may be improved greatly with minor adjustments. Collectively, it consequently performed better that the other hillslope classifications with regards to the delineation of the Back Slope, the Foot Slope and the Toe Slope. With regards to the overall accuracy, it had lower accuracy than the digital hillslope position

delineation, which had an accuracy of 52%. It was, however, more robust, as it did not concentrate most of the sampled sites in one hillslope unit.

Table 3-8: Accuracy assessment of supervised hillslope delineation

		Supervised Hillslope						
		Summit	Shoulder	Back Slope	Foot Slope	Toe Slope	Total	Accuracy (%)
Field	Summit			2	2		4	0
	Shoulder			1	1		2	0
	Back Slope		1	9	8		18	50
	Foot Slope			5	7	1	13	54
	Toe Slope			3	2	6	11	55
	Total	0	1	19	20	6	48	46

6.   Final Hillslope Units

None of the implemented hillslope classification systems was able to effectively delineate all hillslope units. Some, like the TPI Landform were good for the delineation of the summit / shoulder, the upland areas (culmination area) and the lowland areas, while others, like the supervised classification system, were better for the delineation of the back slope, the foot slope and the toe slope. Consequently, to arrive at the final soil units, these two methods were combined.

Figure 3-7 shows a map generated from the combination of the Supervised Hillslope and the TPI Landform Classes. The Top / Shoulder of the TPI landforms was adopted, while all other units of the Supervised Hillslope were retained. Furthermore, the Low Stream Beds were merged with the Streams, while the High Stream Beds were merged with the Toe Slope. The final map has five units, viz. Back Slope, Foot Slope, Streams, Summit/Shoulder and Valley Floor.
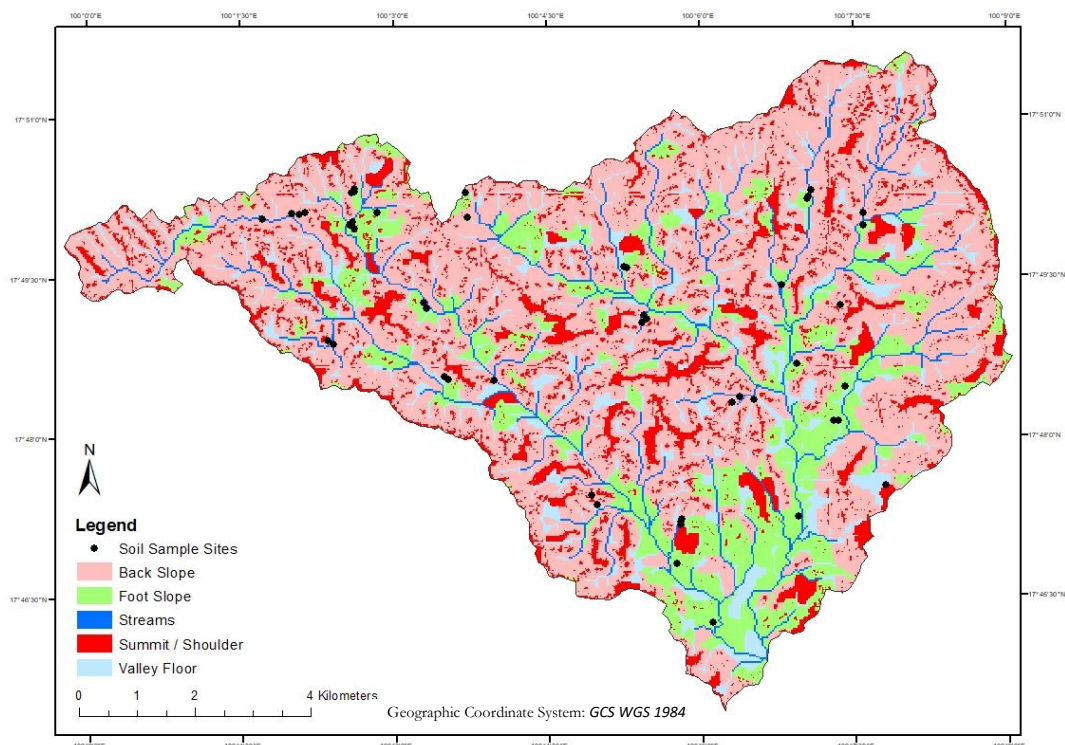
Figure 3-7: Geomorphic map units for characterizing soil variation across the watershed

3.1.3. Assessment of the Soil Variation Across the Landscape

The field-generated soil data are presented in tables and graphs in this section. Appendix 3-1 shows the morphologic properties of the sample sites while Appendix 3-2 shows the physicochemical properties. Figure 3-8a to Figure 3-8f and Figure 3-9a to Figure 3-9d depict the minimum, median, maximum, range and mean of different physicochemical soil properties in the different hillslope positions of the study area. Figure 3-10a to Figure 3-10f and Figure 3-11a to Figure 3-11d depict the minimum, median, maximum, range and mean of the different physicochemical properties of the soils underlying the sampled land cover types in the study area.

A. Variability of Soil Physicochemical Properties Across the Hillslope Positions

A wide range of variability of sand content was recorded on all the hillslope positions (Figure 3-8a). Except for the Summit/Shoulder, which had the lowest mean (29%) and median values (22%), all the other hillslope positions had similar mean sand content, ranging from 34 to 36%. The lower sand content on the Summit/Shoulder may be attributed to the relatively lower flow accumulation (Figure 3-6a) and slope (Figure 3-6d), which ensured that the less of the finer materials (clay and silt), were eroded and lost. This is in line with the findings of Oku et al. (2010), who reported lower sand content for the Summit of humid tropical forest soils. Overall, the value was similar to the 38% sand content reported by Herrmann et al. (2007) for the soils of Northern Thailand.

Similarly, the mean silt content for the Back Slope, the Foot Slope and the Valley Floor were similar, ranging from 41 to 43%, and lowest on the Summit/Shoulder (38%) (Figure 3-8b). Silt was however higher than the 31 % silt content reported by Herrmann et al. (2007) for the soils of Northern Thailand. This may be attributed to a possible difference in the underlying geologic formations of the two study areas.

Clay content was distinctly higher on the Summit/Shoulder (33%), and least in the Foot Slope (20%) (Figure 3-8c). This is also in line with the findings of Oku et al. (2010) for humid tropical forest soils. This may be attributed to the relatively lower flow accumulation (Figure 3-6a) and slope (Figure 3-6d) in the Summit/Shoulder, coupled with the fact that clay tends to stick together and has relatively greater resistance to detachment than the other particle size fractions.

Bulk density was least on the Summit/Shoulder (1.08 Mg/m³), progressively increasing from the Summit/Shoulder to the Valley Floor (1.31 Mg/m³), where it was highest (Figure 3-8d). This may be attributed to the impact of different land use types, as much of the Summit/Shoulder are either natural forest or plantations. The reduced human activities result in reduced compaction, which in turns, results in reduced bulk density. On the other hand, the valley floor, which had the highest bulk density of 1.31 Mg/m³, was dedicated almost exclusively to arable crops. These agricultural and other anthropogenic activities result in increased soil bulk density. This is in line with the contention of Kodiwo et al. (2014) that increased intensity of agricultural activities results in increased soil compaction, which in turns results in increased bulk density.

Conversely, soil porosity was highest on the Summit/Shoulder (59%), and least on the Valley Floor (51%) (Figure 3-9a). Naturally, it may have been expected that since the Summit/Shoulder had more clay, it should be less porous than the other hillslope positions with lower clay. However, the effect of human activities on bulk density also translates into the reduced porosity of the arable soils on the Valley Floor. This is in line with the contention of Balan et al. (2009) that a negative correlation exists between bulk density and soil porosity. Similarly, Pagliai & Vignozzi (2006) reported that soil porosity decreases with increase in soil compaction.

The widest range of shear strength was recorded on the Summit/Shoulder (2.43 to 6.05 kPa), which also, incidentally, had the lowest median values of 4.70 kPa (Figure 3-9b). The average shear strength was least

on the Summit/Shoulder (4.48 kPa) and the Valley Floor (4.44 kPa), while the highest mean value was recorded on the Back Slope (5.09 kPa). The low shear strength of the Valley Floor may be attributed to the effect of tillage activities in the agricultural fields, which break up the soil structure, reducing their resistance to rupture. On the other hand, the lower shear strength of the Summit/Shoulder may be attributed to the effects of large trees roots moving through the soil and the activities of a diverse range of soil macro fauna. In line with this, Whitford & Eldridge (2013) contended that the activities of termites, like many other macrofauna, affect the bulk density, porosity, aeration, infiltration, water holding capacity, turnover and homogenization dynamics of tropical soils. This complex interaction may account for the reduced compaction and shear strength of forest soils.

Figure 3-8: Spatial variability of sand (a), silt (b), clay (c) and bulk density (d) across the study area
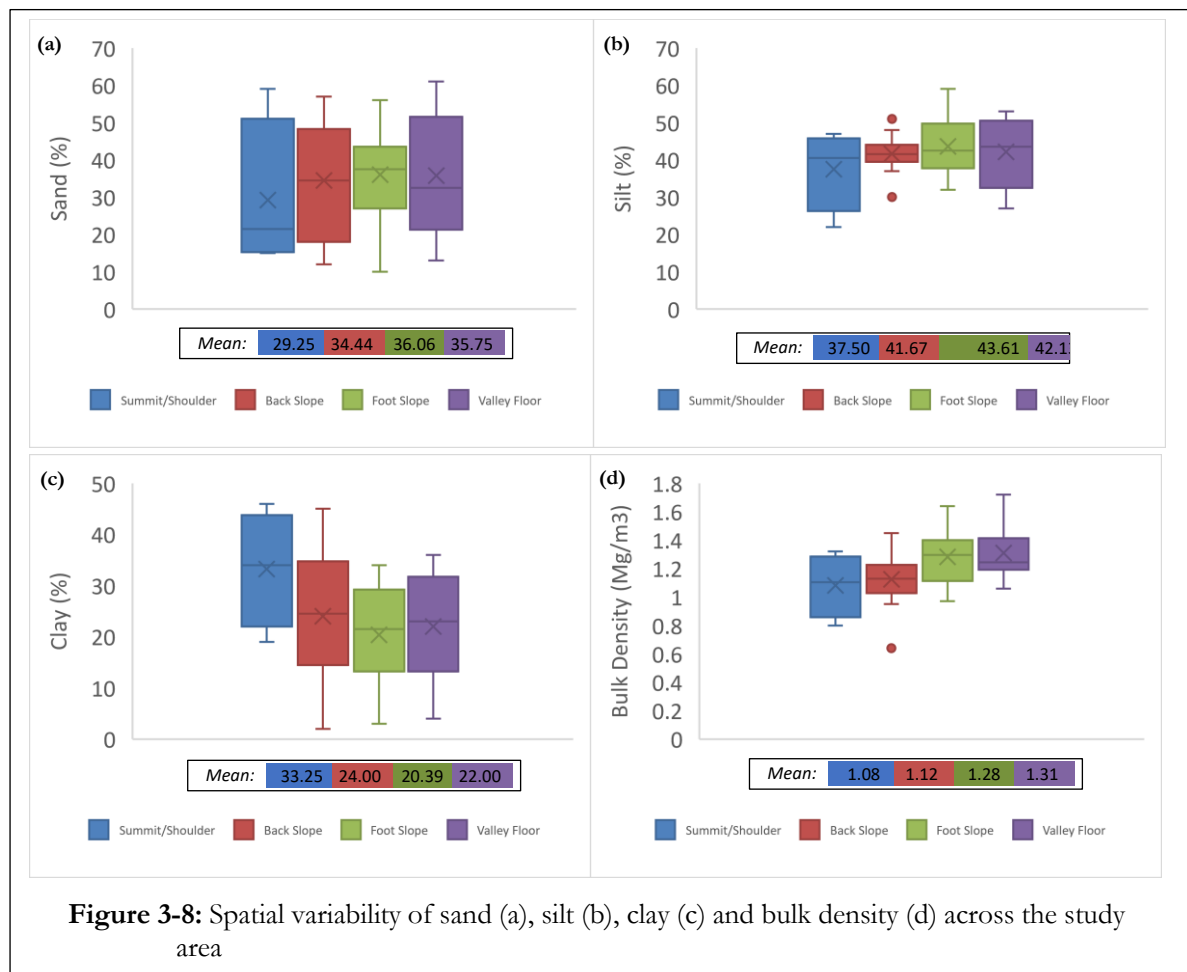
The soil unit with the highest range and extent of saturated hydraulic conductivity (12.15 to 98.43 mm/hr) was located on the Foot Slope (Figure 3-9c). The least mean saturated hydraulic conductivity of 11.15 mm/hr was recorded on the Summit/Shoulder, which incidentally, also has the highest clay content (Figure 3-8c). The fact that saturated hydraulic conductivity of the Summit/Shoulder was distinctly different may be attributed to the fact that its texture was also distinctly different (Figure 3-8a, b, c). This is in line with the findings of Sarki et al. (2014) that, relative to other textural classes, soils with high clay content have very low saturated hydraulic conductivity.

Moisture content at field capacity (Figure 3-9e) and wilting point (Figure 3-9f) were higher on the Summit/Shoulder (35% and 21% respectively), generally decreasing down the slope. This is also attributable to the soil texture, as clayey tends to have higher moisture holding capacity than sandy soils. It may consequently be concluded that the Summit/Shoulder had higher moisture content at field capacity and

wilting point because it had higher clay content. This agrees with the findings of Easton & Bock (2016) that clayey soils have higher water content at field capacity and wilting point than other soil textural classes.

Soil organic matter was highest on the Back Slope (5.13%) and least on the Valley Floor (3.63%) (Figure 3-9d). The low organic matter on the Valley Floor is attributable to its predominantly arable land use. This is in line with the contention of Haynes et al. (2003) that agricultural activities tend to reduce soil organic matter and microbial biomass. The dominant vegetation on other hillslope positions are trees, which, according to Munoz et al. (2007), improves soil organic matter content.
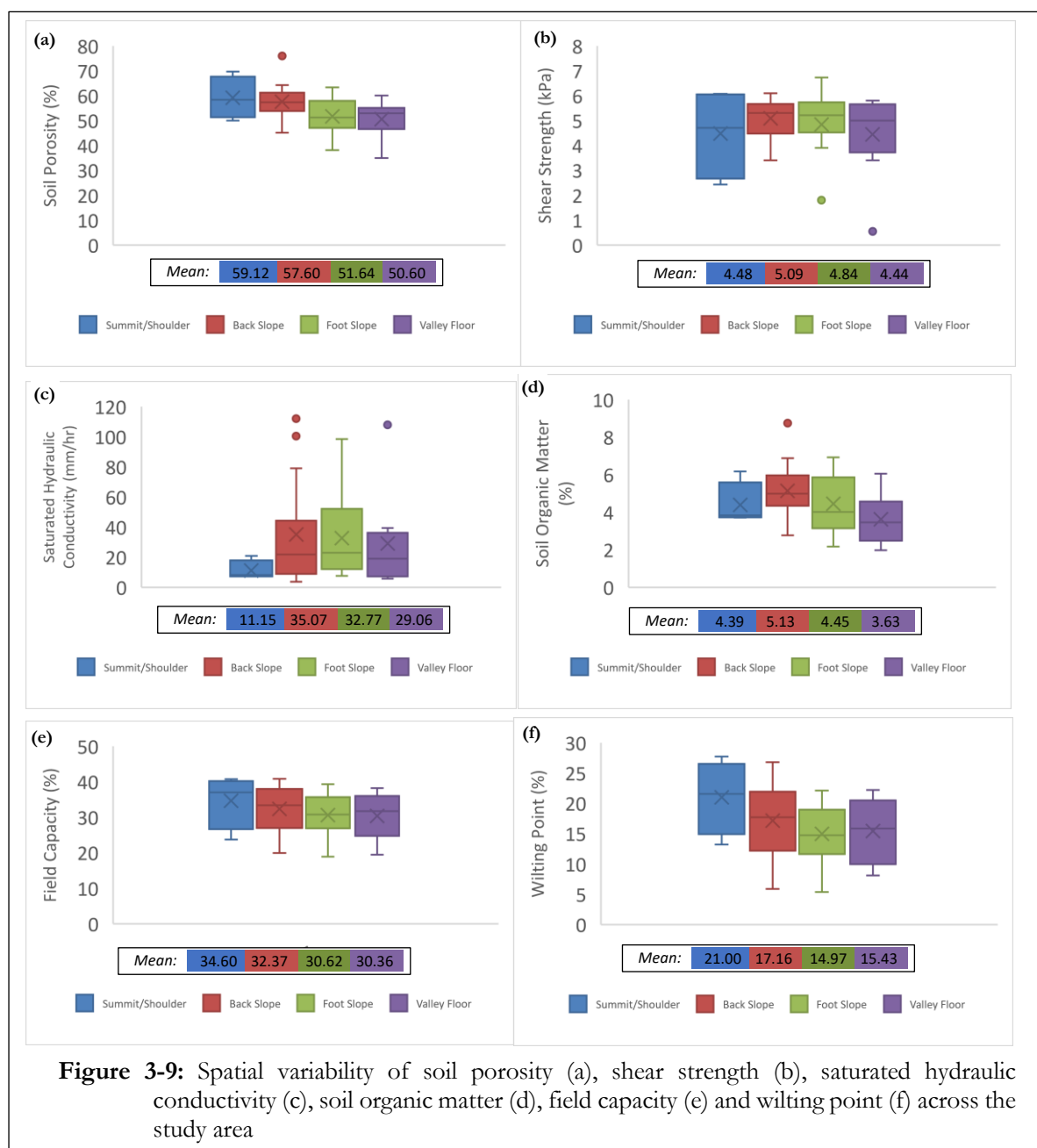
Figure 3-9: Spatial variability of soil porosity (a), shear strength (b), saturated hydraulic conductivity (c), soil organic matter (d), field capacity (e) and wilting point (f) across the study area

B.   Variability of Soil Properties Underlying Different Land Cover Types

The widest range of organic matter was recorded in the orchards (2.18 to 8.75%), the highest mean value (5.57%) in the fallow lands and the least values (2.52%) in the arable lands (Figure 3-10a). The low organic matter on arable land is attributable to the removal of the crops and crop residues for consumption and

industrial purposes. This is in direct contrast to forests, plantations, orchards and fallow lands where the plants remain in the field for prolonged periods of time; and even when they die or drop their leaves, these plant remains decay on the same land and get converted into soil organic matter. As such, Haynes et al. (2003) asserted that agricultural activities reduce soil organic matter and microbial biomass.

Sand content had the highest range of variability (9.58 to 55.4%) in the long kong orchards (Figure 3-10b). The mean values were, however, highest in the teak plantations (52%) and lowest in the forests (25%). Silt content was least on arable lands (35%) and highest in the long kong orchards (45%) (Figure 3-10c). Clay content was most variable in the long kong orchard (5 to 45%), least mean value was recorded in teak plantations (8%) and highest in forested lands (32%) (Figure 3-10d). Nevertheless, the land use does not play a prominent role in determining the soil texture. On the contrary, the soil texture determines the land use type adopted. Lowland rice fields, for instance, would not be located on sandy soils if clayey soils are available in adequate amount. Nonetheless, on the long run, the land use may come to affect the soil texture as certain land uses, like arable land use on steep slopes, may predispose the soil to erosion, and the eventual loss of much of the silt content of such soils.

Bulk density was highest on arable lands (1.54 Mg/m³) and least on forested (1.08 Mg/m³) and fallow lands (1.07 Mg/m³) (Figure 3-10e). This is due to human activities or its absence. As Haynes et al. (2003) pointed out, agricultural activities tend to reduce soil organic matter and microbial biomass. The activities of soil micro and macro fauna, including the pores they create when they bore through the soil and the consumption and defecation of soil and organic materials increases soil porosity, which in turns reduces bulk density. Similarly, the continued addition of organic matter to the soil also reduces soil bulk density (Sakİn, 2012). These factors account for the lower bulk density on forested and fallow lands and the increased bulk density on arable lands. Furthermore, Hakansson (2005) asserted that increased use of agricultural machineries results in increased soil compaction, which in turns, results in increased bulk density.

Shear strength was lowest on arable lands (2.26 kPa) and highest in long kong orchards (5.22 kPa) (Figure 3-10f). This is also attributable to the impact of tillage activity on soil structure. Tillage tends to break up the soil structure, consequently decreasing their resistance to rupture, which in turns leads to decreased shear strength. On the other hand, the soils of the long kong orchards had higher shear strength because in addition to not being tilled, the persistent movement of humans through the orchard results in increased compaction and greater shear strength. Similarly, Genet et al. (2008) asserted that trees increase shear strength through their root system, but Genet et al. (2006), contended that due to their higher root area ratio, the impacts of young trees is greater than that of older trees. This was reiterated by Genet et al. (2008), Genet et al. (2010) and Fattet et al. (2011), who contended that root biomass density was lower in old natural forests, which may account for relatively lower impacts on increased shear strength. This may explain why the soils of long kong orchards, which are relatively younger trees than natural forests and teak plantations, had higher shear strength.

Soil porosity was highest on fallow lands (60%) and forests (59%) and least on arable lands (42%) (Figure 3-11a). This may be attributed to increased organic matter and activities of soil flora and fauna in the forested and fallow lands. Saturated hydraulic conductivity was most variable on teak plantations (26.20 to 112.08 mm/hr) and fallow lands (26.38 to 103.55 mm/hr) (Figure 3-11d). The mean value was lowest on forested soils (12.23 mm/hr) and arable lands (16.42 mm/hr). The low saturated hydraulic conductivity on forested soils may be attributed to its predominantly clayey texture, while that of arable lands may be attributed to soil compaction by tillage operations, machineries and other anthropogenic activities. The highest average saturated hydraulic conductivity of 84 mm/hr was recorded in the soils underlying the teak plantations. This high conductivity may be attributed to its very low clay content of 8% (Figure 3-11d).

Moisture content at field capacity (Figure 3-11b) and wilting point (Figure 3-11c) were highest on forested lands (36% and 21% respectively) and least on teak plantations (22% and 8% respectively). The higher field capacity and wilting point in the forest soils may be attributed to its high clay content of up to 32% (Figure 3-11d). Furthermore, the constituent flora and fauna and the organic matter generated also play a crucial role. Bhadha et al. (2017) reported that increased soil organic matter results in increased soil water holding capacity. The forests have a dense undergrowth of grasses, shrubs, ferns and herbs, all of which support a diverse variety of soil fauna, resulting in increased soil organic matter. On the other hand, the teak plantations were usually almost bare, with relatively few dead leaves to be decomposed and converted into organic matter. Consequently, the organic matter dynamics in both soils account for some of the variation in soil water content at field capacity and wilting point.
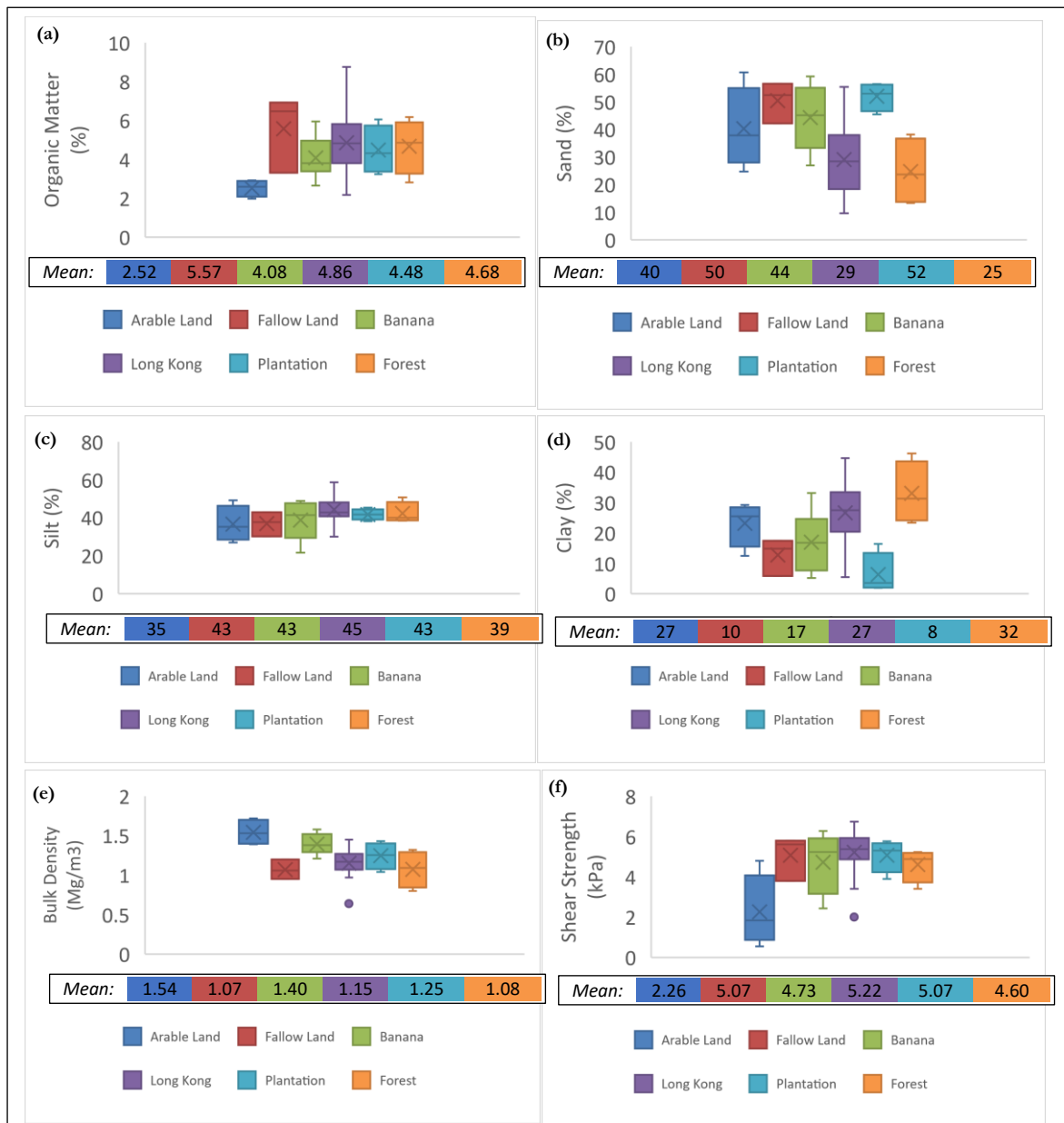
Figure 3-10: Spatial variability of organic matter (a), sand (b), silt (c), clay (d), bulk density (e) and shear strength (f) in the soils underlying the various land cover types of the study area

Figure 3-11: Spatial variability of soil porosity (a), field capacity (b), wilting point (c) and saturated hydraulic conductivity (d) in the soils underlying the various land cover types of the study area
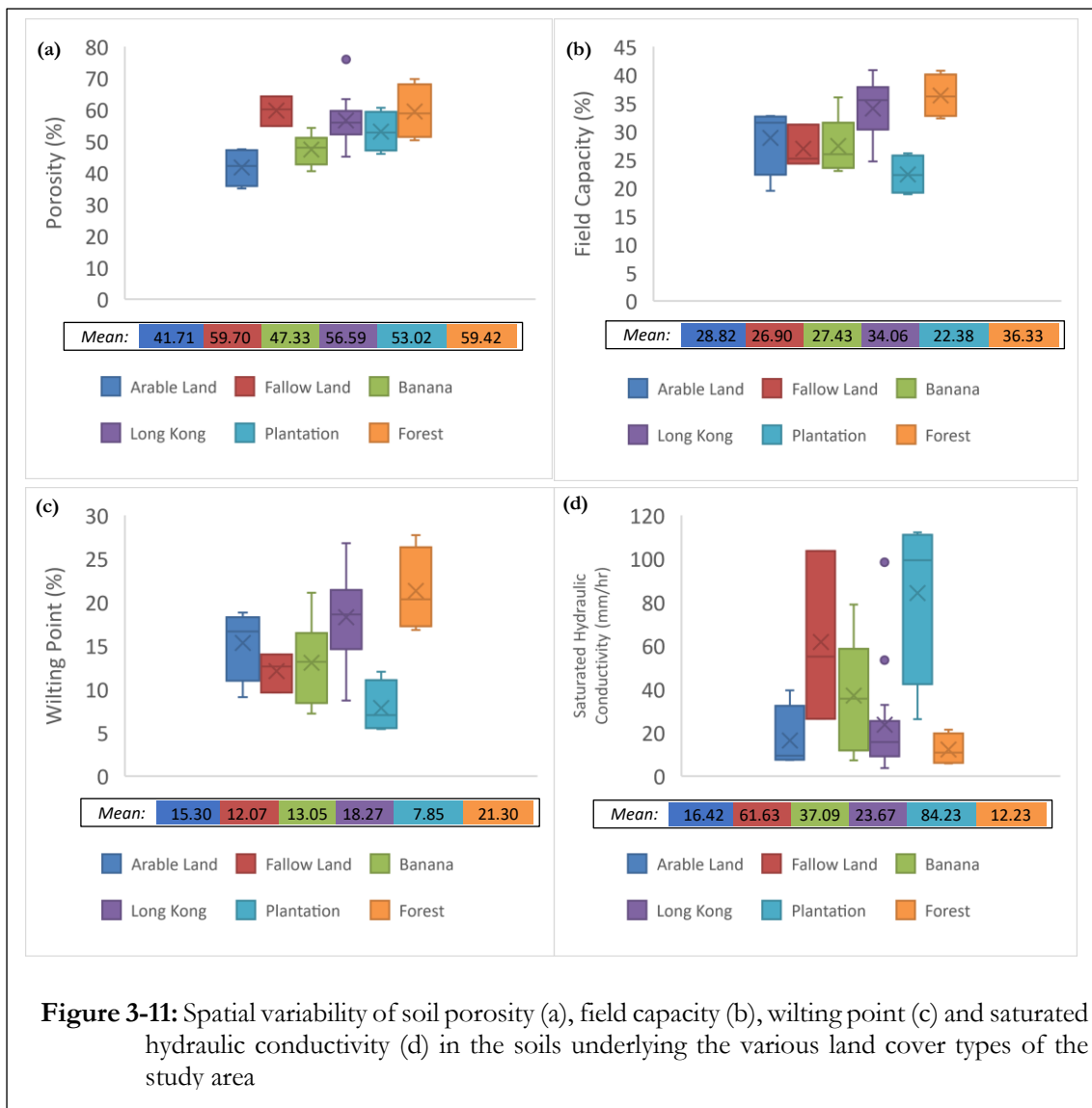
3.1.4. Comparative Analysis of Field and SoilGrids250m Data

SoilGrids250m and Field-based data were assessed to determine the degree of similarity of the two data sources. Owing to the perception that parcel-based averages for both data sources might be similar even when point-based data are not similar, point-based and parcel-based assessments were both conducted. The results are presented in tables and charts.

A. Point-based Assessment of the Different Soil Datasets

Figure 3-12a to Figure 3-12e depict box plots of point-based field and SoilGrids250m data. The figures show that the field-based data consistently has a greater degree of variability than the SoilGrids250m data. This gives the impression that both data sources are quite distinct from each other. Organic matter seemed to be the only soil property for which both data sources have a similar range; but even then, the SoilGrids250m data had relatively higher values. This perceived difference is attributable to the nature of the two data sources. Field measurements would expectedly have higher variability, as soils tend to differ from place to place. This is in line with the contention of Illinois Soil Classifiers Association (2010), who

asserted that soils can vary greatly within a very short distance. On the other hand, models are a simplification of reality; and simplicity comes at a cost.

The Euclidean distance between the data sources and other statistics are shown in Table 3-9. The Euclidean distance between the two datasets is 167.35 while the normalized Euclidean distance is 0.17. The closer the Euclidean distance is to zero, the more similar the data sources are considered to be. The very low normalized Euclidean distance, which is closer to 0 than it is to 1, indicates that the two datasets are not very different. Nevertheless, statistical tests were conducted to determine whether there is a statistically significant difference between both datasets.

A skewness and kurtosis z-value (at P>0.05) generally within the range of -1.96 and +1.96 and a Shapiro-Wilk P-Value consistently greater than 0.05 (Table 3-9), indicated that both the SoilGrids250m data and the Field-based data are approximately normally distributed. Nevertheless, a Levene's Test P-value generally less than 0.05 indicated that the variance was not homogenous for both datasets. As such, T-Test could not be used to compare the means, in order to determine the degree of similarity between the two data sources. In its stead, Wilcoxon Signed Rank Test was conducted.

Table 3-9 show that only clay had a P-Value greater than 0.05, meaning that in terms of clay the two soil datasets were not significantly different. This implies that for management or modelling purposes that require detailed on-site data, SoilGrids250m may not be a very reliable alternative for the study area. On the other hand, if the assessment is hinged more on the clay content of the soil, then SoilGrids250m is an acceptable alternative to field-based data.

Finally, an assessment of the scatter plots of the two datasets shows that they are not significantly correlated. One dataset can consequently not be used to predict the other.

Table 3-9: Point-based comparative statistics of the soil datasets

	Parameter	Mean	Skew	Std. Error	Skew Z-Value	Kurt.	Std. Error	Kurt. Z-Value	Shapiro-Wilk P-Value	Levene Test P-Value	Euclid. Dist.	Norm. Euclid. Dist.	Wilkoxon Signed Rank Test P-Value
SoilGrids-250m	Sand	41.06	0.277	0.343	0.808	0.076	0.674	0.113	0.075	0.000	167.35	0.17	0.012
	Silt	32.56	-0.473	0.343	-1.379	-0.515	0.674	-0.764	0.004	0.000			0.000
	Clay	26.21	0.2	0.343	0.583	-0.274	0.674	-0.407	0.24	0.000			0.119
	Bulk Density	1.30	-0.001	0.343	-0.003	0.642	0.674	0.953	0.889	0.000			0.003
	Organic Matter	5.86	0.019	0.343	0.055	-1.049	0.674	-1.556	0.022	0.010			0.000
Field-based Data	Sand	34.78	0.049	0.343	0.143	-1.088	0.674	-1.614	0.084				
	Silt	42.11	-0.327	0.343	-0.953	0.805	0.674	1.194	0.367				
	Clay	23.12	-0.05	0.343	-0.146	-0.662	0.674	-0.982	0.536				
	Bulk Density	1.21	0.002	0.343	0.006	0.892	0.674	1.323	0.742				
	Organic Matter	4.56	0.408	0.343	1.190	-0.133	0.674	-0.197	0.331				

NOTE: Skew = Skewness, Std. Error = Standard Error, Kurt. = Kurtosis, Norm. Euclid. Dist. = Normalized Euclidean Distance

Figure 3-12: Comparative point-based assessment of sand (a), silt (b), clay (c), bulk density (d) and organic matter (e) from field-based and SoilGrids250m data
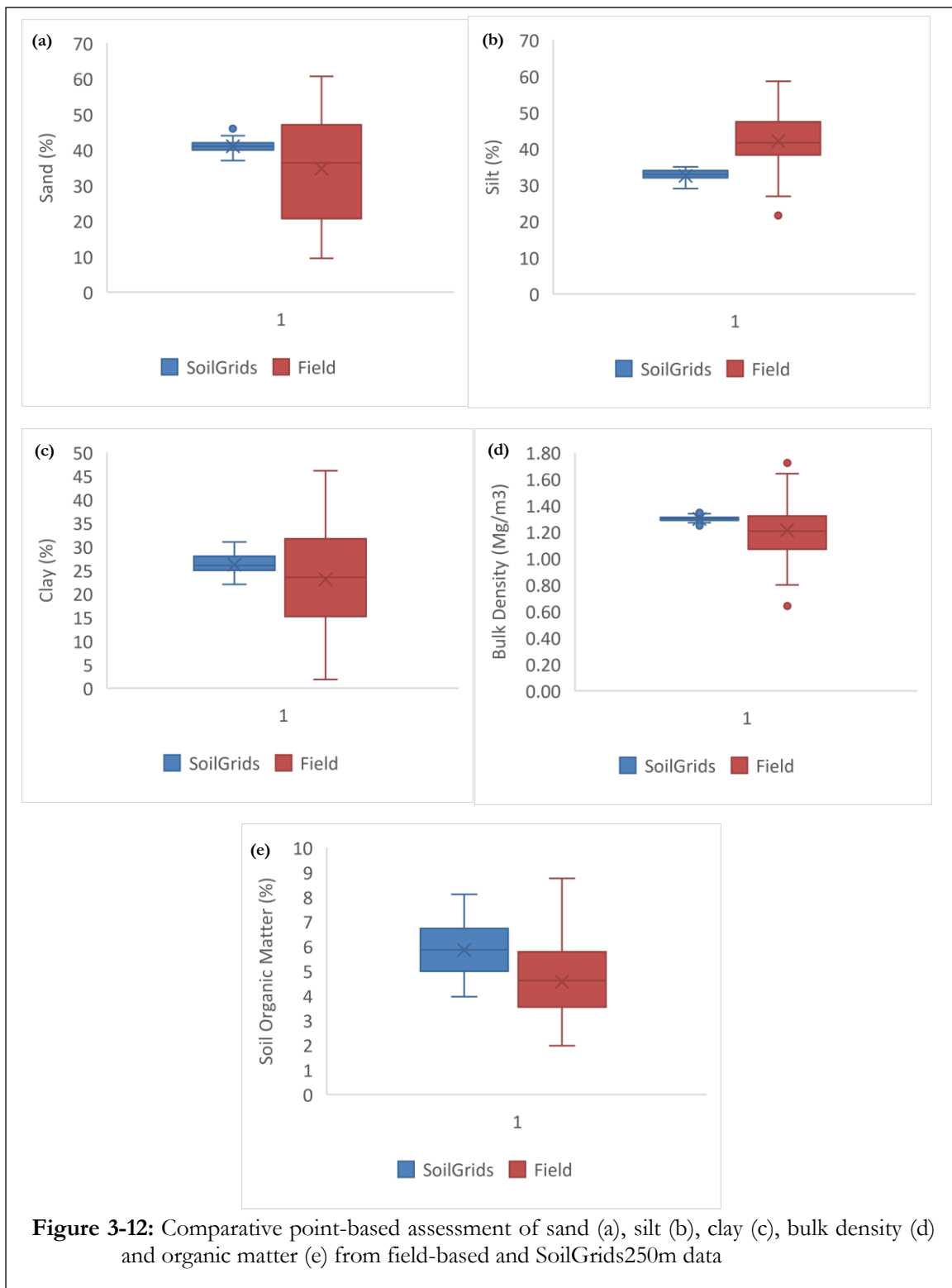
B. Parcel-based Assessment of the Different Soil Datasets

Figure 3-13a to Figure 3-13e depicts box plots of parcel-based field and SoilGrids250m data. The average soil unit data were compared with the average SoilGrid250m data that corresponds to the same area. The results show that the field-based data still consistently had a greater degree of variability. Also, the SoilGrids250m data tended to have higher values, with the exception of silt content, which was somewhat higher for the field-based data (Figure 3-13b).

The Euclidean distance between the data sources and other statistics are shown in Table 3-10. The Euclidean distance between the two datasets was 26.25 while the normalized Euclidean distance was 0.19. Even though the Euclidean distance is much lower that the value (167.35) recorded during the point-based assessment, the normalized Euclidean distance was still very close to the value (0.17) reported for point-based assessment. This may be attributed to the fact that irrespective of the fact that the number of values being compared are different, the datasets are still the same. The very low normalized Euclidean distance, corroborates the results from the point-based assessment, indicating that the datasets may be similar.

To determine whether the difference was statistically significant, a test of normality and homogeneity of variance was first conducted to determine which statistical method was appropriate for the available data. The skewness z-value and the kurtosis z-value (between -1.96 and +1.96) and Shapiro-Wilk P-value (> 0.05), all indicate that both datasets are approximately normal. The Levene Test results show that only silt and organic matter had approximately homogenous variance at P>0.05, but at P>0.01, all of them, with the exception of bulk density, recorded approximate homogeneity of variance. Because the number of parcels (hillslope units) were equal to 4, which is less than the minimum of 6 samples recommended by Dytham (2011) as a pre-condition for performing the Wilcoxon Signed Rank Test, the T-Test was calculated at 0.01 level of significance.

T-Test P-values of 0.624 and 0.189, for clay and bulk density respectively, indicate that these parameters were not significantly different for both data sources at P>0.05. Similarly, a P-value of between 0.011 and 0.019 indicate that sand and organic matter are not significantly different for both data sources at P>0.01. Silt, with a P-value of 0.008, was however, significantly different at both levels of significance.

This implies that, though the SoilGrids250m and the field-based data were significantly different when compared point by point, they are quite similar when the average values of an area are compared. Consequently, when detailed on-site data are not required to effectively implement a project or inform a decision-making process, SoilGrids250m is a good alternative to field-based soil data. In such a situation, the use of SoilGrids250m data will save a lot of time, money and energy.

Table 3-10: Parcel-based comparative statistics of the soil datasets

	Parameter	Mean	Skew	Std. Error	Skew Z-Value	Kurt.	Std. Error	Kurt. Z-Value	Shapiro-Wilk P-Value	Levene Test P-Value	Euclid. Dist.	Norm. Euclid. Dist.	T-Test P-Value
SoilGrids-250m	Sand	41.02	-1.298	1.014	-1.28	1.098	2.619	0.419	0.338	0.032	26.25	0.19	0.019
	Silt	32.46	-0.106	1.014	-0.11	1.277	2.619	0.488	0.887	0.072			0.008
	Clay	26.52	1.119	1.014	1.10	0.927	2.619	0.354	0.076	0.036			0.624
	Bulk Density	1.29	0.383	1.014	0.38	-2.918	2.619	-1.114	0.624	0.000			0.189
	Organic Matter	6.10	-1.095	1.014	-1.08	-0.036	2.619	-0.014	0.296	0.736			0.011
Field-based Data	Sand	33.82	-1.952	1.014	-1.93	3.853	2.619	1.471	0.016				
	Silt	41.23	-1.09	1.014	-1.08	1.941	2.619	0.741	0.601				
	Clay	24.95	1.827	1.014	1.80	3.438	2.619	1.313	0.594				
	Bulk Density	1.20	-0.093	1.014	-0.09	-5.206	2.619	-1.988	0.226				
	Organic Matter	4.39	-0.193	1.014	-0.19	1.491	2.619	0.569	0.759				

NOTE: Skew = Skewness, Std. Error = Standard Error, Kurt. = Kurtosis, Norm. Euclid. Dist. = Normalized Euclidean Distance

Figure 3-13: Comparative parcel-based assessment of sand (a), silt (b), clay (c), bulk density (d) and organic matter (e) from field-based and SoilGrids250m data
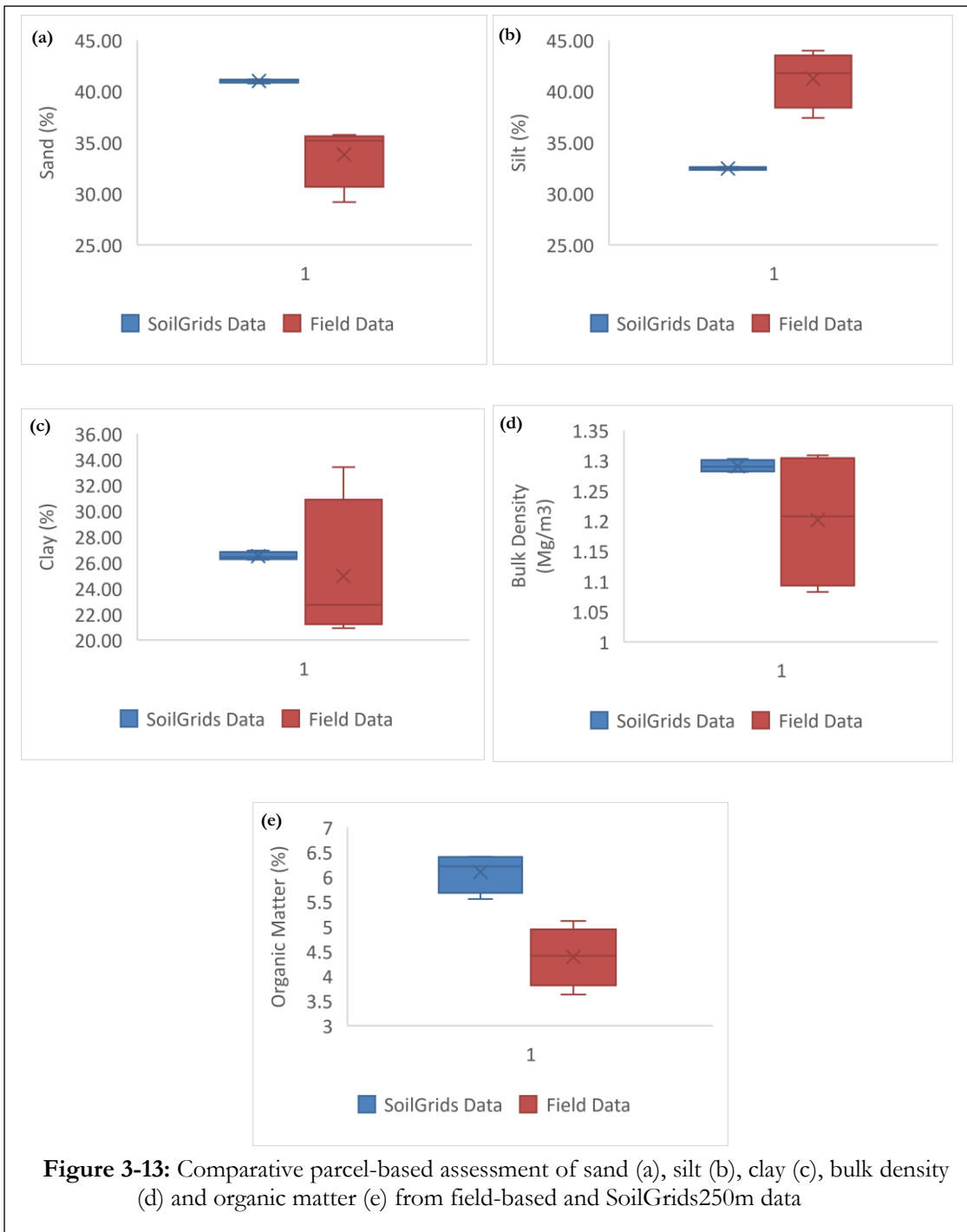
3.2. Land Use / Land Cover Map

The land use map of the watershed is shown in Figure 3-14. The dominant land uses in the area are arable farming, orchards – mostly long kong orchard – teak plantations, natural forests and built-up areas. The accuracy assessment report and confusion matrix for the land use classification is shown in Table 3-11. The overall accuracy of the land use map is 68%. Natural Forest had a low accuracy of 43% and was mostly misclassified as Teak Forest or Orchards. This is similar to the findings of Gebhardt et al. (2015), who reported an accuracy of 50% for secondary forest because it was usually confused with primary forests. These can be attributed to the fact that all the afore-mentioned land cover types are populated by trees. The similarity of the two land cover classes is evident in Table 3-13. The canopy cover (92 – 95 %), the plant

height (19 – 20m), leaf area index (6 – 7 m²/m²)) and the Et/Eo (0.90 – 0.95), all had similar values. They may consequently have similar pixel values.

Furthermore, the relatively low producer accuracy recorded for built-up areas (53%) may be attributed to the misclassification of built-up areas as arable land. Ideally, it is expected that arable land and built-up areas would have very distinct pixel values. Nevertheless, the watershed is located in a rural setting where a building might be surrounded by farms, orchards or trees. As such, the building may be located in a pixel dominated by arable land, resulting in its classification as an arable land. However, with respect to erosion assessment for the watershed, most of the arable lands and built-up areas are located in relatively flat, low-lying areas that are less prone to erosion. The misclassification may consequently not have a major effect on the model-generated erosion prediction.

Forest, arable land and teak had the lowest kappa coefficient of 0.40, 0.53 and 0.56 respectively, whereas, Built-up recorded the highest coefficient of 1.0. This means that the probability that all the areas classified as Built-up were built-up is very high. The overall kappa coefficient was 0.60. Due to the overlap between Teak and Forest, both classes were merged. Table 3-12 shows that this increased the overall accuracy to 79% and the overall kappa coefficient to 0.70. Nevertheless, even though merging Teak and Forest increased the accuracy of the classification, the original map with 68% accuracy was retained and used in the RMMF modelling process. This was because the Teak and the forest had distinct features, with particular reference to surface cover, which play crucial roles in determining the erosion rates within the watershed.

Finally, the ratio of actual to potential evapotranspiration (Et/Eo), canopy cover (CC), crop management factor (C), effective hydrological depth (EHD), surface cover (SC), plant height (PH), crop coefficient (Kc), leaf area index (LAI), maximum plant canopy storage (Smax) and proportion of rainfall intercepted by vegetation (A) were generated for each land cover type (Table 3-13).
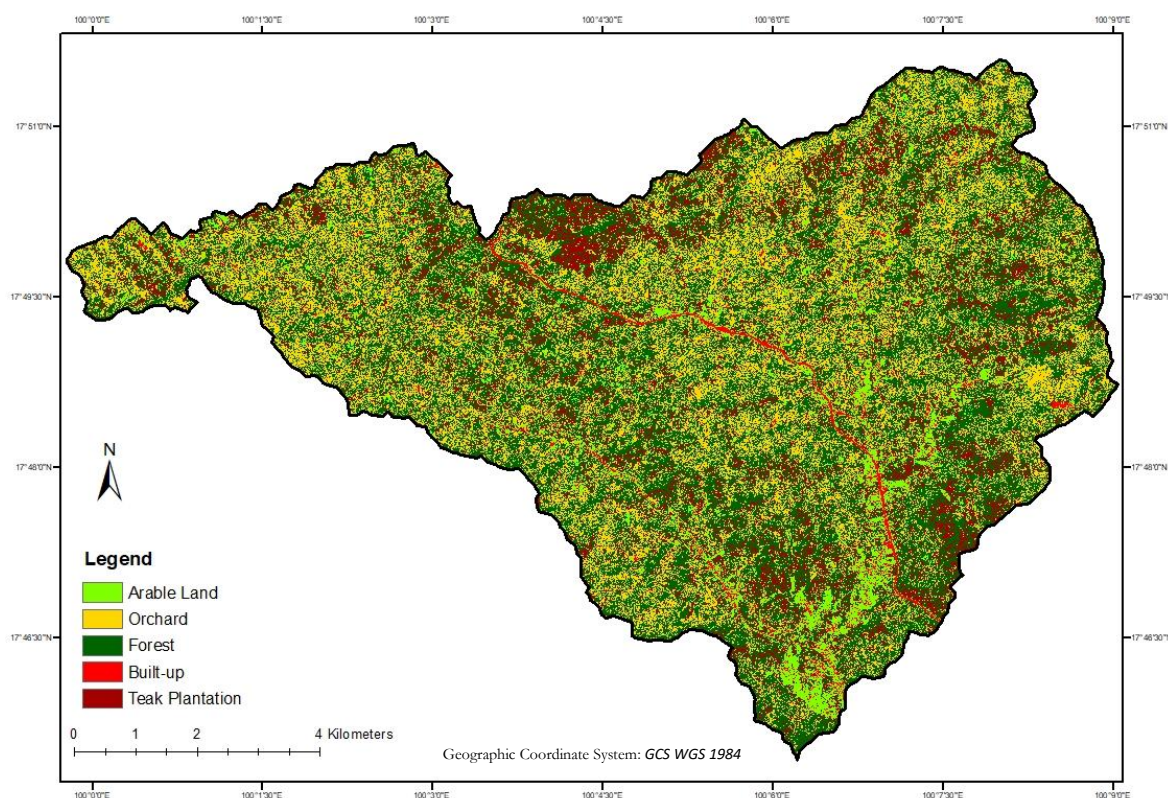
Figure 3-14: Land use / land cover map of the Ban Dan Na Kham Watershed

Table 3-11: Accuracy assessment report for land use / land cover classification

Error Matrix						
Classified Data	Arable Land	Orchard	Natural Forest	Built-up	Teak Forest	Row Total
Arable Land	28	1	0	14	2	45
Orchard	0	23	7	0	0	30
Natural Forest	1	5	13	0	6	25
Built-up	0	0	0	16	0	16
Teak Forest	1	1	10	0	22	34
Column Total	30	30	30	30	30	150

Accuracy Totals					
Class Name	Reference Totals	Producers Accuracy (%)	Users Accuracy (%)	Overall Accuracy (%)	Kappa Coefficient
Arable Land	30	93.33	62.22	68.00	0.5278
Orchard	30	76.67	76.67		0.7083
Natural Forest	30	43.33	52.00		0.4000
Built-up	30	53.33	100.00		1.0000
Teak Forest	30	73.33	64.71		0.5588
Overall	150	-	-	68.00	0.6000

Table 3-12: Accuracy assessment report for land use / land cover classification (without teak plantation)

Error Matrix					
Classified Data	Arable Land	Orchard	Forest	Built-up	Row Total
Arable Land	28	1	1	14	44
Orchard	0	22	7	0	29
Forests	2	7	52	0	61
Built-up	0	0	0	16	16
Column Total	30	30	60	30	150

Accuracy Totals					
Class Name	Reference Totals	Producers Accuracy (%)	Users Accuracy (%)	Overall Accuracy (%)	Kappa Coefficient
Arable Land	30	93.33	63.64	78.67	0.5455
Orchard	30	73.33	75.86		0.6983
Forests	60	86.67	85.25		0.7541
Built-up	30	53.33	100.00		1.0000
Overall	150	-	-	78.67	0.7032

Table 3-13: Attributes generated for each land cover type

Land Cover	Et/Eo	C (0-1)	EHD (m)	A (0-1)	CC (0-1)	SC (0-1)	PH (m)	Kc (0-1)	LAI (m²/m²)	Smax (mm)
Arable Land	0.60	0.51	0.12	0.16	0.49	0.16	1.42	1.00	1.68	1.77
Orchard	0.77	0.33	0.18	0.20	0.67	0.70	10.60	0.68	2.77	2.27
Forest	0.95	0.05	0.20	0.55	0.95	0.61	19.88	0.98	7.49	6.12
Built-up Areas	0.00	1.00	0.00	0.00	0.00	0.00	0.00	0.00	0.00	0.00
Teak Plantation	0.90	0.08	0.20	0.47	0.92	0.26	20.35	0.98	6.31	5.16

Where Et/Eo = Ratio of Actual to Potential Evapotranspiration Ratio, C = Crop Management Factor, EHD = Effective Hydrologic Depth (m), A = Rainfall Interception by Vegetation (0-1), CC = Canopy Cover (0-1), SC = Surface Cover (0-1), PH = Plant Height (m), Kc = Crop Coefficient, LAI = Leaf Area Index, Smax = Maximum Canopy Storage (mm)

3.3. Assessment of the Results of the RMMF Modelling Process for Both Data Sources

The third and fourth research questions focussed on the assessment of the predicted soil erosion using SoilGrids250m and Field-based soil data. The findings related to those research questions were discussed in section 3.3.1.

3.3.1. Comparative Assessment of SoilGrids250m and Field-based Model Outputs

The modelled soil loss maps from both data sources and the difference map are shown in Figure 3-15a to Figure 3-15c. Appendix 3-3 to Appendix 3-8 show the detachment by raindrops, detachment by runoff, total detachment, runoff, runoff transport capacity and deposition maps generated from both data sources and the respective difference maps.

For a large part of study area, the generated data were similar, while for other areas, the SoilGrids250m data generated higher values (Appendix 3-5c and Figure 3-15c). On the other hand, Appendix 3-8c shows that unlike detachment (Appendix 3-5c) and erosion (Figure 3-15c), while a large portion of the area still had relatively similar sediment deposition predictions and a major portion of the remaining area still recorded higher deposition estimates for SoilGrids250m data, a large portion recorded higher values for field-based data. The predominant trend, as shown in the detachment by raindrops (Appendix 3-3), detachment by runoff (Appendix 3-4), runoff (Appendix 3-6) and runoff transport capacity (Appendix 3-7) maps are in line with those of detachment (Appendix 3-5) and erosion (Figure 3-15). This may be attributed to the fact as shown in Figure 3-12a to Figure 3-12e and Figure 3-13a to Figure 3-13e that the values of the soil characteristics represented in SoilGrids250m data were consistently higher than the field-based data, with the singular exception of silt content. Statistical analysis was subsequently conducted to determine whether the difference between the two set of outputs are statistically significant.

A. Point-based Assessment of the RMMF Model Outputs

The point-based field and SoilGrids250m output data, and the residual values after field-based values were subtracted from SoilGrids250m-based values are shown in Figure 3-16a to Figure 3-16f. The figures show that unlike the case of the inputs where the field-based data consistently seemed to have a greater degree of variability than the SoilGrids250m data, the range and variability of the output data were relatively similar. This gives the impression that the outputs from both data sources may not be very different from each other. This is attributable to the fact that soil data is not the only input data used in the RMMF model. The integrated effect of the land cover and rainfall inputs played a key role in homogenizing the variability.

Total detachment for SoilGrids250m and field-based data are 317 and 304 ton/ha respectively, with a mean difference of 13 ton/ha (Figure 3-16c). Sediment deposition for SoilGrids250m and field-based data are 298 and 287 ton/ha respectively, with a mean difference of 10 ton/ha (Figure 3-16e). Soil erosion for SoilGrids250m and field-based data are 20 and 17 ton/ha respectively, with a mean difference of 3 ton/ha (Figure 3-16f). Similar trends were recorded for all other erosional processes. The difference between the outputs seem conservative, even though in reality, it may make a lot of difference. This informed the need to assess these data further to determine whether the modelled output from one dataset can be used to predict the output from the other dataset. SoilGrids250m data is currently available and has a global coverage, while field data may need to be generated whenever the need arises. The question then arises as to whether we can use the modelled values from SoilGrids250m to predict the values of the different erosional processes that would have been generated if field-based data were used instead of SoilGrids250m data.

Figure 3-15: Soil erosion (ton/ha) map from SoilGrids250m (a), field-based data (b) and the difference map (c)
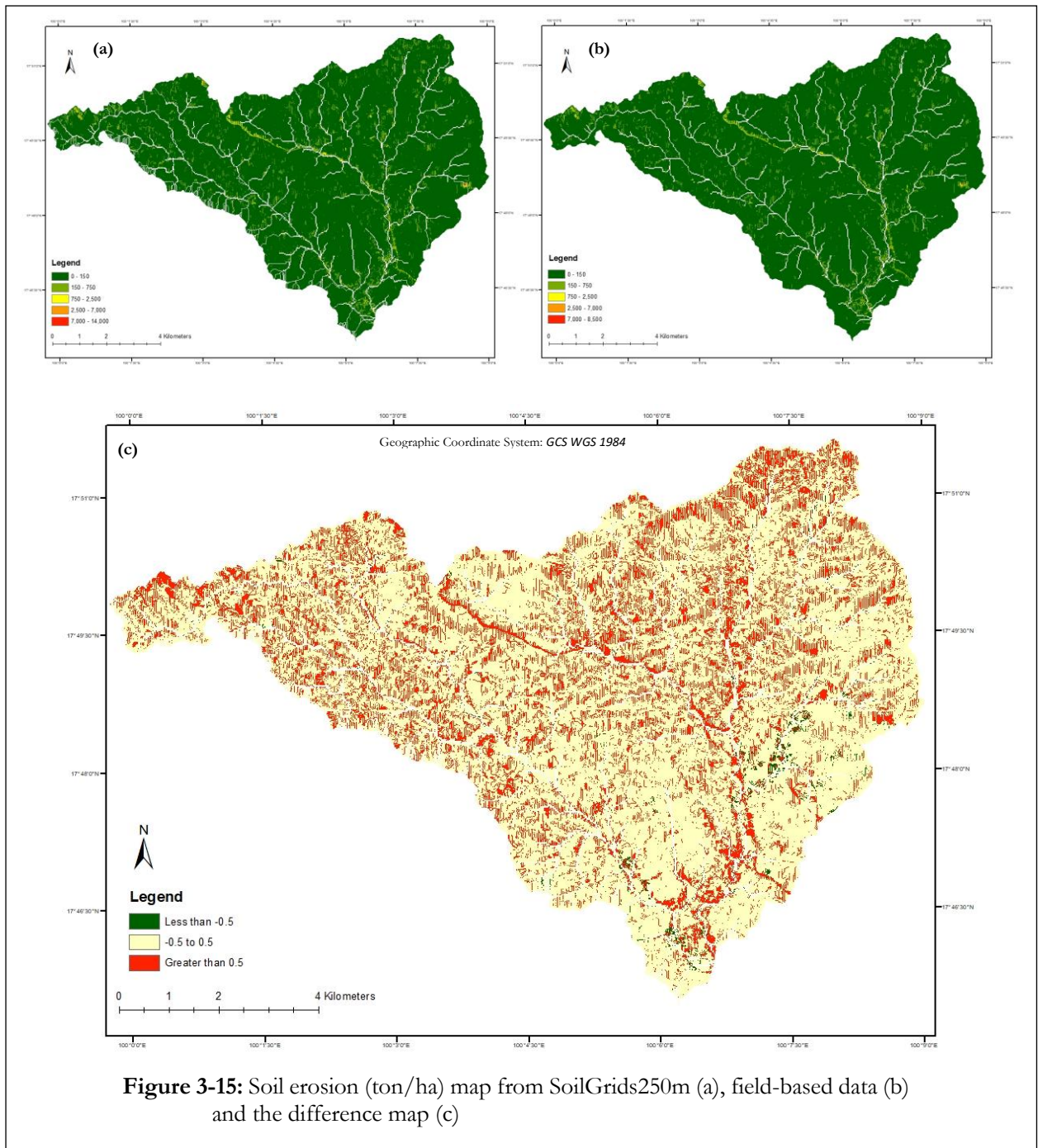
The regression graphs of erosional processes generated from SoilGrids250m and field-based soil data are shown in Figure 3-17a to Figure 3-17f. The graphs show that there is a positive correlation between the two sets of outputs, as higher values in one correspond with higher values in the other. As such, using the accompanying equation, each erosional process generated from SoilGrids250m data can be used to quantitatively predict the possible erosional process that would be generated from field-based data. More so, the very high R^2 values, ranging from 0.92 to 0.99, shows that a great proportion of the variability in the one set of output can be explained by the other set of outputs. This implies that the relationship between SoilGrids250m and field-based soil data accounts for 92 to 99% of the variations that are noticed in each of the graphs in Figure 3-17.

Furthermore, having concluded that the outputs from the two datasets are different, as shown in Figure 3-16, the next step was to determine to what extent they were different. The Euclidean distance between

the two sets of outputs and other statistics are shown in Table 3-14. The Euclidean distance between the two sets of outputs was 409.02 while the normalized Euclidean distance was 0.07. The very low normalized Euclidean distance, which is closer to 0 than it is to 1, indicates that the two datasets are similar. Nevertheless, statistical tests were conducted to determine whether there is a statistically significant difference between both datasets.

Figure 3-16: Comparative assessment of point-based detachment by raindrops (a), detachment by runoff (b), total detachment (c), runoff transport capacity (d), sediment deposition (e) and soil erosion (f) from SoilGrids250m and field-based soil data
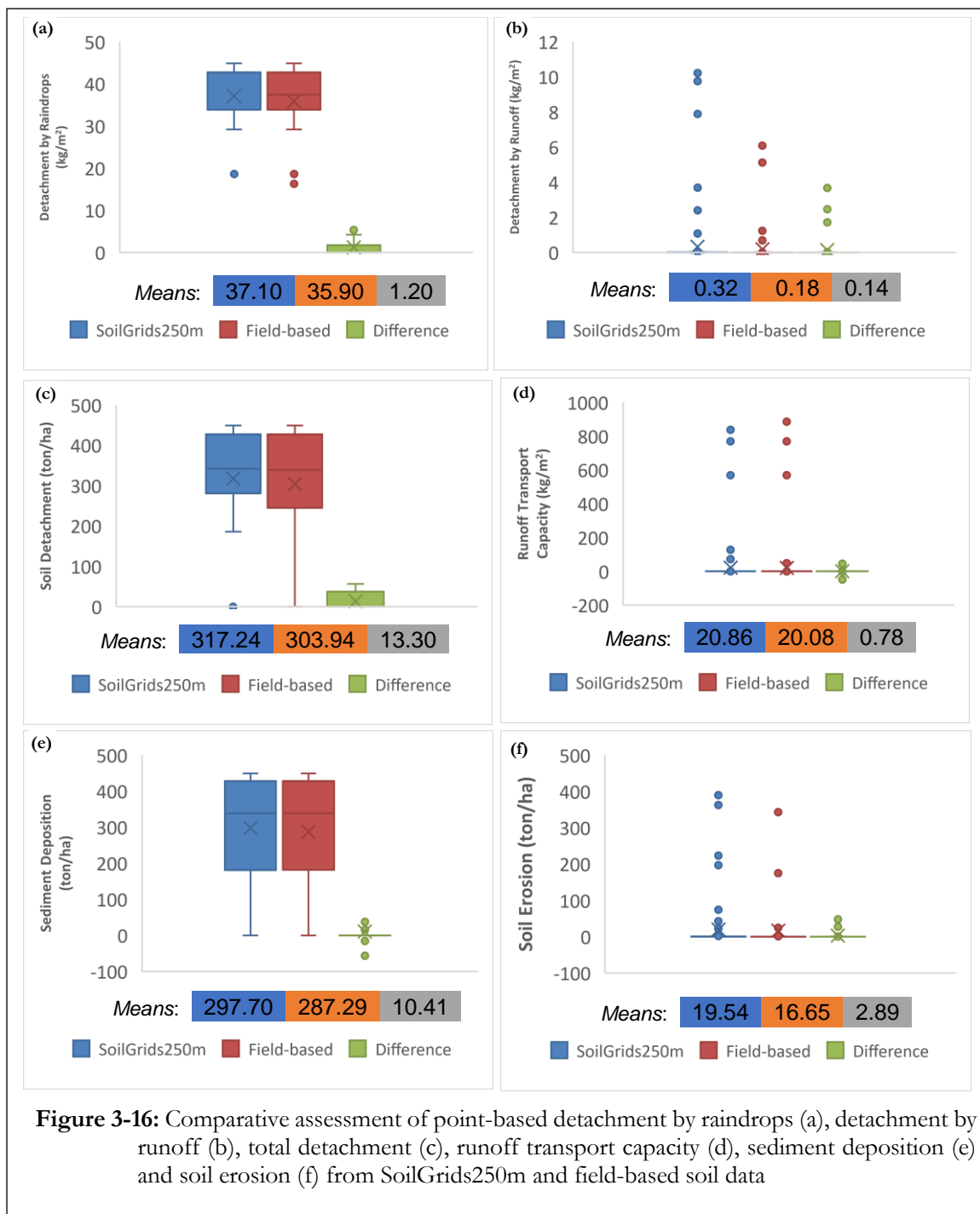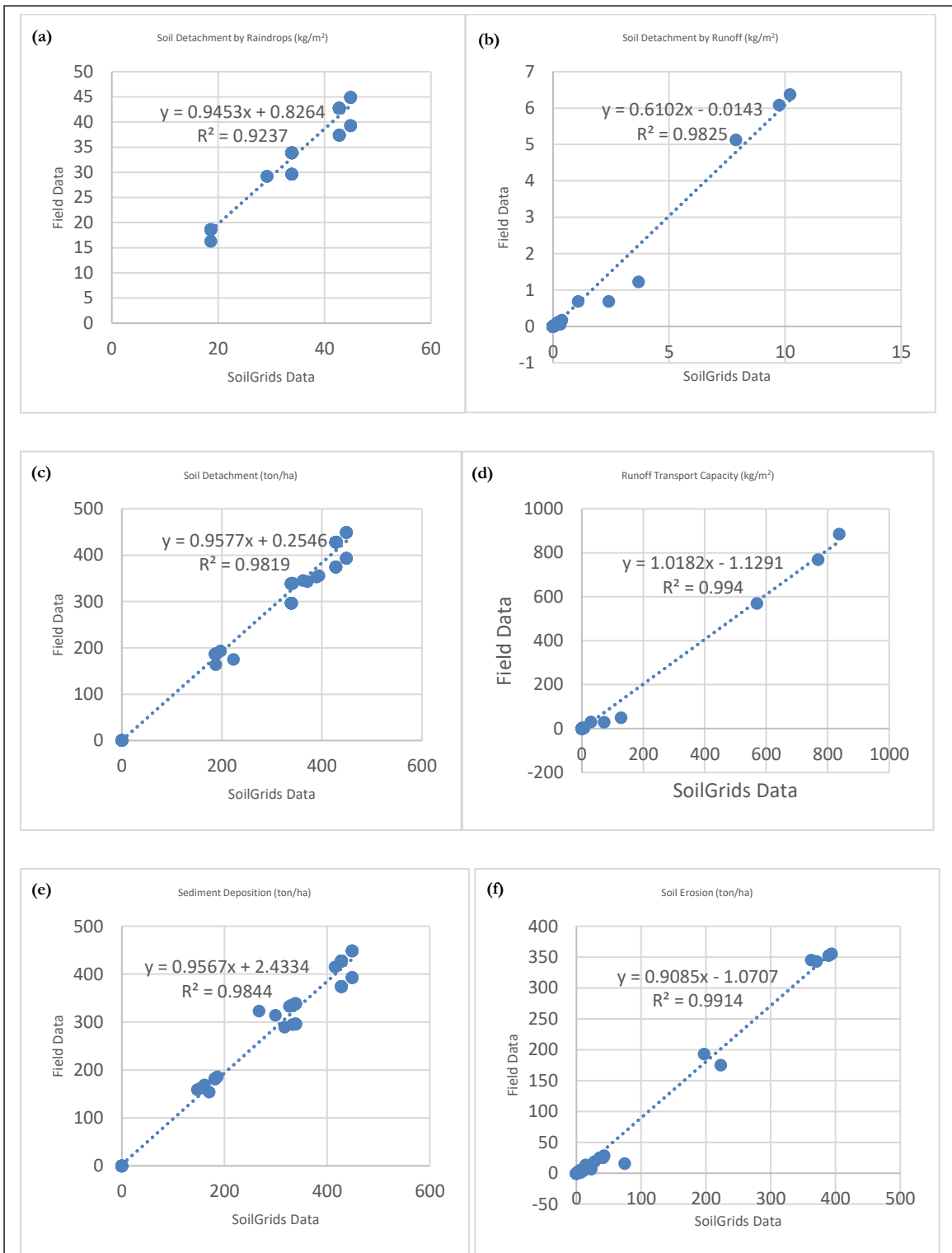
Figure 3-17: Regression analysis of point-based detachment by raindrops [kg/m²] (a), detachment by runoff [kg/m²] (b), total detachment [ton/ha] (c), runoff transport capacity [kg/m²] (d), sediment deposition [ton/ha] (e) and soil erosion [ton/ha] (f) from SoilGrids250m and field-based soil data

The skewness and kurtosis z-value for several of the parameters (at $P>0.05$) were outside the range of -1.96 and +1.96 and their Shapiro-Wilk P-value were also consistently less than 0.05 (Table 3-14). This indicates that most of the output parameters for both data sources are not normally distributed. Nevertheless, a

Levene Test P-value generally higher than 0.05 indicated that the variance was approximately homogenous for both sets of output. The homogeneity notwithstanding, the data did not fulfil the requirements for performing a T-Test, which according to Dytham (2011), included approximate normality and homogeneity of variance. Wilcoxon Signed Rank Test was conducted in place of the T-Test.

Table 3-14 shows that the Wilcoxon Signed Rank Test P-values for each set of outputs were consistently lower than 0.05, indicating that the outputs from both soil data sources are significantly different. This is still in line with the results from the comparison of soil datasets (Table 3-9). Nevertheless, with the models shown in Figure 3-17 and Table 3-14, the soil loss generated from an available soil dataset can be used to predict the soil loss from the unavailable soil dataset.

Table 3-14: Point-based comparative statistics for RMMF model outputs

	Parameter	Mean	Skew	Std. Error	Skew Z-Value	Kurt.	Std. Error	Kurt. Z-Value	Shapiro-Wilk P-Value	Levene Test P-Value	Euclid. Dist.	Norm. Euclid. Dist.	Wilkoxon Signed Rank Test P-Value
SoilGrids-250m	MMF_FA	37.10	-1.186	0.221	-5.367	0.691	0.438	1.578	0.000	0.5322	409.02	0.07	0.000
	MMF_HA	0.314	5.698	0.221	25.783	32.708	0.438	74.676	0.000	0.1203			0.000
	Detachment	312.1	-1.176	0.221	-5.321	-0.105	0.438	-0.240	0.000	0.6823			0.000
	Runoff	0.041	5.731	0.221	25.932	32.893	0.438	75.098	0.000	0.8926			0.000
	Runoff TC	20.33	6.259	0.221	28.321	39.047	0.438	89.148	0.000	0.9350			0.000
	Deposition	290.3	-0.861	0.221	-3.896	-0.930	0.438	-2.123	0.000	0.5459			0.003
	Erosion	19.05	4.427	0.221	20.032	18.931	0.438	43.221	0.000	0.6035			0.000
											Model		**R-square**
Field-based Data	MMF_FA	35.90	-1.030	0.221	-4.661	0.488	0.438	1.114	0.000	y = 0.9453x + 0.8264			0.9237
	MMF_HA	0.177	6.034	0.221	27.303	35.994	0.438	82.178	0.000	y = 0.6102x - 0.0143			0.9825
	Detachment	299.2	-1.117	0.221	-5.054	-0.161	0.438	-0.368	0.000	y = 0.9577x + 0.2546			0.9819
	Runoff	0.038	5.832	0.221	26.389	33.770	0.438	77.100	0.000	y = 0.9959x - 0.0028			0.9978
	Runoff TC	19.58	6.421	0.221	29.054	41.051	0.438	93.724	0.000	y = 1.0182x - 1.1291			0.9940
	Deposition	280.1	-0.846	0.221	-3.828	-0.904	0.438	-2.064	0.000	y = 0.9567x + 2.4334			0.9844
	Erosion	16.23	4.545	0.221	20.566	19.813	0.438	45.235	0.000	y = 0.9085x - 1.0707			0.9914

NOTE: Skew = Skewness, Kurt. = Kurtosis, Std. Error = Standard Error, Norm. Euclid. Dist. = Normalized Euclidean Distance, MMF_FA = Soil Detachment by Raindrops, MMF_HA = Soil Detachment by Runoff, Runoff TC = Runoff Transport Capacity, y = Field-based Data, x = SoilGrids250m Data

B. Parcel-based Assessment of RMMF Model Outputs

Having concluded that grid cell values (point data) comparison show that the erosional processes generated from the two datasets are significantly different, the need arose to determine whether they still differ when zonal averages are compared.

Figure 3-18a to Figure 3-18f depicts box plots of parcel-based field and SoilGrids250m output data. The parcels were based on the hillslope units generated in the course of soil delineation. The average output values generated for the parcels from both data sources were compared to determine whether they are significantly different. The results show that the both sets of outputs had similar range of values, with the exception of detachment by runoff, where the SoilGrids250m output recorded a distinctly wider range (Figure 3-18b). Also, the SoilGrids250m outputs tended to have higher values, with the exception of detachment by raindrops (Figure 3-18a) where they recorded similar values. This is also in line with the findings for the parcel-based soil data comparison (Figure 3-13).

It is noteworthy that the mean detachment by raindrops for both data sources were very similar, resulting in a residual value equal to zero (Figure 3-18). As was the case in the point-based assessment (Figure 3-16), with the exception of detachment by runoff, the difference between the two means for all the output sets, seemed relatively small. Total detachment ranged from 332 ton/ha for field-based data to 350 ton/ha for SoilGrids250m, with a mean difference of 19 ton/ha (Figure 3-18c). Sediment deposition ranged from 312 ton/ha for field-based data to 326 ton/ha for SoilGrids250m data, with a mean difference of 14 ton/ha

(Figure 3-18e). Soil loss ranged from 20 ton/ha for field-based data to 24 ton/ha for SoilGrids250m data (Figure 3-18f). Consequently, as was the case with the point-based assessment, the data required further analysis.
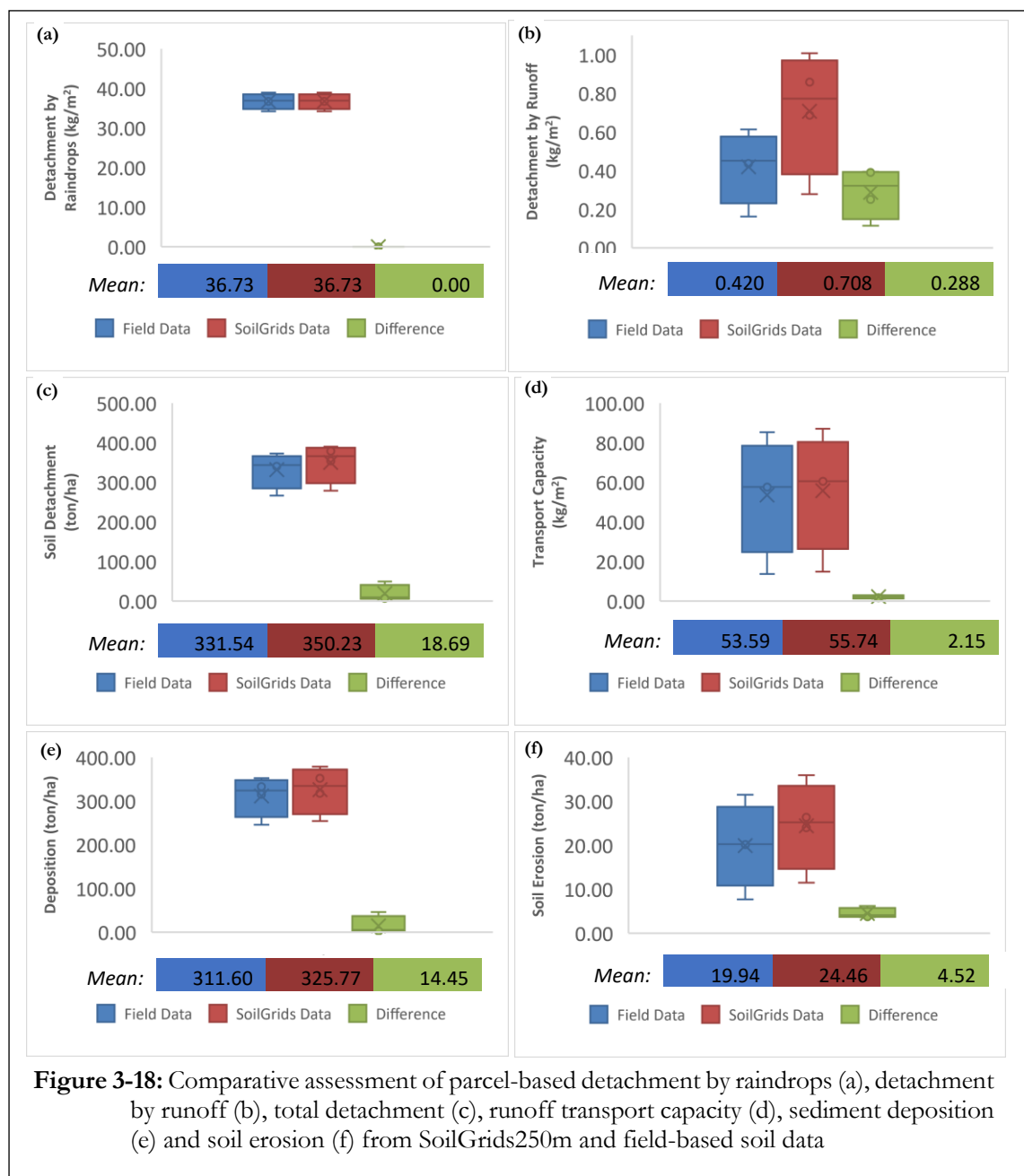
Figure 3-18: Comparative assessment of parcel-based detachment by raindrops (a), detachment by runoff (b), total detachment (c), runoff transport capacity (d), sediment deposition (e) and soil erosion (f) from SoilGrids250m and field-based soil data

Table 3-15 shows the data generated from further quantitative analysis of the model outputs. The Euclidean distance between the two sets of outputs was 70.90 while the normalized Euclidean distance was 0.03. Even though the Euclidean distance is much lower that the value (409.02) recorded during the point-based assessment, the normalized Euclidean distance was still very close to the value (0.07) reported for point-based assessment. This may be attributed to the fact that irrespective of the fact that the number of values being compared are different, the datasets are still the same. The very low normalized Euclidean distance, corroborates the results from the point-based assessment, indicating that the datasets similar.

To determine whether the difference was statistically significant for the other sets of outputs T-Test was calculated for each set. The skewness z-value, kurtosis z-value and Shapiro-Wilk P-value, all indicated that

both sets of outputs are approximately normal (Table 3-15). Similarly, the Levene Test, with P-values consistently higher than 0.05 (Table 3-15), indicated that all the output data has approximately homogenous variability. They consequently met the requirements for implementing the T-Test, as documented by Dytham (2011).

The T-Test P-values (Table 3-15) show that at $P>0.05$, the estimates for detachment by raindrops, total detachment and deposition were not significantly different for both datasets; at $P>0.01$, the estimates for detachment by runoff, runoff and runoff transport capacity were not significantly different. However, a P-value of 0.005, indicates that the erosion data generated from the two data sources were significantly different.

Table 3-15: Hillslope parcel-based comparative statistics for RMMF model outputs

	Parameter	Mean	Skew	Std. Error	Skew Z-Value	Kurtosis	Std. Error	Kurtosis Z-Value	Shapiro-Wilk P-Value	Levene Test P-Value	Euclid. Dist.	Norm. Euclid. Dist.	T-Test P-Value
SoilGrids-250m	MMF_FA	37	-0.506	1.014	-0.499	1.438	2.619	0.549	0.824	1.000	70.90	0.03	***
	MMF_HA	0.708	-1.046	1.014	-1.032	0.969	2.619	0.370	0.674	0.398			0.023
	Detachment	350	-1.491	1.014	-1.470	2.103	2.619	0.803	0.285	0.873			0.173
	Runoff	0.038	0.533	1.014	0.526	-3.004	2.619	-1.147	0.281	0.880			0.041
	Runoff TC	56	-0.930	1.014	-0.917	1.989	2.619	0.759	0.502	0.971			0.016
	Deposition	326	-0.845	1.014	-0.833	0.240	2.619	0.092	0.781	0.740			0.281
	Erosion	24	-0.434	1.014	-0.428	1.342	2.619	0.512	0.859	0.903			0.005
Field-based Data	MMF_FA	37	-0.506	1.014	-0.499	1.438	2.619	0.549	0.824				
	MMF_HA	0.420	-0.967	1.014	-0.954	1.921	2.619	0.733	0.616				
	Detachment	332	-1.427	1.014	-1.407	2.614	2.619	0.998	0.332				
	Runoff	0.035	0.477	1.014	0.470	-3.171	2.619	-1.211	0.393				
	Runoff TC	54	-0.807	1.014	-0.796	1.867	2.619	0.713	0.546				
	Deposition	312	-1.375	1.014	-1.356	2.102	2.619	0.803	0.429				
	Erosion	20	-0.196	1.014	-0.193	1.519	2.619	0.580	0.698				

NOTE: Skew = Skewness, Kurt. = Kurtosis, Std. Error = Standard Error, Norm. Euclid. Dist. = Normalized Euclidean Distance, MMF_FA = Soil Detachment by Raindrops, MMF_HA = Soil Detachment by Runoff, Runoff TC = Runoff Transport Capacity, *** = Exactly the same values (could not be computed because the standard error of the difference is 0)

Because erosion control or prevention may not usually target the erosion itself, but its predisposing factors, the data from SoilGrids250m is still valuable. It can be used to target zones with excessive runoff, zones with high detachment by raindrops, zones with high detachment by runoff and zones with high runoff transport capacity. Soil conservation measures implemented in these zones will ultimately lead to reduced soil loss. Similarly, it can be used to quantify the off-site effect of soil erosion as the sediment deposition generated by both datasets were also very similar.

However, the fact that the erosional processes which were significantly different when point-based assessment was done, turned out to be similar when parcel-based assessment was performed, has implications relating to the scale at which the SoilGrid250m generated erosional processes can be applied in soil conservation or land use planning. The SoilGrids250m-generated outputs are more useful for regional, district or provincial soil conservation / land use planning, where very detailed estimates of the erosional processes are not required. If more detailed, site-specific information are required, then, in the absence of field-generated data, SoilGrids250m can be used to predict the annual extent of the erosional processes, after which the models in Figure 3-17 and Table 3-14 can be used to predict the field-based estimates.

3.3.2. Assessment of the Sensitivity of the Model Parameters

The fifth and the sixth research questions were related to the determination of the soil and land cover parameters that the modelled erosional processes are more sensitive to. The findings are discussed in this

section. Figure 3-19 to Figure 3-22 and Appendix 3-9 to Appendix 3-11 graphically depict the percent change in the average predicted erosional processes in the watershed for every 20% increase in input parameters.

A. **Sensitivity of Rainfall Parameters:** Detachment by raindrops (Appendix 3-9), detachment by runoff (Appendix 3-10), total detachment (Figure 3-19), runoff (Figure 3-20), runoff transport capacity (Appendix 3-11) and soil erosion (Figure 3-22) were all more sensitive to rainfall amount than they are to number of rainy days. Nevertheless, sediment deposition (Figure 3-21) appears to be marginally more sensitive to number of rainy days as 100% increase in number of rainy days resulted in a 22% increase in deposition, while a 100% increase in rainfall amount resulted in only 18% increase in sediment deposition. This is in line with the findings of Morgan & Duzant (2008) that erosional processes are more sensitive to rainfall amount. With regards to deposition, it seems odd that increase in rainfall amount should result in increase in deposition. This apparent anomaly may be attributed to the fact that as rainfall increases, detachment also increases, but since the runoff transport capacity is low, the high detachment will also result in high deposition.

B. **Sensitivity of Soil Parameters:** Appendix 3-9 shows that besides soil erodibility, detachment by raindrops was not sensitive to any other soil parameter. Indeed, a 100% increase in soil erodibility equally results in a 100% increase in detachment by raindrops. One would, however, have expected that detachment by raindrops would be sensitive to cohesion as cohesive soils are less easily detached than non-cohesive soils. But the model does not seem to be sensitive to it. This is perhaps, due to the contention of Mahalder et al. (2016) that prediction of cohesive soil erodibility is difficult because credible models that capture its dynamics are currently not available. On the other hand, besides soil erodibility, detachment by runoff (Appendix 3-10) was sensitive to all other soil parameters. It was, however, most sensitive to moisture content at field capacity and effective hydrological depth. In both cases, a 100% increase resulted in an 84% decrease in soil detachment by runoff. Figure 3-19 shows that total detachment was most sensitive to soil erodibility, as it increased by 95% with 100% increase in erodibility. It is noteworthy that total detachment is sensitive to all soil parameters, albeit, marginal for field capacity, cohesion and effective hydrological depth. With respect to runoff estimate, it was equally sensitive to moisture content at field capacity and effective hydrological depth, as a 100% increase in any of them resulted in a 72% decrease in estimated runoff. Runoff was nonetheless, not sensitive to cohesion and erodibility (Figure 3-20). Expectedly, runoff transport capacity was also not sensitive to cohesion and erodibility, but equally sensitive to field capacity and effective hydrological depth – runoff transport capacity decreases by 89% with every 100% increase in field capacity or effective hydrological depth (Appendix 3-11). Figure 3-21 shows that sediment deposition is most sensitive to soil erodibility, as 100% increase in soil erodibility results in up to 114% increase in deposition. It was also sensitive to field capacity and effective hydrological depth, but not sensitive to cohesion. With respect to soil erosion (Figure 3-22), moisture content at field capacity and effective hydrological depth had the highest sensitivity of up to 80%, while cohesion had the least sensitivity of 7%. It is important to note that only soil erodibility had a position relationship with soil erosion; the other parameters had an inverse relationship with soil erosion.

C. **Sensitivity of Land Cover Parameters:** Appendix 3-9 shows that detachment by raindrops was most sensitive to water interception by vegetation (A), as 100% increase in interception results in a 66% decrease in detachment by raindrops. It was also sensitive to canopy cover (CC) and plant height (PH), as 100% increase in any of the variables results in over 25% increase in detachment by raindrops. Detachment by raindrops was not sensitive to any of the other land cover parameters. Detachment by runoff (Appendix 3-10) was most sensitive to the ratio of actual to potential evapotranspiration, which had a sensitivity of 84%. This is in line with the findings of Morgan & Duzant (2008) that runoff is highly sensitive to evapotranspiration. Detachment by runoff was also sensitive to interception by

vegetation and surface cover, but not sensitive to crop management factor, canopy cover and plant height. Total detachment (Figure 3-19) was most sensitive to rainfall interception by vegetation with a sensitivity of up to 53%. The only land cover parameter that it was not sensitive to was crop management factor. Runoff estimate (Figure 3-20) was most sensitive to the ratio of actual to potential evapotranspiration – which is in accord with the findings of Morgan & Duzant (2008) – with a sensitivity of up to 72%. The only other land cover parameter it was sensitive to was interception by vegetation. Runoff transport capacity (Appendix 3-11) was most sensitive to crop management factor, which had a sensitivity of up to 100%. It was not sensitive to canopy cover, surface cover and plant height. Sediment deposition (Figure 3-21) was most sensitive to interception by vegetation, with a sensitivity of up to 52%. Besides surface cover, it was sensitive to all other parameters. Soil erosion (Figure 3-22) was most sensitive to the ratio of actual to potential evapotranspiration, with a sensitivity of up to 80%. It was sensitive to all land cover parameters, but least sensitive to canopy cover (7 %).

D. Overall Sensitivity: Appendix 3-9 shows that, overall, detachment by raindrops was most sensitive to rainfall amount (100%) and soil erodibility (100%). Detachment by runoff (Appendix 3-10), total detachment (Figure 3-19), runoff estimate (Figure 3-20), runoff transport capacity (Appendix 3-11) and soil erosion (Figure 3-22), were all most sensitive to changes in rainfall amount. The only parameter that was an exception was soil deposition (Figure 3-21), which was most sensitive to soil erodibility (114%). The findings of this study is in line with those of Morgan & Duzant (2008), which were reiterated by Choi et al. (2016), that soil loss and runoff estimates are most sensitive to variations in rainfall amount. Furthermore, Morgan & Duzant (2008) asserted that for bare soils, besides rainfall, the MMF model estimates of soil loss is more sensitive to soil parameters, but that with increase in vegetation cover, land cover becomes progressively more important. They, however, also stated that irrespective of the vegetation cover or the lack of it, in addition to rainfall, runoff was also sensitive to soil moisture storage (soil moisture content at field capacity and effective hydrological depth) and evapotranspiration (ratio of actual to potential evapotranspiration) as was also evident in Figure 3-20.

Factors	Parameters	Baseline	20%	40%	60%	80%	100%
Climate	RF	236.60	23.76	49.89	78.76	110.70	145.96
	RD	236.60	-1.69	-2.74	-3.37	-3.80	-4.08
Soil	MS	236.60	-1.65	-2.74	-3.38	-3.81	-4.08
	K	236.60	19.03	38.05	57.08	76.10	95.13
	COH	236.60	-0.82	-1.40	-1.83	-2.17	-2.44
	EHD	236.60	-1.68	-2.75	-3.36	-3.82	-4.08
	Et/Eo	236.60	-1.68	-2.74	-3.37	-3.80	-4.08
Land Cover	C	236.60	0.00	0.00	0.00	0.00	0.00
	A	236.60	-13.80	-26.95	-40.15	-53.40	-34.34
	CC	236.60	5.30	10.96	16.22	21.88	27.19
	SC	236.60	-0.49	-1.00	-1.53	-2.02	-2.51
	PH	236.60	5.66	10.86	15.70	20.25	24.55

RF = Rainfall (mm), RD = Rainy Days, MS = Field Capacity (%), K = Erodibility (kg/J), COH = Cohesion (kPa), EHD = Effective Hydrological Depth (m), Et/Eo = Ratio of Actual to Potential Evapotranspiration, C = Crop Management Factor, A = Rainfall Interception by Vegetation (mm), CC = Canopy Cover (%), SC = Surface Cover (%), PH = Plant Height (m)

Figure 3-19: Sensitivity of total soil detachment to various input parameters
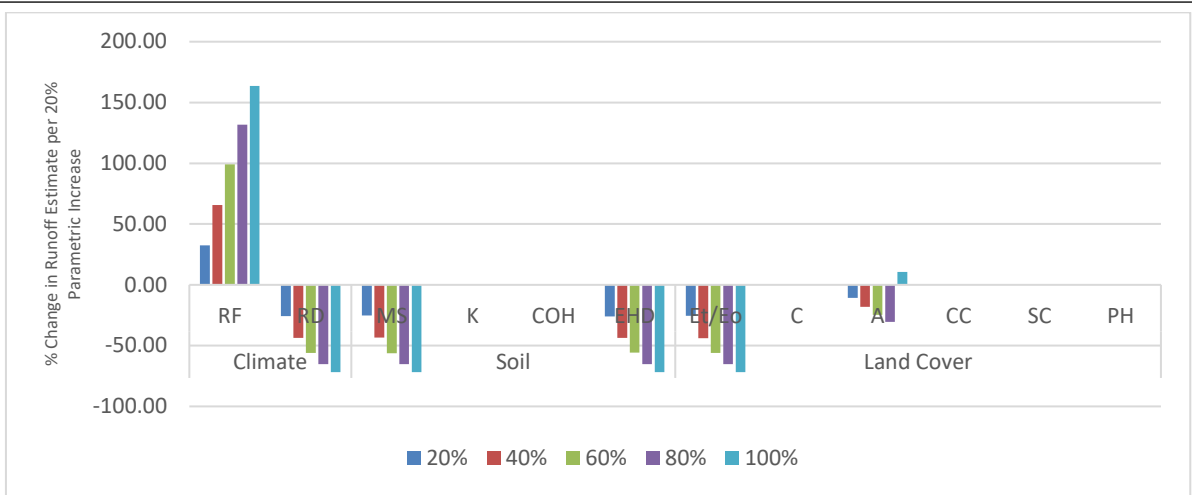
Factors	Parameters	Baseline	20%	40%	60%	80%	100%
Climate	RF	0.08	32.55	65.77	99.00	131.76	163.71
	RD	0.08	-25.65	-43.71	-55.90	-65.16	-71.79
Soil	MS	0.08	-25.11	-43.38	-56.15	-65.33	-71.79
	K	0.08	0.00	0.00	0.00	0.00	0.00
	COH	0.08	0.00	0.00	0.00	0.00	0.00
	EHD	0.08	-25.96	-43.67	-55.85	-65.30	-71.79
Land Cover	Et/Eo	0.08	-25.39	-43.78	-55.87	-65.19	-71.79
	C	0.08	0.00	0.00	0.00	0.00	0.00
	A	0.08	-10.62	-18.02	-24.67	-30.33	10.52
	CC	0.08	0.00	0.00	0.00	0.00	0.00
	SC	0.08	0.00	0.00	0.00	0.00	0.00
	PH	0.08	0.00	0.00	0.00	0.00	0.00

RF = Rainfall (mm), RD = Rainy Days, MS = Field Capacity (%), K = Erodibility (kg/J), COH = Cohesion (kPa), EHD = Effective Hydrological Depth (m), Et/Eo = Ratio of Actual to Potential Evapotranspiration, C = Crop Management Factor, A = Rainfall Interception by Vegetation (mm), CC = Canopy Cover (%), SC = Surface Cover (%), PH = Plant Height (m)

Figure 3-20: Sensitivity of runoff estimate to various input parameters
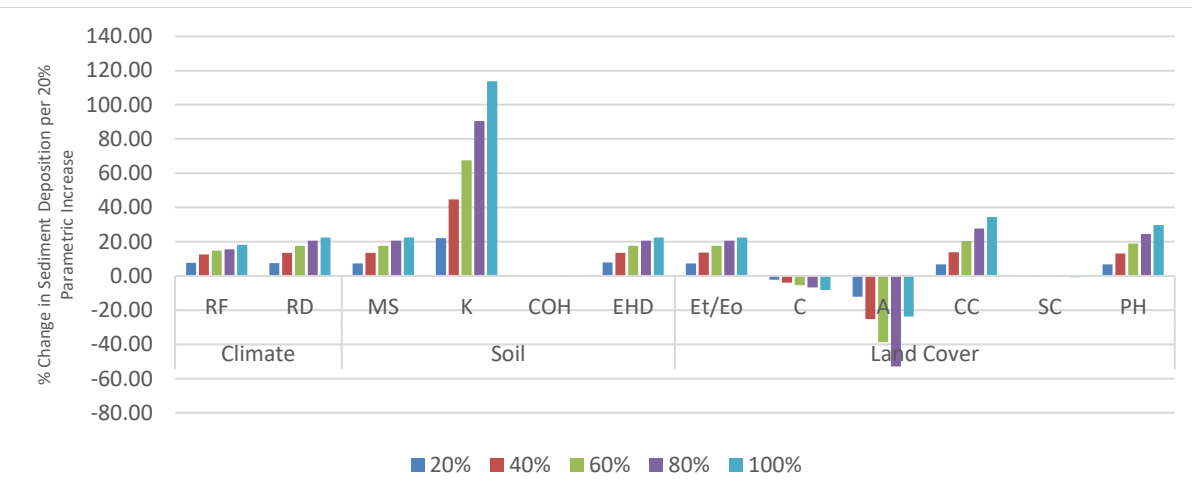
Factors	Parameters	Baseline	20%	40%	60%	80%	100%
Climate	RF	175.09	7.63	12.54	14.86	15.57	18.21
	RD	175.09	7.52	13.57	17.61	20.52	22.45
Soil	MS	175.09	7.29	13.53	17.64	20.59	22.45
	K	175.09	22.17	44.65	67.45	90.48	113.69
	COH	175.09	-0.20	-0.35	-0.46	-0.54	-0.60
	EHD	175.09	7.88	13.48	17.63	20.55	22.45
Land Cover	Et/Eo	175.09	7.37	13.62	17.59	20.53	22.45
	C	175.09	-2.22	-3.88	-5.47	-6.79	-8.16
	A	175.09	-12.15	-25.28	-38.74	-52.89	-23.70
	CC	175.09	6.65	13.79	20.46	27.64	34.38
	SC	175.09	-0.14	-0.29	-0.44	-0.58	-0.72
	PH	175.09	6.81	13.09	18.95	24.47	29.71

RF = Rainfall (mm), RD = Rainy Days, MS = Field Capacity (%), K = Erodibility (kg/J), COH = Cohesion (kPa), EHD = Effective Hydrological Depth (m), Et/Eo = Ratio of Actual to Potential Evapotranspiration, C = Crop Management Factor, A = Rainfall Interception by Vegetation (mm), CC = Canopy Cover (%), SC = Surface Cover (%), PH = Plant Height (m)

Figure 3-21: Sensitivity of sediment deposition to various input parameters

RF = Rainfall (mm), RD = Rainy Days, MS = Field Capacity (%), K = Erodibility (kg/J), COH = Cohesion (kPa), EHD = Effective Hydrological Depth (m), Et/Eo = Ratio of Actual to Potential Evapotranspiration, C = Crop Management Factor, A = Rainfall Interception by Vegetation (mm), CC = Canopy Cover (%), SC = Surface Cover (%), PH = Plant Height (m)

Figure 3-22: Sensitivity of soil loss estimation to various input parameters
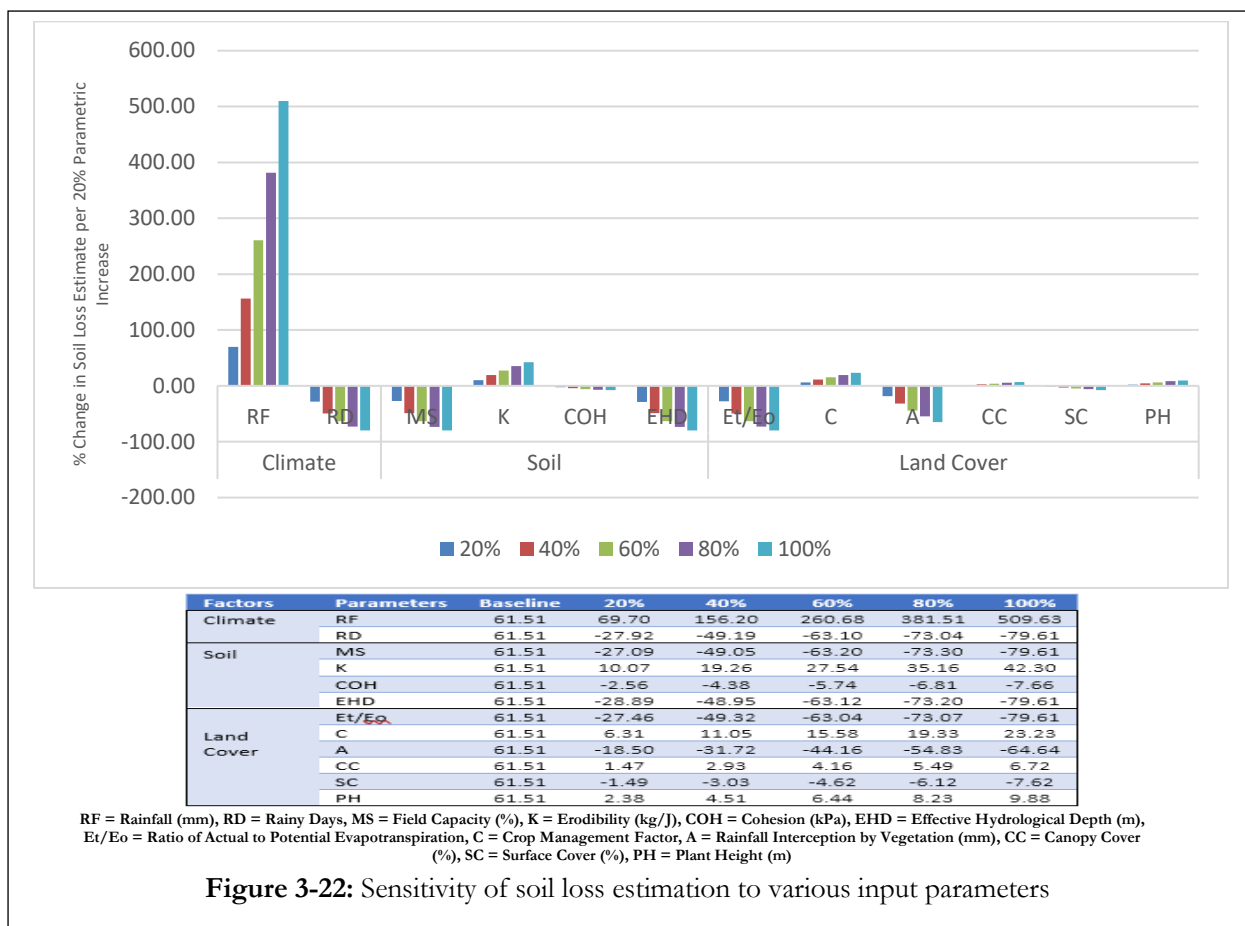
3.3.3. Assessment of the Spatial Extent of Soil Erosion within the Different Land Cover and Slope Units of the Watershed

The seventh and eight research questions focussed on the assessment of which land cover and hillslope units are more prone to soil erosion. It is noteworthy that field assessment of erosional processes within the study area could not be conducted. Similarly, secondary validation data was also not available. Nevertheless, Morgan (2001) validated the runoff and soil loss generated by the RMMF model for 91 sites in 17 different countries, including Thailand. The findings of the assessment of the erosional processes in the study area are discussed in this section. The output data are presented in maps, tables and graphs.

A. **Erosional Processes Under Different Slope Conditions:** Figure 3-23 depicts the detachment, deposition and soil loss from different slope units. Figure 3-23 shows that soil detachment was highest in the steep slopes (399 ton/ha/annum) and least in the gentle slopes (317 ton/ha/annum). Soil loss, which ranges from 18 to 30 ton/ha/annum, was however, much lower than detachment. This may be attributed to the low runoff volume (Table 3-16), which in turns translated into low runoff transport capacity (Table 3-16). Because the runoff does not have the capacity to transport the detached sediments out of the watershed, a very large proportion of the detached sediments are re-deposited within the vicinity of the area from which they were detached. This was why the deposition is also quite high (274 to 354 ton/ha/annum), almost at par with detachment. Given the relatively high rate of detachment on steep slopes, land uses, like arable farming, that may predispose the soil to the direct impact of raindrops and runoff, ought to be discouraged on steep slopes. Ideally, it would have been expected that soil loss would be highest on the steep slope, but it turned out to be highest on the gentle slopes. This may be attributed to the fact that all the runoff from the steep and moderate slopes get accumulated on the gentle slopes, increasing runoff volume and runoff transport capacity. This is in

line with the findings of Medeiros et al. (2010) and Santos et al. (2017) that low runoff volume results in low runoff transport capacity, which in turn results in reduced soil loss. The reverse can consequently also be true. As such, though a relatively lower amount of sediment was detached on the gentle slopes, the increased runoff transport capacity ensures that a greater proportion of the detached sediments are transported out of the watershed. Also, the steep and moderate slopes are usually forested, unlike the gentle slopes, which are mostly used for arable farming. This agrees with the assertion of Lorsirirat & Maita (2006) that arable farming predisposes the soil to greater magnitude of land degradation.

Slope	Area (km²)	Detachment	Deposition	Erosion
Gentle	13.27	317.36	274.13	27.03
Moderate	62.42	374.98	345.38	18.21
Steep	5.96	398.85	354.04	29.55

Figure 3-23: Detachment, deposition and soil loss under different slope conditions
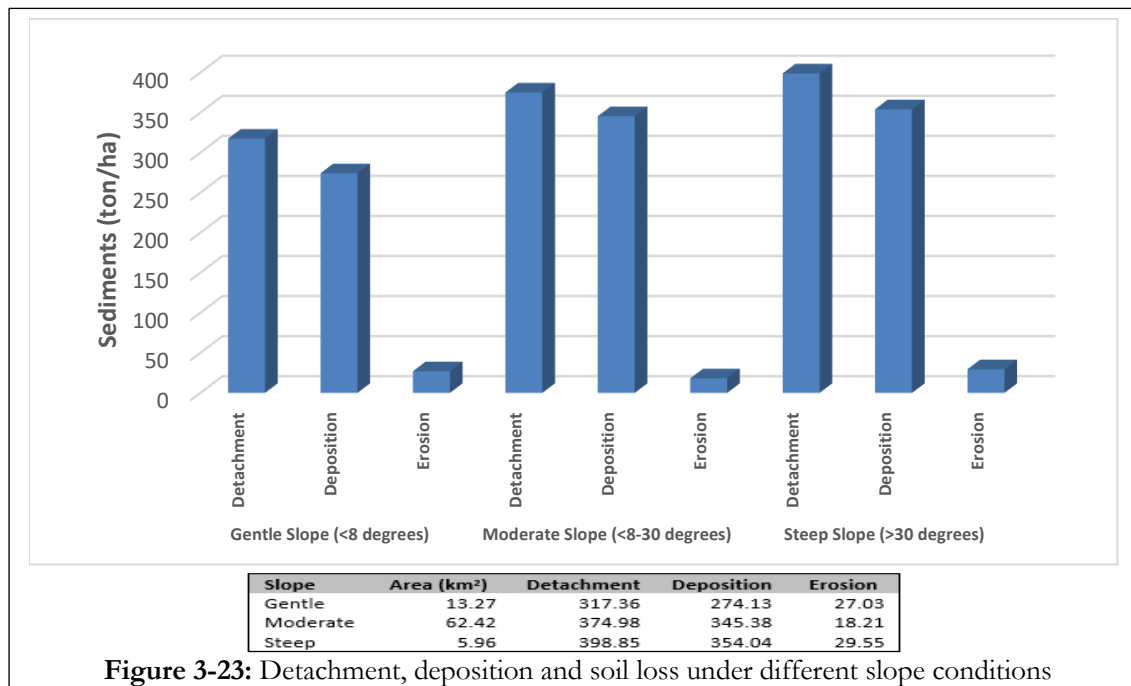
B. **Erosional Processes Across Different Hillslope Units:** Figure 3-24 depicts the detachment, deposition and soil loss across different hillslope units. It shows that detachment and deposition were highest on the back slope and least on the valley floor. The high detachment may be attributed the steep slopes of the back slope which results in the generated runoff moving down the slope at higher velocity, which increases its capacity to cut through the soil. Nevertheless, since the runoff volume is not large enough to have a high carrying capacity, much of the detached soils were still deposited within the hillslope unit. The back slope was consequently not the unit with the highest soil loss. Similarly, due to its gentle slope and low runoff volume and carrying capacity, the Summit/Shoulder was the hillslope unit with the lowest soil loss. This is in line with the assertion of Tingting et al. (2008) that erosion risks in northern Thailand is lower on higher altitudes. Tingting et al. (2008) however, attributed the low erosion to the predominance of forest land cover in these areas and the high capacity of forests to conserve water efficiently. The foot slope recorded the highest soil loss, which may be attributed to its accumulated runoff and increased runoff carrying capacity. It may, however, have been expected that soil loss would be highest on the valley floor, since this is the ultimate destination of all the runoff. This was not the case since the valley floor is virtually level, resulting in reduced runoff speed and longer residence time, which may have enabled some of its sediment load to be re-deposited. To reduce soil loss in the region, arable cropping may have to be discouraged on the back slope to avoid undue increase in soil detachment. Also, farmers may be encouraged to practice conservation tillage, leave behind crop residues after crop harvest and / or grow cover crops after crop removal as a way to slow down water movement on the foot slope and allow enough time for deposition to occur.

Hillslope Unit	Detachment	Deposition	Soil Loss
Summit/Shoulder	340.45	332.72	7.73
Back Slope	372.73	352.57	20.16
Foot Slope	346.79	315.29	31.50
Valley Floor	266.19	245.83	20.35
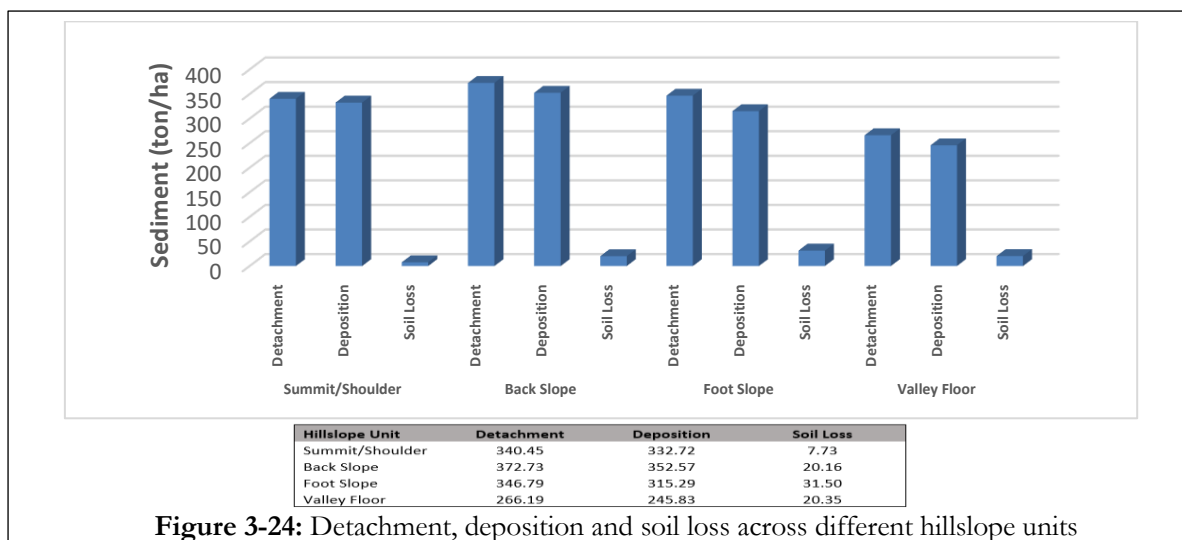
Figure 3-24: Detachment, deposition and soil loss across different hillslope units

C. **Erosional Processes Under Different Land Cover Types:** Figure 3-25 depicts the detachment, deposition and soil loss under the various land cover types delineated in the watershed. It shows that detachment and deposition were highest in teak plantations (416 and 403 ton/ha respectively) and least on arable soils (185 and 115 ton/ha respectively). The relatively high detachment in forests and teak plantation may be attributed to the predominance of tall trees in both land cover types, which invariably increases detachment by raindrops (leaf drainage). Detachment by raindrops was, however, much more severe in teak plantations due to the virtual nonexistence of undergrowth in the plantation, unlike was the case in forests. This may have informed the higher detachment in teak plantations as Labrière et al. (2015) asserted that in the humid tropics, soil loss is highest when there is no extra vegetation layer under the forest canopy. Similarly, Tingting et al. (2008) also contended that plantations are relatively more prone to erosion. Consequently, the cultivation of shade-loving plants under the canopy of the teak trees may be recommended, especially for regions on steep slopes. However, even though detachment was least on arable lands, soil loss was highest – as high as 69 ton/ha. This is in line with the contention of Lorsirirat & Maita (2006) that in Northern Thailand, agricultural practices predispose the soils to erosion. This may be attributed to increased runoff and runoff carrying capacity in the foot slope and valley floor where most of the arable lands are located. In addition to that, agricultural practices that lead to the soil being bare for prolonged periods of time may also be a contributory factor.

Land Use	Area (km²)	Detachment	Deposition	Erosion
Arable Land	6.03	184.53	115.17	69.36
Orchard	24.97	306.17	291.89	14.28
Forest	38.59	392.67	385.21	7.46
Teak Plantation	12.29	415.91	402.62	13.29
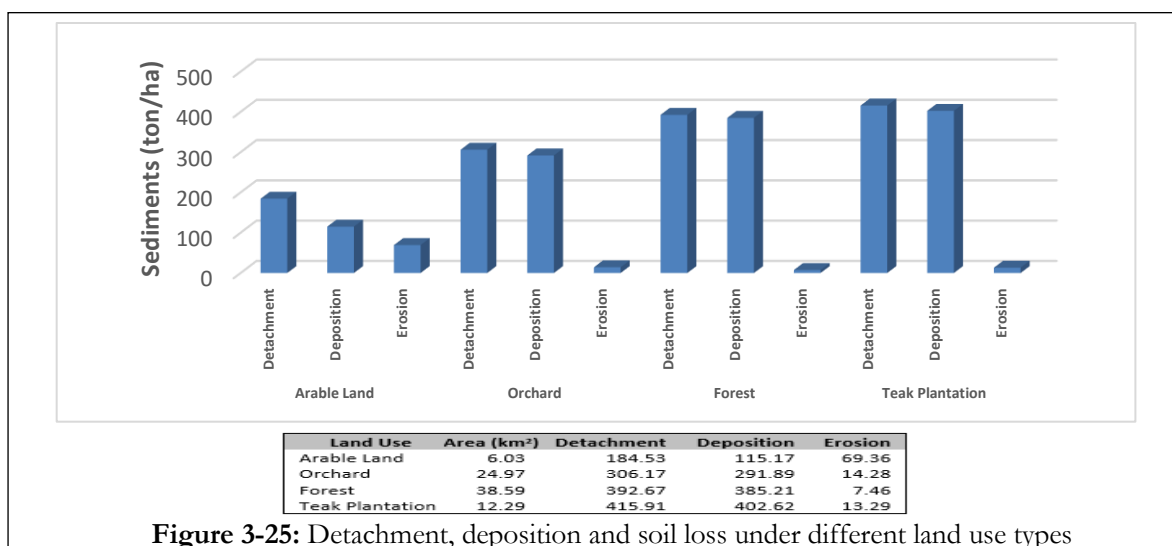
Figure 3-25: Detachment, deposition and soil loss under different land use types

D. **Erosional Processes Under Different Land Cover-Slope Units:** Figure 3-26 shows a map of the study area, depicting the location and extent of the various land use types under different slope conditions, while Table 3-16 shows the predicted values of the erosional processes taking place in each unit. Table 3-16 shows that for each land cover type, detachment was highest on the steep slopes and least on the gentle slopes. Overall, it was highest on teak plantation soils on steep slopes (431 ton/ha) and least on arable soils on gentle slopes (169 ton/ha). Due the relatively low runoff volume and transport capacity, deposition followed the same trends as did detachment. The exception to the rule was the arable lands, where deposition was highest on the gentle slopes and lowest on steep slopes. This may be attributed to the fact that the gentle slopes allowed enough time for the accumulated runoff to deposit a relatively larger proportion of its sediment load, a phenomenon that is not feasible on steep slopes. Figure 3-27 depicts the soil loss across the land cover-slope units of the watershed. It shows that though total detachment was lowest on arable lands (Table 3-16), soil loss was highest, ranging from 46 ton/ha on gentle slopes to 132 ton/ha on steep slopes. This is in line with the assertion of Tingting et al. (2008) that arable soils, especially those on steep slopes, are very prone to erosion. Similarly, Vlassak et al. (1993), Panomtaranichagul et al. (2002), Panomtaranichagul & Nareuban (2005) and Wicharuck et al. (2010) contended that agricultural activities on the highlands of northern Thailand results in 5 to 297 ton/ha soil loss per annum. The high soil loss is attributable to the land use type, which does not protect the soil adequately and the increased runoff and runoff transport capacity on moderate to gentle slopes. The lower soil loss on gentle slopes for all land use types may be attributed to the relatively lower runoff velocity and energy on gentle slopes, and the increased residence time, which permits a greater degree of deposition.

Furthermore, with regards to the soil loss tolerance, Hudson (1981) and Morgan (2005) reported that a mean annual soil loss of 11 ton/ha is generally considered acceptable for soils that are up to 1m deep, but that the acceptable soil loss can be as low as 2 t/ha for sensitive areas where soils are thin or highly erodible. It has also been recommended that in regions where soils are over 2m deep, the soil loss tolerance can be increased to 15 – 20 ton/ha (Schertz, 1983; Morgan, 2005). Therefore, with a soil loss ranging from 6.5 ton/ha for gentle slopes to 10.48 ton/ha for steep slopes, soil loss in forest is still within the acceptable range. With respect to orchards, only those on gentle slopes had soil losses (9.11 ton/ha) within the tolerable limit of less than 11 ton/ha. Nevertheless, because most of the soils of the watershed are deep, and the soil loss for both moderate slope (14.93 ton/ha) and steep slope (18.16 ton/ha) are still less than 20 ton/ha, the predicted soil loss may be acceptable. Notwithstanding that the soil loss is below 20 ton/ha, it is still important to implement some soil conservation measure, particularly on steep slopes.

Teak plantations on both gentle (12.36 ton/ha) and moderate slopes (12.65 ton/ha) had soil loss values exceeding 11 ton/ha, but because it was just marginally higher and very much less than 15 ton/ha, teak can still be sustainably grown under these slope conditions. The planting of shade-loving plants under the dense canopy of the teak trees may improve the situation further. On the other hand, with a soil loss of 22.52 ton/ha, teak plantations on steep slopes exceed the maximum acceptable soil loss tolerance. Establishing teak plantations on steep slopes may consequently be discouraged. If they must be established, then soil conservation measures that reduce detachment and soil loss should be implemented as a precondition for establishing the plantations.

Irrespective of the condition of the slope, soil loss on arable lands, by far, exceed the maximum acceptable soil loss of 20 ton/ha. Arable farming on steep slopes, with a soil loss of up to 131.61 ton/ha should be outrightly discouraged. If arable farming is to be implemented on the moderate slopes, then soil conservation measures like terracing (with hedge plants or trees along the contours), should first be put in place. On gentle slopes, the soil loss was still as high as 45.67 ton/ha.

Consequently, even on gentle slopes, soil conservation measures and farming practices that discourage soil degradation by reducing the period during which the soil is bare, reducing runoff velocity, increasing runoff residence time and organic matter content, should be practiced.

Figure 3-26: Map of the watershed showing the different land use types and their respective slope classes
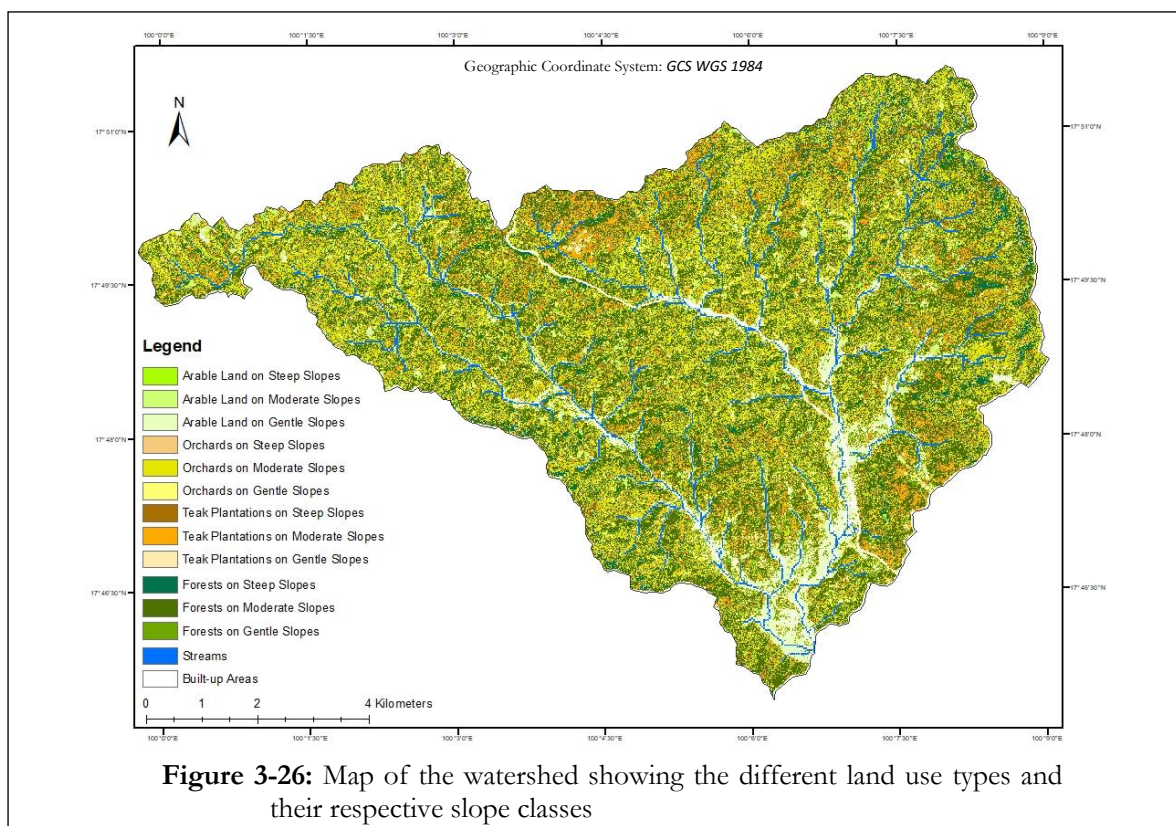
Table 3-16: Soil erosion processes in the different landscape units of the watershed

Landscape Unit	Area (km²)	MMF_FA (kg/m²)	MMF_HA (kg/m²)	MMF_Det (ton/ha)	RF (mm)	MMF_TC (kg/m²)	MMF_Dep (ton/ha)	Erosion (ton/ha)
AL-Gentle (< 8°)	2.49	18.521	0.920	169.494	0.106	115.831	123.820	45.67
AL-Moderate (8-30°)	3.16	18.233	1.780	192.747	0.098	172.935	110.940	81.81
AL-Steep (> 30°)	0.34	18.289	4.041	218.851	0.097	520.552	87.238	131.61
OR-Gentle (< 8°)	3.39	33.214	0.044	266.405	0.008	8.192	257.297	9.11
OR-Moderate (8-30°)	19.82	33.343	0.151	311.320	0.008	29.055	296.392	14.93
OR-Steep (> 30°)	1.61	33.397	0.179	325.807	0.008	33.017	307.651	18.16
FO-Gentle (< 8°)	4.97	41.897	0.070	356.170	0.000	1.543	349.669	6.50
FO-Moderate (8-30°)	30.25	41.992	0.146	396.948	0.000	3.294	389.599	7.35
FO-Steep (8-30°)	3.10	42.021	0.284	409.206	0.000	7.725	398.728	10.48
TP-Gentle (< 8°)	2.08	44.200	0.189	387.661	0.001	3.746	375.299	12.36
TP-Moderate (8-30°)	9.22	44.098	0.295	420.820	0.001	4.649	408.170	12.65
TP-Steep (> 30°)	0.92	44.132	0.674	430.527	0.001	12.049	408.004	22.52

NOTE: MMF_FA = Detachment by Raindrops (kg/m²), MMF_HA = Detachment by Runoff (kg/m²), RF = Runoff (mm), MMF_TC = Runoff Transport Capacity (kg/m²), MMF_Det = Total Soil Detachment (ton/ha), MMF_Dep = Sediment Deposition (ton/ha), Erosion = Soil Erosion (ton/ha), AL-Gentle = Arable Land on Gentle Slopes, AL-Moderate = Arable Land on Moderate Slopes, AL-Steep = Arable Land on Steep Slopes, OR-Gentle = Orchards on Gentle Slopes, OR-Moderate = Orchards on Moderate Slopes, OR-Steep = Orchards on Steep Slopes, FO-Gentle = Forests on Gentle Slopes, FO-Moderate = Forests on Moderate Slopes, FO-Steep = Forests on Steep Slopes, TP-Gentle = Teak Plantations on Gentle Slopes, TP-Moderate = Teak Plantations on Moderate Slopes, TP-Steep = Teak Plantations on Steep Slopes
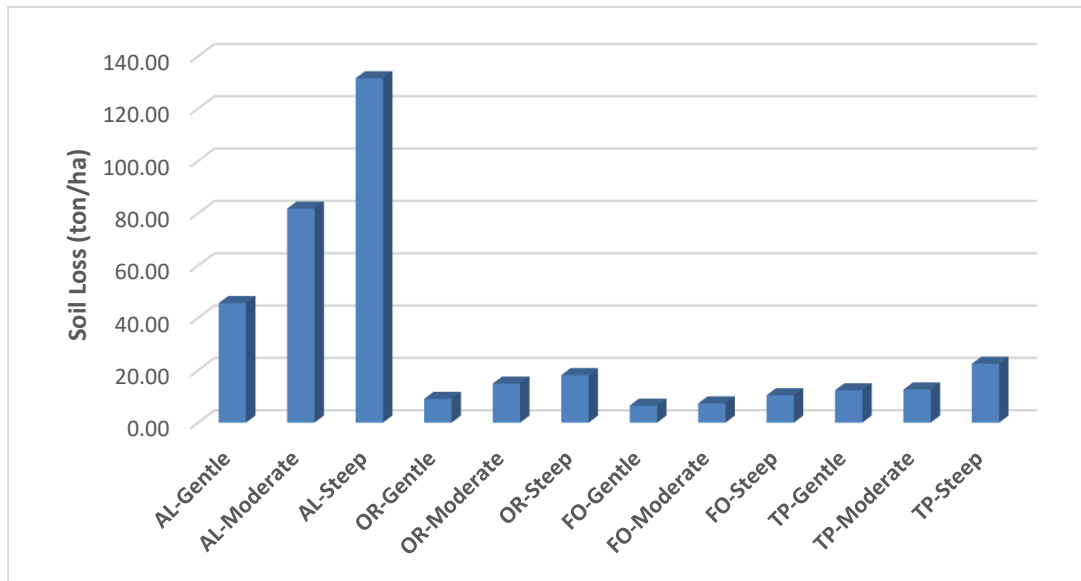
AL = Arable Land, OR = Orchard, FO = Forest, TP = Teak Plantation, Gentle = < 8° slope, Moderate = 8 – 30° slope, Steep = > 30° slope

Figure 3-27: Soil erosion (ton/ha) on different land cover-slope units

4. CONCLUSION AND RECOMMENDATIONS

4.1. Conclusion

Soil erosion is a global phenomenon that is more preponderant in the humid tropics, especially soil erosion by water. Given its devastating off-site and on-site impacts, there has over the years, been a consensus that it should be built into land evaluation and land use planning projects. As such, soil erosion assessment is a necessary prerequisite to sustainable natural resources management. The acquisition of the input data for the modelling is, however, time-consuming and capital-intensive. This is more so for soil survey data, which requires extensive fieldwork. SoilGrids250m, which is available at a global scale, could potentially solve the problem relating to the scarcity of soil data for erosion assessment. This study consequently assessed the value of SoilGrids250m data for erosion modelling, relative to field-generated soil data.

The comparative assessment of the SoilGrids250m and the field-based soil data was performed at two scales – point and areal. Point-based assessment indicated that the two soil datasets are significantly different. The only exception to this rule was clay content, for which both datasets were not significantly different. On the other hand, for the area-based assessment – which was based on the parametric average values of both datasets for each of the delineated hillslope units in the study area – only silt content was significantly different at $P>0.01$. All the other soil parameters were similar for both datasets. It may consequently be concluded that for regional studies, which require the average soil property for delineated areal units, SoilGrids250m data may be a good alternative to field data.

After assessing soil erosion for the study area using both datasets, the outputs relating to the erosional processes (detachment by raindrops, detachment by runoff, total detachment, runoff, runoff transport capacity, deposition and soil loss) were also compared to determine the extent of their similarities. As was the case with the point-based assessment of the soil datasets, the point-based assessment of the model outputs show that all the outputs generated were significantly different. Similarly, just like the area-based assessment of the input data, the assessment of the outputs show that they are not significantly different at $P>0.01$, with the exception of soil loss, for which the soil loss modelled from the SoilGrids250m was significantly higher. This also implies that when planning land evaluation or soil conservation projects at a regional scale areal averages of runoff and detachment from SoilGrids250m data may be adequate.

Nevertheless, for more site-specific erosion assessment in Northern Thailand, if time and funds are not available for the acquisition of additional field data, SoilGrids250m data can be used to assess soil erosion. Subsequently, using the models generated in this study, expected erosional processes from field-based data can be predicted. It is also noteworthy that all erosional processes generated from the RMMF, besides sediment deposition, were most sensitive to rainfall amount. Sediment deposition was most sensitive to soil erodibility. Also, besides rainfall, soil loss estimate was quite sensitive to soil parameters (moisture content at field capacity and effective hydrological depth) and land cover parameters (ratio of actual to potential evapotranspiration and rainfall interception by vegetation). Extra care should consequently be taken when running the RMMF model to ensure that these input parameters are of good quality.

Finally, the hillslope unit that is most susceptible to the forces of detachment (raindrop and runoff) is the back slope, but the low runoff transport capacity makes it less susceptible to soil loss than the foot slope which has lower detachment but greater soil loss. Slope classes below 8° are less prone to soil loss than other slope classes. The land cover type most susceptible to erosion in the study area was the arable lands, while forests were least susceptible.

4.2. Limitations

Some of the limitations encountered in the course of this study are:

- Lack of data for the validation of the RMMF model outputs.
- Inability to acquire a fine resolution DEM that will enable more accurate soil delineation.
- Inability to acquire a detailed geologic maps of the area, which would have been a necessary tool for proper delineation of the soil map units.
- Available hillslope delineation algorithms were designed to use high resolution terrain data, like LiDAR DEM or the airborne laser-derived DEM, which are usually not available in developing countries
- The ruggedness of the terrain, which made it difficult to access of the pre-defined sample sites.

4.3. Recommendations

In terms of the methods, if similar studies are to be conducted, it may be necessary to delineate the hillslope units prior to the fieldwork. The soil sampling scheme should be based on the delineated hillslope units. This would eliminate the ambiguity inherent in trying to compare two sets of outputs that are not comparable. With regards to the findings of this study, it is recommended that:

- Arable farming should be discouraged on steep and moderate slopes. Even on gentle slopes, arable farming should be accompanied by sustainable soil conservation practices.
- The establishment of teak plantations and orchards on steep slopes should be discouraged; and the implementation of land conservation measures should be a precondition for establishing teak plantations or orchards on moderate slopes.
- Shade-loving plants may need to be grown in teak plantations to reduce soil detachment and soil loss, and increase deposition by obstructing the flow of runoff.

4.4. Further Studies

In terms of the outcome of this study, some of the areas that require further research are:

- Validation of the outputs of the RMMF model for the watershed through field measurements of runoff, soil loss and / or other erosional processes.
- Assessment of the value of SoilGrids250m data for daily soil erosion modeling.
- Generation of soil loss tolerance and other indices that can be used as a baseline to determine the extent of soil loss that is acceptable in the region.
- Downscaling of soil delineation algorithms to permit the use of coarse resolution DEM (which are available for developing countries) to generate hillslope units that effectively reflect the soil-landscape relationship.

LIST OF REFERENCES

Alexakis, D. D., Hadjimitsis, D. G., & Agapiou, A. (2013). Integrated Use of Remote Sensing, GIS and Precipitation Data for the Assessment of Soil Erosion Rate in the Catchment Area of " Yialias " in Cyprus. *Atmospheric Research*, *131*, 108–124.

Avwunudiogba, A., & Hudson, P. F. (2014). A Review of Soil Erosion Models with Special Reference to the needs of Humid Tropical Mountainous Environments. *European Journal of Sustainable Development*, *3*(4), 299–310. https://doi.org/10.14207/ejsd.2014.v3n4p299

Baartman, J. E. M., Jetten, V. G., Ritsema, C. J., & Vente, J. (2012). Exploring Effects of Rainfall Intensity and Duration on Soil Erosion at the Catchment Scale Using openLISEM: Prado Catchment, SE Spain. *Hydrological Processes*, *26*(7), 1034–1049. https://doi.org/10.1002/hyp.8196

Balan, A., Raus, L., & Jitareanu, G. (2009). Effects of Tillage Management on Soil Porosity and Bulk Density on Rape Effects of Tillage Management on Soil Porosity and Bulk Density on Rape (Brasica Napus). *Bulletin UASVM Agriculture*, *66*(1), 260–263.

Beasley, D. B., Huggins, L. F., & Monke, E. J. (1980). Answers - A Model for Watershed Planning. *Transactions of the ASAE*, *23*, 938–944.

Bhadha, J. H., Capasso, J. M., Khatiwada, R., Swanson, S., & LeBorde, C. (2017). Raising Soil Organic Matter Content to Improve Water Holding Capacity. Gainesville: University of Florida Institute of Food and Agricultural Sciences. Retrieved from http://edis.ifas.ufl.edu.

Choi, K., Huwe, B., & Reineking, B. (2016). Commentary on "Modified MMF (Morgan-Morgan-Finney) Model for Evaluating Effects of Crops and Vegetation Cover on Soil Erosion" by Morgan and Duzant (2008). *ArXiv:1612.08899v2 [Physics.Geo-Ph]*, 13. Retrieved from http://arxiv.org/abs/1612.08899

Clutario, M. V. A., & David, C. P. C. (2014). Event-based Soil Erosion Estimation in a Tropical Watershed. *International Journal of Forest, Soil and Erosion (IJFSE)*, *4*(2), 51–57. Retrieved from http://ijfse.com/index.php/IJFSE/article/view/242

De Roo, A. P. J., Wesseling, C. G., & Ritsema, C. J. (1996). LISEM: A Single-Event Physically Based Hydrological and Soil Erosion Model for Drainage Basins. I: Theory, Input and Output. *Hydrological Processes*, *10*(8), 1107–1117. https://doi.org/10.1002/(SICI)1099-1085(199608)10:8<1107::AID-HYP415>3.0.CO;2-4

De Vente, J., Poesen, J., Verstraeten, G., Govers, G., Vanmaercke, M., Rompaey, A. Van, … Boix-Fayos, C. (2013). Predicting Soil Erosion and Sediment Yield at Regional Scales: Where do we Stand? *Earth-Science Reviews*, *127*, 16–29. https://doi.org/10.1016/j.earscirev.2013.08.014

Deumlich, D., Schmidt, R., & Sommer, M. (2010). A Multiscale Soil-landform Relationship in the Glacial-drift Area Based on Digital Terrain Analysis and Soil Attributes. *Journal of Plant Nutrition and Soil Science*, *173*(6), 843–851. https://doi.org/10.1002/jpln.200900094

Dor, E. Ben, & Banin, A. (1989). Determination of Organic Matter Content in Arid - Zone Soils using a Simple "Loss - on - Ignition" Method. *Communications in Soil Science and Plant Analysis*, *20*(15–16), 1675–1695. https://doi.org/10.1080/00103628909368175

Dytham, C. (2011). *Choosing and Using Statistics: A Biologist's Guide* (Third). Chichester: Wiley-Blackwell.

Easton, Z. M., & Bock, E. (2016). Soil and Soil Water Relationships. Petersburg: Virginia Cooperative Extension, College of Agriculture and Life Sciences, Virginia State University.

FAO, & ITPS. (2015). *Status of the World's Soil Resources (SWSR) - Main Report*. (F. Nachtergaele, Ed.), *Food and Agriculture Organization of the United Nations and Intergovernmental Technical Panel on Soils*. Rome: Food and Agriculture Organization of the United Nations and Intergovernmental Technical Panel on Soils. https://doi.org/ISBN 978-92-5-109004-6

Fattet, M., Fu, Y., Ghestem, M., Ma, W., Foulonneau, M., Nespoulous, J., … Stokes, A. (2011). Effects of Vegetation Type on Soil Resistance to Erosion: Relationship between Aggregate Stability and Shear Strength. *Catena*, *87*, 60–69. https://doi.org/10.1016/j.catena.2011.05.006

Gebhardt, S., Maeda, P., Espinoza, J. E., Wehrmann, T., & Schmidt, M. (2015). A proper Land Cover and Forest Type Classification Scheme for Mexico. In *36th International Symposium on Remote Sensing of Environment held from 11–15 May 2015 in Berlin, Germany* (pp. 383–390). Berlin: The International Archives of the Photogrammetry, Remote Sensing and Spatial Information Sciences. https://doi.org/10.5194/isprsarchives-XL-7-W3-383-2015

Gee, G. W., & Bauder, J. W. (1986). Particle-Size Analysis. In A. Klute (Ed.), *Methods of Soil Analysis, Part 1. Physical and Mineralogical Methods, Agronomy Monograph No. 9* (2nd ed., pp. 383–411). Madison, WI: American Society of Agronomy.

Genet, M., Kokutse, N., Stokes, A., Fourcaud, T., Cai, X., Ji, J., & Mickovski, S. (2008). Root Reinforcement in Plantations of Cryptomeria japonica D . Don: Effect of Tree Age and Stand Structure on Slope Stability. *Forest Ecology and Management*, *256*, 1517–1526. https://doi.org/10.1016/j.foreco.2008.05.050

Genet, M., Stokes, A., Fourcaud, T., Cai, X., & Lu, Y. (2006). Soil Fixation by Tree Roots: Changes in Root Reinforcement Parameters with Age in Cryptomeria J aponica D . Don . Plantations. In *Disaster Mitigation of Debris Flows, Slope Failures and Landslides* (pp. 535–542). Tokyo: Universal Academy Press, Inc.

Genet, M., Stokes, A., Fourcaud, T., & Norris, J. E. (2010). The Influence of Plant Diversity on Slope Stability in a Moist Evergreen Deciduous Forest. *Ecological Engineering, 36*, 265–275. https://doi.org/10.1016/j.ecoleng.2009.05.018

Giang, P., Giang, L., & Toshiki, K. (2017). Spatial and Temporal Responses of Soil Erosion to Climate Change Impacts in a Transnational Watershed in Southeast Asia. *Climate, 5*, 22. https://doi.org/10.3390/cli5010022

Hajigholizadeh, M., Melesse, A., & Fuentes, H. (2018). Erosion and Sediment Transport Modelling in Shallow Waters: A Review on Approaches, Models and Applications. *International Journal of Environmental Research and Public Health, 15*, 518. https://doi.org/10.3390/ijerph15030518

Hakansson, I. (2005). *Compaction of Arable Soils: Incidence, Consequences and Counter Measures*. Uppsala: Department of Soil Sciences, Swedish University of Agricultural Sciences.

Haynes, R. J., Dominy, C. S., & Graham, M. H. (2003). Effect of Agricultural Land Use on Soil Organic Matter Status and the Composition of Earthworm Communities in KwaZulu-Natal , South Africa. *Agriculture, Ecosystems and Environment, 95*, 453–464. https://doi.org/10.1016/S0167-8809(02)00223-2

Herrmann, L., Spohrer, K., Schuler, U., Stahr, K., Anongrak, N., Hongsak, T., & Manajuti, D. (2007). Variability of Soil Resources in Northern Thailand. In F. Heidhues, L. Herrmann, A. Neef, S. Neidhart, J. Pape, P. Sruamsiri, … A. Valle Zárate (Eds.), *Sustainable Land Use in Mountainous Regions of Southeast Asia: Meeting the Challenges of Ecological, Socio-Economic and Cultural Diversity* (pp. 21–36). Berlin: Springer. Retrieved from https://link-springer-com.ezproxy2.utwente.nl/content/pdf/10.1007%2F978-3-540-71220-6.pdf

Hudson, N. W. (1981). *Soil Conservation* (2nd ed.). London: Batsford.

Hunink, J. E., Terink, W., Contreras, S., & Droogers, P. (2015). *Scoping Assessment of Erosion Levels for the Mahale region, Lake Tanganyika, Tanzania*. Wageningen: FutureWater. Retrieved from https://www.futurewater.nl/wp-content/uploads/2015/12/LakeTanganyikaErosion_FW148.pdf

Illinois Soil Classifiers Association. (2010). Understanding Soil. Washington, D.C.: United States Department of Agriculture. Retrieved from http://www.illinoissoils.org/Links_Files/Understanding Soils_Final2.pdf

ISRIC. (2017). SoilGrids - Global Gridded Soil Information. Retrieved May 27, 2018, from https://www.soilgrids.org/#!/?layer=taxnwrb_250m

Jasiewicz, J., & Stepinski, T. F. (2013). Geomorphons - A Pattern Recognition Approach to Classification and Mapping of Landforms. *Geomorphology, 182*, 147–156. https://doi.org/https://doi.org/10.1016/j.geomorph.2012.11.005

Jenness, J. (2006). Topographic Position Index (tpi_jen.avx) Extension for ArcView 3.x, v. 1.2. Jenness Enterprises. Retrieved from http://www.jennessent.com/arcview/tpi.htm

Jetten, V. (2018a). *OpenLISEM - Multi-Hazard Land Surface Process Model: Documentation & User Manual*. Enschede: Faculty of Geoinformation Science and Earth Observation, University of Twente. Retrieved from https://blackboard.utwente.nl/bbcswebdav/pid-1150496-dt-content-rid-3065950_2/courses/M18-AES-113/documentation15_OpenLISEM.pdf

Jetten, V. (2018b). Saxtons Pedotransfer Function SWAP Model 2005 for SoilGrids. Enschede: ITC.

Klute, A., & Dirksen, C. (1986). Hydraulic Conductivity and Diffusivity. Laboratory Methods. In A. Klute (Ed.), *Methods of Soil Analysis, Part 1. Physical and Mineralogical Methods* (pp. 687–734). Madison, WI: American Society of Agronomy.

Kodiwo, M., Oindo, B., & Ang'awa, F. (2014). Intensity of Farmland Cultivated and Soil Bulk Density in Different Physiographic Units in Nyakach District. *Journal of Humanities and Social Science, 19*(1), 86–91. Retrieved from www.iosrjournals.org

Kramm, T., Hoffmeister, D., Curdt, C., Maleki, S., Khormali, F., & Kehl, M. (2017). Accuracy Assessment of Landform Classification Approaches on Different Spatial Scales for the Iranian Loess Plateau. *International Journal of Geoinformation, 6*(366), 1–22. https://doi.org/10.3390/ijgi6110366

Labrière, N., Locatelli, B., Laumonier, Y., Freycon, V., & Bernoux, M. (2015). Soil Erosion in the Humid Tropics: A Systematic Quantitative Review. *Agriculture, Ecosystems and Environment, 203*, 127–139. https://doi.org/10.1016/j.agee.2015.01.027

Lorsirirat, K., & Maita, H. (2006). Soil Erosion Problems in Northeast Thailand: A Case Study from the View of Agricultural Development in a Rural Community Near Khon Kaen General status of soil erosion and agricultural development in Thailand. In *Disaster Mitigation of Debris Flows, Slope Failures and Landslides* (pp. 675–686). Tokyo: Universal Academy Press, Inc.

Mahalder, B., Schwartz, J., Palomino, A. M., & Zirkle, J. (2016). Relationship between Cohesive Soil Erosion Behavior and the Physical and Geochemical Properties of Soil in Tennessee, USA. In *Proceedings of the 2016*

World Environmental and Water Resources Congress (pp. 352–361). World Environmental And Water Resources Congress. https://doi.org/10.1061/9780784479872.036

Martin, W. E., & Bridgmon, K. D. (2012). *Quantitative and Statistical Research Methods: From Hypothesis to Results*. New Jersey: John Wiley & Sons.

Medeiros, P. H. A., Guntner, A., Francke, T., Mamede, G. L., & Araujo, J. C. de. (2010). Modelling Spatio-temporal Patterns of Sediment Yield and Connectivity in a Semi-arid Catchment with the WASA-SED Model. *Hydrological Sciences Journal*, *55*(4), 1–13. https://doi.org/10.1080/02626661003780409

Melaku, N. D., Renschler, C. S., Holzmann, H., Strohmeier, S., Bayu, W., Zucca, C., … Klik, A. (2018). Prediction of Soil and Water Conservation Structure Impacts on Runoff and Erosion Processes Using SWAT Model in the Northern Ethiopian Highlands. *Journal of Soils and Sediments*, *18*, 1743–1755. https://doi.org/10.1007/s11368-017-1901-3

Miller, B. A. (2014). Relief Analysis Toolbox. Retrieved January 24, 2019, from http://glsi.agron.iastate.edu/relief-analysis-toolbox/

Miller, B. A., & Schaetzl, R. J. (2015). Digital Classification of Hillslope Position. *Soil Science Society of America Journal*, *79*(1), 132. https://doi.org/10.2136/sssaj2014.07.0287

Mohamadi, M. A., & Kavian, A. (2015). Effects of Rainfall Patterns on Runoff and Soil Erosion in Field Plots. *International Soil and Water Conservation Research*, *3*, 273–281. https://doi.org/10.1016/j.iswcr.2015.10.001

Moonjun, R. (2007). *Application of Artificial Neural Network and Decision Tree in A GIS-based Predictive Soil Mapping for Landslide Vulnerability Study: A Case Study of Hoi Num Rin Sub-watershed, Thailand. (Masters Thesis).* International Institute for Geo-Information Science and Earth Observation, Enschede, The Netherlands. Retrieved from https://webapps.itc.utwente.nl/librarywww/papers_2007/msc/aes/ruamporn.pdf

Morgan, R. P. C. (2001). A Simple Approach to Soil Loss Prediction: A Revised Morgan-Morgan-Finney Model. *Catena*, *44*(4), 305–322. https://doi.org/10.1016/S0341-8162(00)00171-5

Morgan, R. P. C. (2005). *Soil Erosion and Conservation* (3rd ed.). Malden: Blackwell Publishing. Retrieved from http://svgaos.nl/wp-content/uploads/2017/02/Morgan_2005_Soil_Erosion_and_Conservation.pdf

Morgan, R. P. C., & Duzant, J. H. (2008). Modified MMF (Morgan–Morgan–Finney) Model for Evaluating Effects of Crops and Vegetation Cover on Soil Erosion. *Earth Surf. Process. Landforms*, *32*, 90–106. https://doi.org/10.1002/esp.1530

Morgan, R. P. C., Quinton, J. N., Smith, R. E., Govers, G., Poesen, J. W. A., Auerswald, K., … Silsoe. (1998). *The European Soil Erosion Model (EUROSEM): Documentation and User Guide*. Silsoe College, Cranfield University, Bedford.

Munoz, C., Zagal, E., & Ovalle, C. (2007). Influence of Trees on Soil Organic Matter in Mediterranean Agroforestry Systems: An Example from the ' Espinal ' of Central Chile. *European Journal of Soil Science*, *58*, 728–735. https://doi.org/10.1111/j.1365-2389.2006.00858.x

Näschen, K., Diekkrüger, B., Leemhuis, C., Steinbach, S., Seregina, L. S., Thonfeld, F., & Linden, R. Van Der. (2018). Hydrological Modeling in Data-Scarce Catchments: The Kilombero Floodplain in Tanzania. *Water*, *10*(599), doi:10.3390/w10050599.

Oku, E., Essoka, A., & Thomas, E. (2010). Variability in Soil Properties Along an Udalf Toposequence in the Humid Forest Zone of Nigeria. *Kasetsart Journal - Natural Science*, *44*(4), 564–573.

Pagliai, M., & Vignozzi, N. (2006). Soil Porosity as an Indicator of Soil Health. *Annals of Arid Zone*, *45*(3&4), 259–286.

Panagos, P., Jones, A., Bosco, C., & Senthil, K. P. S. (2011). European Digital Archive on Soil Maps (EuDASM): Preserving Important Soil Data for Public Free Access. *International Journal of Digital Earth*, *4*(5), 434–443.

Panomtaranichagul, M., & Nareuban, S. (2005). Improvement of Water Harvesting and Anti-Erosive Cultural Practices for Sustainable Rainfed Multiple Crop Production on Sloping Land. In *Conference on International Agricultural Research for Development Improvement held on 11-13 October 2005 at Stuttgart-Hohenheim, Germany* (pp. 1–5). Stuttgart-Hohenheim. Retrieved from http://www.tropentag.de/2005/abstracts/full/490.pdf

Panomtaranichagul, M., Sukkasem, C., Peukrai, S., & Deedlek, S. (2002). *Comparative Evaluation of Cultural Practices to Improve Soil Productivity and Crop Water Use Efficiency on Highland Slope in Northern Thailand. Improving the Productivity and Sustainability of Crop Systems on fragile Slopes in the Highlands of South East Asia, SHASEA Project, Final Report*. Brussels: International Cooperation with Developing Countries.

Renard, K. G., Foster, G. R., Weesies, G. A., & Porter, J. I. (1991). RUSLE: Revised Universal Soil Loss Equation. *Journal of Soil and Water Conservation*, *46*(1), 30–33. Retrieved from https://www.tucson.ars.ag.gov/unit/publications/PDFfiles/775.pdf

Sakİn, E. (2012). Organic Carbon, Organic Matter and Bulk Density Relationships in Arid-Semi Arid Soils in Southeast Anatolia Region. *African Journal of Biotechnology*, *11*(6), 1373–1377. https://doi.org/10.5897/AJB11.2297

Santos, J. C. N. dos, Andrade, E. M. De, Henrique, P. H. A., Medeiros, A., Guerreiro, M. J. S., & Palácio, H. A. de Q. P. (2017). Land Use Impact on Soil Erosion at Different Scales in the Brazilian Semi-Arid. *Revista Ciência Agronômica*, *48*(2), 251–260. https://doi.org/10.5935/1806-6690.20170029

Sarkar, T., & Mishra, M. (2018). Soil Erosion Susceptibility Mapping with the Application of Logistic Regression and Artificial Neural Network. *Journal of Geovisualization and Spatial Analysis*, *2*, 8. https://doi.org/10.1007/s41651-018-0015-9

Sarki, A., Mirjat, M. S., Mahessar, A. A., Kori, S. M., & Qureshi, A. L. (2014). Determination of Saturated Hydraulic Conductivity of Different Soil Texture Materials. *Journal of Agriculture and Veterinary Science*, *7*(12), 56–62. https://doi.org/10.9790/2380-071245662

Saxton, K. E., & Rawls, W. J. (2006). Soil Water Characteristic Estimates by Texture and Organic Matter for Hydrologic Solutions. *Soil Science Society of America Journal*, *70*, 1569–1578. https://doi.org/10.2136/sssaj2005.0117

Saxton, K. E., Rawls, W. J., Romgerger, J. S., & Pipendick, R. I. (1986). Estimating Generalized Soil Water Characteristics from Texture. *Transactions of ASAE*, *50*, 1031–1035.

Schertz, D. L. (1983). The Basis for Soil Loss Tolerance. *Journal of Soil and Water Conservation*, *38*, 10–14.

Scholten, J. J., & Siriphant, C. (1973). *Soils and Land Forms of Thailand*. Bangkok: Soil Survey Division of the Ministry of Agriculture and Cooperatives. Retrieved from https://library.wur.nl/isric/fulltext/isricu_i3963_001.pdf

Schoorl, J. M., Sonneveld, M. P. W., & Veldkamp, A. (2000). Three-dimensional Landscape Process Modelling: The Effect of DEM Resolution. *Earth Surface Processes and Landforms*, *25*(9), 1025–1034. https://doi.org/10.1002/1096-9837(200008)25:9<1025::AID-ESP116>3.0.CO;2-Z

Schuler, U., Choocharoen, C., Elstner, P., Neef, A., Stahr, K., Zarei, M., & Herrmann, L. (2006). Soil Mapping for Land-use Planning in a Karst Area of N. Thailand with due Consideration of Local Knowledge. *Journal of Plant Nutrition and Soil Science*, *169*, 444–452. https://doi.org/10.1002/jpln.200521902

Shrestha, D. P. (2018). Vegetation Canopy Changes and Use of SoilGrids Data for Assessing the Effect of Extreme Rains on Annual Soil Losses. In *Asian Conference on Remote Sensing Held on 15 - 19 October 2018 at Renaissance Hotel, Kuala Lumpur, Malaysia* (pp. 763–770).

Shrestha, D. P., & Jetten, V. J. (2018). Modelling Erosion on a Daily Basis: An Adaptation of the MMF Approach. *International Journal of Applied Earth Observation and Geoinformation*, *64*, 117–131. https://doi.org/10.1016/j.jag.2017.09.003

Shrestha, D. P., Suriyaprasit, M., & Prachansri, S. (2014). Assessing soil erosion in inaccessible mountainous areas in the tropics: The use of land cover and topographic parameters in a case study in Thailand. *Catena*, *121*, 40–52. https://doi.org/10.1016/j.catena.2014.04.016

Soil Survey Staff. (2014). *Soil Survey Field and Laboratory Methods Manual*. (R. Burt & Soil Survey Staff, Eds.) (2nd ed.). Washington, D.C.: United States Department of Agriculture, Natural Resources Conservation Service.

Sonneveld, M. P. W. A., Temme, A. J. A. M. A., Schoorl, J. M. A., Claessens, L. A., Viveen, W. A., & Baartman, J. E. M. A. (2010). Landscape - Soilscape Evolution Modelling: LAPSUS. In *19th World Congress of Soil Science, Soil Solutions for a Changing World held on 1 – 6 August 2010 at Brisbane, Australia* (pp. 12–15). Brisbane: World Congress of Soil Science.

Starkloff, T., & Stolte, J. (2014). Applied Comparison of the Erosion Risk Models EROSION 3D and LISEM for a Small Catchment in Norway. *Catena*, *118*, 154–167. https://doi.org/10.1016/j.catena.2014.02.004

Stocking, M. (1981). *A Working Model for the Estimation of Soil Loss Suitable for Underdeveloped Areas*. Norwich: School of Development Studies, University of East Anglia.

Tingting, L. V., Xiaoyu, S., Dandan, Z., Zhenshan, X., & Jianming, G. (2008). Assessment of Soil Erosion Risk in Northern Thailand. *International Archives of the Photogrammetry, Remote Sensing and Spatial Information Sciences*, *XXXVII*(B8), 703–708.

Veselsky, M., Bandura, P., Burian, L., Harcinikova, T., Bella, P., & Gis, G. (2015). Semi-automated Recognition of Planation Surfaces and other Flat Landforms: A Case Study from the Aggtelek Karst, Hungary. *Open Geosciences*, *7*(1), 7–9. https://doi.org/10.1515/geo-2015-0063

Vlassak, K. S., Ongprasert, A., Tancho, K., Look, V., Turkelboom, F., & Ooms, L. (1993). *Soil Fertility Conservation: Research Report. 1989 – 1992*. Brussels: MJU, Thailand-KULeuven, VLIR-ABOS.

Wang, W., Yin, S., Xie, Y., Liu, B., & Liu, Y. (2016). Effects of Four Storm Patterns on Soil Loss from Five Soils under Natural Rainfall. *Catena*, *141*, 56–65. https://doi.org/10.1016/j.catena.2016.02.019

Weiss, A. D. (2001). Topographic Position and Landforms Analysis (Poster Presentation). In *ESRI International User Conference, held at San Diego, USA*. Retrieved from http://www.jennessent.com/downloads/tpi-poster-tnc_18x22.pdf

Whitford, W. G., & Eldridge, D. J. (2013). Effects of Ants and Termites on Soil and Geomorphological Processes. *Ecogeomorphology*, *12*, 281–292. https://doi.org/10.1016/B978-0-12-374739-6.00335-3

Wicharuck, S., Erbe, P., Schuler, U., Inthasan, J., Herrmann, L., & Stahr, K. (2010). Influence of Land Use Systems on Soil Resources in Northern Thailand. In *19th World Congress of Soil Science, Soil Solutions for a Changing World held on 1 – 6 August 2010 at Brisbane, Australia* (pp. 64–67). Brisbane: International Union of Soil Sciences. Retrieved from https://iuss.org/19th WCSS/Symposium/pdf/0344.pdf

Wischmeier, W. H., & Smith, D. D. (1978). *Predicting Rainfall Erosion Losses: A Guide to Conservation Planning*. Washington, D.C.: United States Department for Agriculture.

Woolhiser, D. A., Smith, R. E., & Goodrich, D. C. (1990). *KINEROS, A Kinematic Runoff and Erosion Model: Documentation and User Manual* (ARS-77). Washington, D.C.: United States Department for Agriculture, Agricultural Research Service.

APPENDIX

Appendix 2-1: Data requirements

S/N	FACTOR	PARAMETER	DEFINITION AND REMARK
1.	Rainfall	R	Annual or mean annual rainfall (mm)
		R_n	Number of rainy days per annum
		I	Typical value for intensity of erosive rains (mm/h): 10 for temperate climate, 25 for tropical climate and 30 for strongly seasonal climates (e.g. Monsoon)
2.	Soil	MS	Soil moisture content at field capacity or 1/3 bar tension (5w/w)
		BD	Bulk density of topsoil layer (Mg/m^3)
		EHD	Effective hydrological depth of soil (m); depends on vegetation / crop cover, presence / absence of surface crust, presence of impermeable layer within 0.15m from the surface
		K	Soil detachability index (g/J) defined as the weight of soil detached from the soil mass per unit of rainfall energy
		COH	Cohesion of surface soil (kPa), as measured with the torvane under saturated condition
3	Landform	S	Slope steepness (°)
4	Land Cover	A	Proportion (between 0 and 1) of the rainfall intercepted by vegetation or crop cover
		E_t / E_o	Ratio of actual (E_t) to potential (E_o) evapotranspiration
		C	Crop cover management factor; combines the C and P factors of the Universal Soil Loss Equation
		CC	Percentage canopy cover (expressed as a proportion between 0 and 1)
		GC	Percentage ground cover (expressed as a proportion between 0 and 1)
		PH	Plant height (m) representing the height from which raindrops fall from the crop / vegetation cover to the ground surface

Source: Morgan (2001)

Appendix 2-2: Site description form

Site No:	Described by:		Geology & Parent Material:
Photo No:	Date:		

Location:		Longitude (X):	
		Latitude (Y):	

Classification:	Topography	Land Use:
	Altitude:	
	Slope:	Vegetation:
	Aspect:	
	Landform:	
	Landscape Position:	
	Surface Shape:	

Horizon name	Depth (cm)	Colour (Munsell)	Texture	Structure	Roots	pH	Ksat	Shear Strength (kPa)

Notes:

Land Cover Data Sheet				
Layer	Land Use Type	Height (cm)	Cover (%)	Dominant Species
Grass				
Thicket				
Arable Crops				
Tree Crops				
Trees (Natural)				
Bare				
Water				
Built-up Areas				
Notes:				

Appendix 2-3: PCRaster model codes for SoilGrids250m pedotransfer functions

```
###############################################################
# Model: Saxtons pedotransfer function SWAP model 2005 # #
# input data SOILGRIDS.ORG #
# Date: 05/04/2018 #
# Version: 1.1 #
# Author: V Jetten @ ITC #
###############################################################
# $1 = soilgrids layer indication, e.g. "sl2"
# $2 is lisem layer, 1 or 2
# $3 is the degree of saturation between porosity and field capacity,
# used for the initial moisture content and initial suction head
# $4 is the bulk density you consider normal (uncompacted and not loose) in the area in kg/m3

#! ;; sl2 1 0.7

binding
S = sand1.map; #sand %
C = clay1.map; #clay %
# OC = oc$1.map; #organic carbon in %
Gravel = gravels1.map; #coarse fragments %, note in excel sheet it says g/cc
# but this is not correct, it is used as a volume fraction
OC = oc1.map;
bdsg=bulk1.map; #bulkdensity kg/m3
standardBD = scalar(1470); # <= used to calibrate output
fractionmoisture = scalar(0.7);
#inital moisture as fraction between porosity and field capacity
# 0 = init moist is at FC, 1.0 = init moist is at porosity
POROSITY = pore.map; #porosity (cm3/cm3)
Ksat = ksat.map; # ksat in mm/h
initmoist =thetainit.map; # inital moisture (cm3/cm3)
psi=psi1.map; # suction with init moisture in cm, used in LISEM
se = se.map; # relative moisture content between 0-1
Densityfactor = densfact.map;

BD = bulkdens.map; # ton/m3
WP = wilting.map; # wilting point moisture content
FC = fieldcap.map; # field capacity moisture content
PAW = plantAVW.map;
sand = sand.map;
clay = clay.map;
grav = graveln.map;
dem = dem30.map;

initial

# prep data
S = S/100;
C = C/100;
OC= (OC/1000)*100; # conversion OC from g/kg to percentage
OM = OC/2.0; #conversion org carbon to org matter factor 2
```

```
report om.map = OM;


Gravel = Gravel/100;
report Densityfactor = bdsg/standardBD;#scalar(1.0); # upper boundary 1.15
# calculated as the bulk density from soilgrids divided by some standard bd
# multiple regression from excel


# wilting point stuff
M1500 =-0.024*S+0.487*C+0.006*OM+0.005*S*OM-0.013*C*OM+0.068*S*C+0.031; #W18)
# =-0.024*F18+0.487*G18+0.006*H18+0.005*F18*H18-0.013*G18*H18+0.068*F18*G18+0.031
M1500adj =M1500+0.14*M1500-0.02; #X18) =W18+0.14*W18-0.02
# field capacity stuff
M33 =-0.251*S+0.195*C+0.011*OM+0.006*S*OM-0.027*C*OM+0.452*S*C+0.299; #Y18)
#=-0.251*F18+0.195*G18+0.011*H18+0.006*F18*H18-0.027*G18*H18+0.452*F18*G18+0.299
M33adj = M33+(1.283*M33*M33-0.374*M33-0.015); #Z18) =Y18+(1.283*Y18*Y18-0.374*Y18-0.015)
# porosity - FC
PM33 = 0.278*S+0.034*C+0.022*OM-0.018*S*OM-0.027*C*OM-0.584*S*C+0.078; #AA18)
#=0.278*F18+0.034*G18+0.022*H18-0.018*F18*H18-0.027*G18*H18-0.584*F18*G18+0.078
PM33adj = PM33+(0.636*PM33-0.107); #AB18) =AA18+(0.636*AA18-0.107)
# porosity
SatPM33 = M33adj + PM33adj; #AC18) =AB18+Z18
SatSadj = -0.097*S+0.043; #AD18) =-0.097*F18+0.043
SadjSat = SatPM33 + SatSadj; #AE18) =AC18+AD18
Dens_om = (1-SadjSat)*2.65; #AF18) =(1-AE18)*2.65
Dens_comp = Dens_om * Densityfactor; #AG18) =AF18*(I18)
PORE_comp =(1-Dens_om/2.65)-(1-Dens_comp/2.65); #AI18) =(1-AG18/2.65)-(1-AF18/2.65)
M33comp = M33adj + 0.2*PORE_comp; #AJ18) =Z18+0.2*AI18


#output
report POROSITY = 1-(Dens_comp/2.65); #AH18)
PoreMcomp = POROSITY-M33comp; #AK18)
LAMBDA = (ln(M33comp)-ln(M1500adj))/(ln(1500)-ln(33)); #AL18)
GravelRedKsat =(1-Gravel)/(1-Gravel*(1-1.5*(Dens_comp/2.65))); #AM18)
report Ksat = max(0.0, 1930*(PoreMcomp)**(3-LAMBDA)*GravelRedKsat); #AN18)
report BD = Gravel*2.65+(1-Gravel)*Dens_comp; #U18
report WP = M1500adj;
report FC = M33adj;
report PAW = (M33adj - M1500adj)*(1-Gravel);
report initmoist= fractionmoisture*POROSITY+ (1-fractionmoisture)*FC;


# A = exp[ln(33) + B ln(T33)]
# B = [ln(1500) - ln(33)] / [ln(T33) - ln(T1500)]
bB = (ln(1500)-ln(33))/(ln(FC)-ln(WP));
aA = exp(ln(33)+bB*ln(FC));
report psi= aA * initmoist**-bB *100/9.8;
report se.map = initmoist/POROSITY;



#report av_Ksat.map = areaaverage(Ksat, nominal(landunit.map));
#report area.map = areaarea(nominal(landunit.map));
```

Appendix 2-4: RMMF model codes for PCRaster

```
# Annual soil erosion estimation using RMMF model
# by D. Shrestha, April 2015, ITC


#! --matrixtable --lddout


binding
# input maps
dem = dem.map;
soil = soil.map;
landuse = landuse.map;
landuse_sl = luse_slope.map;
LDD = ldd.map;
mask = mask.map;


# output maps
Ksat = ksat.map; # saturated hydraulic conductivity (mm/day)


Erosion = erosion${1}a.map;
Erosion_rate = erosion_rate${1}a.map;
Detachment = detachment${1}a.map;
Deposition = deposition${1}a.map;
tonhaavg = tonhaavg${1}a.map;
tonhaavg_sl = tonhaavg${1}asl.map;
tonhaavg_tss = tonhaavg${1}a.tss;
tonhaavg_sl_tss = tonhaavg${1}asl.tss;
rofavg = rof${1}a.map;


# input tables
landuse_tbl = landuse.tbl;
soil_tbl = soil.tbl;
infil = infil.map;
MS = fc.map;


# average values for interception fraction, Et/E0 and cover, avg per landuse type
# derived from daily model with areaaverage operation
mmfA = mmfA${1}.map;
mmfEtE0 = mmfEtE0${1}.map;
mmfCC = mmfCC${1}.map;
Et_Eo = Et_Eo.map;
areamap
mask.map;
# timer
# this section is empty since it is annual model
initial


annualrain = 1380.3;
rdays = 117;
ups=accuflux(LDD,cellarea()/10000);
```

```
smallcatchment = mask * scalar(ups le 1);

# soil *= mask;
# landuse *= mask;

#units (1=arable land, 2=orchard, 3=forest, 4=built-up, 5=teak plantation)

## Et_Eo = mmfEtE0;
## A = mmfA;
## CC = mmfCC; # average annual cover per LU class from daily
report Et_Eo = lookupscalar(landuse_tbl, 1, landuse)*mask;
# C = lookupscalar(landuse_tbl, 2, landuse); # Cover factor
# is 1 - CC with absense of management factors
EHD = lookupscalar(landuse_tbl, 3, landuse); # Effective hydrological depth
EHD = EHD * 1000; #mm
# A = lookupscalar(landuse_tbl, 4, landuse); # A is rain interception factor in percentage
CC = lookupscalar(landuse_tbl, 5, landuse); # CC is NDVI canopy cover in percentage
SC = lookupscalar(landuse_tbl, 6, landuse); # SC is surface cover in percentage
PH = lookupscalar(landuse_tbl, 7, landuse); # PH is plant height in m
SC = if(landuse eq 1, 0.33 * CC, SC);
# base SC for non-permanent vegetation on CC
C = 1-CC; # cover factor = 1 - canopy cover


# generating soil attributes from soil map
K = lookupscalar(soil_tbl, 2, soil); # soil erodibility factor
Coh = lookupscalar(soil_tbl, 3, soil); # cohesion of soil in kPa
PORE = lookupscalar(soil_tbl, 6, soil); # soil porosity
MS = lookupscalar(soil_tbl, 7, soil); # soil moisture at field capacity
WP = lookupscalar(soil_tbl, 8, soil);
Ksat =24* lookupscalar(soil_tbl, 5, soil); # reading saturated hydraulic conductivity in mm/hr
#Ksat = if(landuse eq 3 or landuse eq 5, Ksat*1.5, Ksat);
# generating slope gradient and sinus of slope
grad = slope(dem);
sinS = sin(atan(grad));
# calculating A from Smax and rainy days
LAI = ln(1-CC)/-0.4;
Smax1 = 0.935 + 0.498*LAI - 0.00575; # Field crops
Smax2 = 1.46*LAI**0.56; # Olive
Smax3 = max(0, 0.9117*ln(LAI+0.01) + 0.7027); # clumped grass
Smax = if(landuse eq 1, Smax1, if((landuse eq 2 or landuse eq 3 or landuse eq 5), Smax2, Smax3));

A = rdays * Smax/annualrain;

###########################################################

# Computing Kinetic energy of rainfall in J/m2
rain = mask * annualrain;
ER = rain * (1-A); # Effective rainfall
LD = ER * CC; # Computing leaf drainage
DT = ER - LD; # Direct throughfall
KE_DT = DT*(9.81 + 11.25*log10(30)); # kinetic energy of DT in J/m2 according to Zanchi and Torri(1980)
KE_LD = LD*max(0, (15.8*sqrt(PH) - 5.87)); # kinetic energy of LD in J/m2 proposed by Brandt (1990)
```

```
KE_LD = max(KE_LD, 0); # kinetic energy of leaf drainage cannot be negative
KE = KE_DT + KE_LD; # total kinetic energy of rainfall
# Estimation of runoff
theta = MS; #WP+0.5*(MS-WP);
#Rc = (PORE- theta) * EHD * Et_Eo; # NEW runoff fraction calculation)
# OR THE ORIGINAL
Rc = MS * EHD * Et_Eo; # NEW runoff fraction calculation)
Ro = ER/rdays; # average rain in a rainy day
report rofavg = exp(-Rc/Ro);

Q = accuflux(LDD, exp(-Rc/Ro)*ER); # runoff flow accumulation
runon = upstream(LDD, Q);
report infil = max(0, runon+ER-Q);



# Soil particle detachment
F = K * KE* 0.001; # detachment by raindrop Kg/m2
Z = 1/(0.5*Coh);
H = Z * (Q**1.5) * sinS * (1 - SC) * 0.001; # Soil particle detachment by runoff
report mmf_fa.map=F;
report mmf_ha.map=H*smallcatchment;
detach = F + H; # total soil detachment
detach = detach * smallcatchment;
# Transport capacity of runoff
TC = C * (Q**2)* sinS * 0.001;
TC = TC * smallcatchment;
report mmf_TCa.map=TC;
# Estimation of soil loss
eros = min(detach, TC); # soil loss in kg/m2

report Erosion = eros*10*mask; # reporting erosion map
# report Erosion_rate = scalar(if(Erosion le 1, 1, if(Erosion gt 1 and
# Erosion le 10, 10, if(Erosion gt 10 and Erosion le 20,
# 20, if(Erosion gt 20 and Erosion le 50, 50, if(Erosion gt 50 and Erosion le 100, 100, 200))))));

# Estimating sediment deposition
report Detachment = max(0, detach)*10*mask;
report Deposition = max(0, detach - TC)*10*mask;
report tonhaavg = areaaverage(eros*10, nominal(landuse));
report tonhaavg_tss = timeoutput(nominal(landuse), tonhaavg);
# report tonhaavg_sl = areaaverage(eros*10, nominal(landuse_sl));
# report tonhaavg_sl_tss = timeoutput(nominal(landuse_sl), tonhaavg_sl);
```

Appendix 2-5: Daily rainfall data for Uttaradit (2017/2018)

		Days																															
Year	Month	1	2	3	4	5	6	7	8	9	10	11	12	13	14	15	16	17	18	19	20	21	22	23	24	25	26	27	28	29	30	31	Total
2017	Oct.	0	1.7	31.1	6.1	18.1	27.3	0	0	0	21.4	6.8	0	0	0	0	2	0	2.1	0	0.6	0	14.6	0.2	1.3	0	0	0	0	0	0	0	133.3
2017	Nov.	0	0	0	0	0	0.3	0	0	0	0	0	0	0	1.8	0	0	0	0	0	0.5	0	0	2.6	0	0	0	0	0	0	0	-	5.2
2017	Dec.	0	0	0	0	0	0	0	0	0	0	0	0	0	0	0	0	0	0	0	0	0	0	0	0	0	8.1	13.8	3.3	0	0	0	25.2
2018	Jan.	0	0	0	0	0	0	0	0	0	0	2	0	0	0	0	0	0	0	0	0	0	0	0	0	0	5	0	0	0	0	0	7
2018	Feb	0	0	0	0	0	0	0	0	0	0	0	0	0	0	0	0	0	0	0	0	0	12.3	0	0	0	0	0	0	-	-	-	12.3
2018	Mar.	0	0	0	0	0	0	0	0	0	0	0	0	0	0	0	0	0	0	0	0	0	0	0	0	0	0	1.2	0	0	1	1.4	3.6
2018	Apr.	0	1.2	0	27.6	0	0.1	1.9	0	0	0	0	0	0	0	0	24.1	0	0	0	0	0	0	0	0	0	3.1	1.2	2.2	8.1	3.2	-	72.7
2018	May	1	3	0	4.5	0	0	0	0	0	5.3	1.8	5.9	14.5	0.9	0	0	0	56.1	0	0	2.8	0	93.2	1.8	0.4	35.2	36.9	1.6	10.9	4.6	0	280.4
2018	Jun.	0	0	0	0	0.7	3.2	0	0	15.1	23.8	45.7	7	0.2	0	11	6.7	0	0	10.8	0	1	0	0	0	8.5	61.5	4.7	0	0	1	-	200.4
2018	Jul.	4.6	0	0	0	0	0	0	0	1.7	0.6	0	0	0	2.3	0.2	0.5	49.8	14.5	2.6	6.8	3.5	16.5	8	1.3	0	29.4	0.3	0	0.2	0.8	4.3	147.9
2018	Aug.	0	0	6.2	0	28.2	0	0	0	120.6	32.6	0	0	4	0	1.7	0	3.9	6.4	0	2.1	45.1	6.2	0	4.9	0	10	16.6	9.4	0	0	3.1	301
2018	Sep.	0	0	1.4	2.1	8.4	3.4	0	10.3	2.1	0	45.1	0	0	0	0	0	0	63.3	0.4	0	0	T	3.5	0	0	0	0	43.5	1	6.6	-	191.1

Source: Meteorological Station 351201, Uttaradit, Thailand

**Appendix 3-1:** Morphological properties of the soil

| Site	Longitude	Latitude	Soil Map Unit	Altitude	Soil Depth (cm)	Munsell Colour Notation	Soil Colour	% Clay	% Sand	% Silt	Soil Textural Class
1	619771	1967551	Summit/Shoulder	204	80	10R5/1	Reddish Grey	19	59	22	Sandy Loam
2	618856	1968672	Foot Slope	168	90	10YR7/4	Very Pale Brown	29	38	33	Clay Loam
3	618942	1968680	Valley Floor	158	-	10YR5/3	Brown	12	61	27	Sandy Loam
4	618249	1967020	Foot Slope	123	100	7.5YR6/4	Light Brown	25	38	37	Loam
5	618225	1969653	Foot Slope	154	100	10YR7/4	Very Pale Brown	21	37	41	Loam
6	618984	1970672	Back Slope	251	80	7.5YR7/6	Reddish Yellow	45	12	44	Silty Clay
7	617962	1971016	Valley Floor	170	100	7.5YR7/2	Pinkish Grey	26	25	49	Loam
8	617491	1969031	Valley Floor	154	100	10YR7/6	Yellow	36	13	51	Silty Clay Loam
9	617105	1968991	Summit/Shoulder	206	100	10YR6/6	Brownish Yellow	46	15	39	Clay
10	617240	1969081	Back Slope	168	100	10YR7/2	Light Grey	30	29	41	Clay Loam
11	616160	1966187	Foot Slope	129	100	10YR6/4	Light Yellowish Brown	16	45	38	Loam
12	614673	1967368	Back Slope	206	90	10YR6/4	Light Yellowish Brown	42	18	40	Silty Clay
13	614773	1967203	Back Slope	144	100	10YR6/3	Pale Brown	27	31	42	Loam
14	612130	1969421	Back Slope	163	100	10YR6/6	Brownish Yellow	41	16	43	Silty Clay
15	612205	1969377	Valley Floor	168	100	10YR7/3	Very Pale Brown	28	20	53	Silty Clay Loam
16	616224	1966862	Valley Floor	119	100	10YR7/2	Light Grey	17	52	30	Sandy Loam
17	616212	1966923	Back Slope	137	100	10YR7/4	Very Pale Brown	27	32	41	Loam
18	616236	1966966	Back Slope	150	100	10YR7/3	Very Pale Brown	23	38	38	Loam
19	610112	1970044	Back Slope	227	100	10YR7/6	Yellow	33	16	51	Silty Clay Loam
20	610574	1972634	Foot Slope	228	100	10YR6/3	Pale Brown	24	35	42	Loam
21	610571	1972681	Foot Slope	230	100	10YR7/4	Very Pale Brown	30	19	52	Silty Clay Loam
22	610531	1972616	Back Slope	214	80	10YR7/2	Light Grey	23	37	40	Loam
23	609624	1972236	Summit/Shoulder	278	100	10YR6/6	Brownish Yellow	31	27	42	Clay Loam
24	609712	1972273	Back Slope	292	100	10YR6/4	Light Yellowish Brown	26	26	48	Loam
25	609486	1972244	Back Slope	224	60	10YR6/3	Pale Brown	21	49	30	Loam
26	610540	1972106	Foot Slope	200	100	10YR6/4	Light Yellowish Brown	24	24	52	Silty Loam
27	610484	1972051	Foot Slope	220	100	10YR7/3	Very Pale Brown	32	10	59	Silty Clay Loam
28	610577	1971984	Summit/Shoulder	259	100	10YR7/4	Very Pale Brown	37	16	47	Silty Clay Loam
29	610219	1969983	Valley Floor	211	62	10YR6/4	Light Yellowish Brown	20	38	42	Loam
30	612991	1969365	Back Slope	139	100	10YR6/4	Light Yellowish Brown	17	43	41	Loam
31	615578	1970494	Foot Slope	175	100	10YR7/3	Very Pale Brown	34	28	38	Clay Loam
32	615625	1970421	Back Slope	207	100	10YR6/6	Brownish Yellow	40	18	43	Silty Clay
33	615552	1970369	Back Slope	180	61	10YR7/3	Very Pale Brown	17	39	44	Loam
34	615229	1971325	Valley Floor	169	25	10YR7/4	Very Pale Brown	33	27	40	Clay Loam
35	615286	1971318	Foot Slope	177	100	10YR7/6	Yellow	33	19	47	Silty Clay Loam
36	619063	1969265	Foot Slope	162	100	10YR8/2	Very Pale Brown	22	35	43	Loam
37	619363	1972050	Foot Slope	226	90	10YR5/2	Greyish Brown	14	54	32	Sandy Loam
38	619368	1972261	Back Slope	162	100	10YR5/3	Brown	6	57	38	Sandy Loam
39	618396	1972508	Foot Slope	255	100	10YR7/6	Yellow	11	51	37	Loam
40	618421	1972541	Foot Slope	238	100	10YR7/6	Yellow	20	35	45	Loam
41	618471	1972653	Back Slope	217	100	10YR6/4	Light Yellowish Brown	2	56	42	Sandy Loam
42	612490	1972619	Valley Floor	380	100	10YR6/4	Light Yellowish Brown	4	50	45	Sandy Loam
43	612532	1972193	Back Slope	307	100	10YR6/3	Pale Brown	5	48	47	Sandy Loam
44	610959	1972270	Foot Slope	232	100	10YR6/4	Light Yellowish Brown	15	42	43	Loam
45	611772	1970705	Foot Slope	174	100	10YR6/4	Light Yellowish Brown	5	40	55	Silty Loam
46	608972	1972152	Back Slope	233	75	10YR6/3	Pale Brown	7	55	37	Sandy Loam
47	611828	1970614	Foot Slope	160	100	10YR7/3	Very Pale Brown	3	56	42	Sandy Loam
48	616782	1965176	Foot Slope	110	100	10YR7/2	Light Grey	9	43	49	Loam

Appendix 3-2: Physico-chemical properties of the soil

Sample Site	Longitude	Latitude	Soil Map Unit	Bulk Density (Mg/m3)	Porosity (%)	Shear Strength (kPa)	Ksat (mm/hr)	Field Capacity (%)	Wilting Point (%)	Organic Matter (%)
1	619771	1967551	Summit/Shoulder	1.32	50	2.43	20.87	23.7	13.2	3.71
2	618856	1968672	Foot Slope	1.39	47.45	1.8	7.59	32.3	18.8	2.81
3	618942	1968680	Valley Floor	1.72	35.01	0.55	39.48	19.47	9.1	2.37
4	618249	1967020	Foot Slope	1.64	38.11	1.87	11.14	30.8	16.6	2.92
5	618225	1969653	Foot Slope	1.29	51.41	2	12.49	28.6	14	2.18
6	618984	1970672	Back Slope	1.21	54.42	4.8	3.74	40.8	26.8	2.78
7	617962	1971016	Valley Floor	1.42	46.26	4.8	7.46	32.7	16.7	1.98
8	617491	1969031	Valley Floor	1.2	54.74	4.7	5.8	38.2	22.2	2.82
9	617105	1968991	Summit/Shoulder	0.8	69.73	3.4	7.39	40.7	27.7	6.17
10	617240	1969081	Back Slope	1.45	45.12	4.4	7.44	34.2	19.2	2.86
11	616160	1966187	Foot Slope	1.43	45.96	3.9	26.2	26.1	12	3.23
12	614673	1967368	Back Slope	1.07	59.71	5	6.28	39.8	25.7	4.83
13	614773	1967203	Back Slope	0.99	62.7	5.4	19.4	35.3	19	5.93
14	612130	1969421	Back Slope	1.2	54.59	4.1	9.14	39.8	25.3	5.65
15	612205	1969377	Valley Floor	1.22	53.78	5.2	13.25	35.9	18.6	4.16
16	616224	1966862	Valley Floor	1.06	60.06	5.8	26.38	25.2	12.6	3.31
17	616212	1966923	Back Slope	0.98	62.92	5.07	14.35	34.1	18.5	4.6
18	616236	1966966	Back Slope	1.32	50.3	5.23	21.38	32.3	16.8	5.11
19	610112	1970044	Back Slope	1.09	58.73	5.63	8.26	37.3	20.8	3.52
20	610574	1972634	Foot Slope	1.3	51.04	6.73	15.65	32	16.7	3.96
21	610571	1972681	Foot Slope	1.07	59.64	4.97	10.16	36.2	19.4	3.69
22	610531	1972616	Back Slope	1.08	59.31	5.93	22.37	32.6	16.9	5.32
23	609624	1972236	Summit/Shoulder	1.18	55.59	6.07	8.98	35.5	20.1	3.81
24	609712	1972273	Back Slope	1.24	53.28	6.1	23.24	35.9	18.5	6.09
25	609486	1972244	Back Slope	1.29	51.28	6.05	27.06	30.3	16.4	5.67
26	610540	1972106	Foot Slope	1.36	48.73	4.87	25.32	35.5	17.3	5.82
27	610484	1972051	Foot Slope	1.09	58.91	6.57	24.14	39.3	21.1	6.67
28	610577	1971984	Summit/Shoulder	1.03	61.17	6	7.37	38.5	23	3.85
29	610219	1969983	Valley Floor	1.27	52.14	5.33	25.01	30.8	15	4.71
30	612991	1969365	Back Slope	1.22	54.03	4.5	25.75	27.4	12.8	3.6
31	615578	1970494	Foot Slope	1.12	57.63	5.2	9.54	37	22.1	5.07
32	615625	1970421	Back Slope	0.64	75.95	3.4	15.1	40	25.4	8.75
33	615552	1970369	Back Slope	1.07	59.5	5.57	32.77	29.8	13.6	4.88
34	615229	1971325	Valley Floor	1.39	47.65	3.4	7.26	36	21.1	3.62
35	615286	1971318	Foot Slope	1.27	52.2	4.9	12.84	37.8	21.4	5.24
36	619063	1969265	Foot Slope	1.58	40.51	5.73	13.27	30	14.9	2.66
37	619363	1972050	Foot Slope	1.37	48.19	4.73	51.78	27.1	13.1	5.95
38	619368	1972261	Back Slope	0.95	64.22	3.8	103.55	24.3	9.6	6.48
39	618396	1972508	Foot Slope	1.15	56.79	5.37	53.34	24.7	10.5	4.7
40	618421	1972541	Foot Slope	1.03	61.07	5.77	21.78	30.7	14.6	4.07
41	618471	1972653	Back Slope	1.04	60.64	5.37	112.08	19.9	5.9	4.83
42	612490	1972619	Valley Floor	1.19	55.17	5.77	107.85	24.6	8.1	6.05
43	612532	1972193	Back Slope	1.21	54.25	5.8	78.95	23	7.2	4.63
44	610959	1972270	Foot Slope	1.2	54.82	5.6	54.96	31.2	14	6.93
45	611772	1970705	Foot Slope	0.97	63.33	5.57	98.43	28.1	8.7	6.44
46	608972	1972152	Back Slope	1.17	55.91	5.47	100.37	25.8	10.4	6.88
47	611828	1970614	Foot Slope	1.32	50.31	5.23	90.77	18.9	5.4	3.81
48	616782	1965176	Foot Slope	1.5	43.38	6.27	50.42	24.8	8.8	3.89

Appendix 3-3: Soil detachment by raindrops (kg/m²) map from SoilGrids250m (a) and field-based data (b) and the difference map (c)
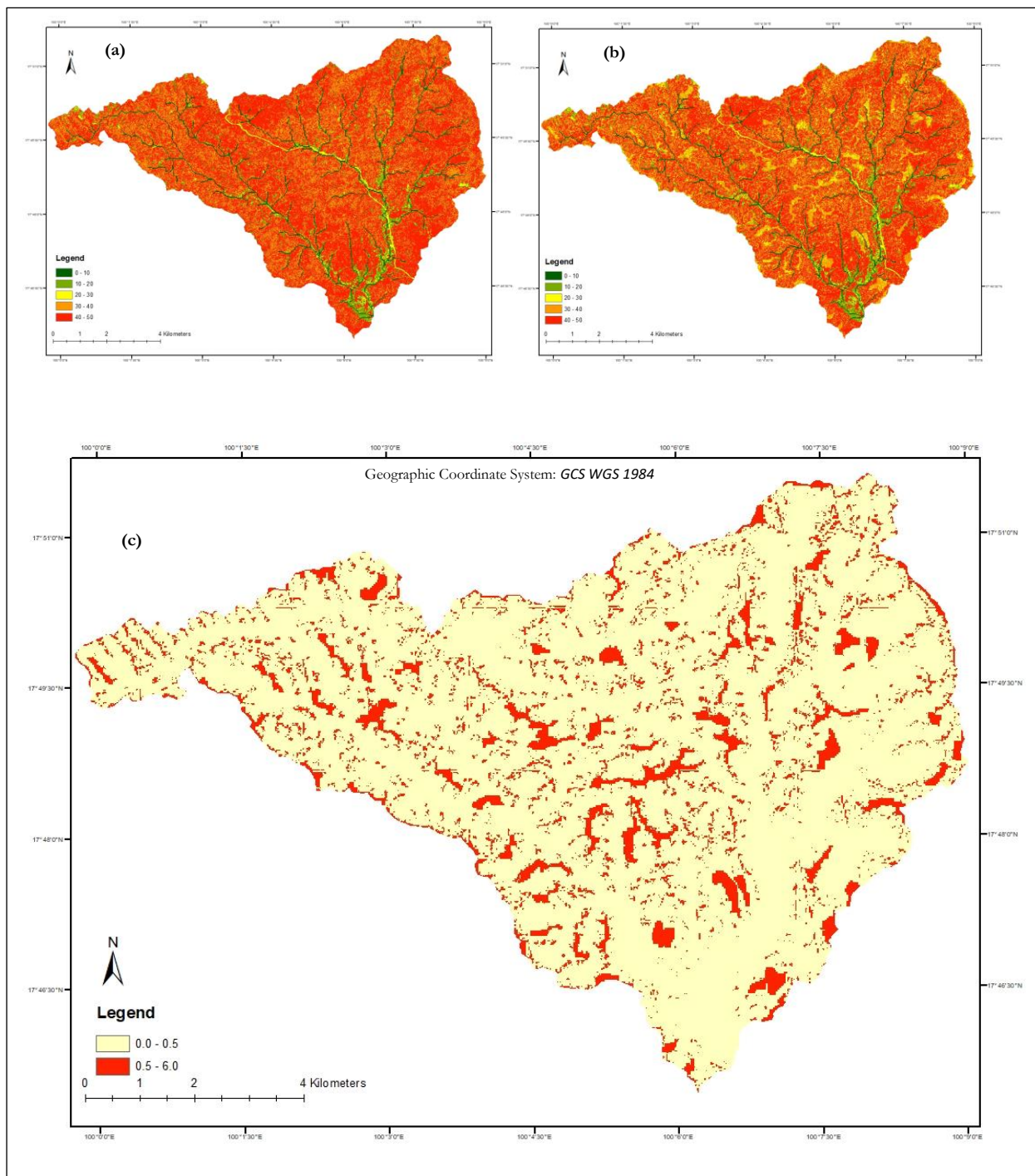
Appendix 3-4: Soil detachment by runoff (kg/m²) map from SoilGrids250m (a) and field-based data (b) and the difference map (c)
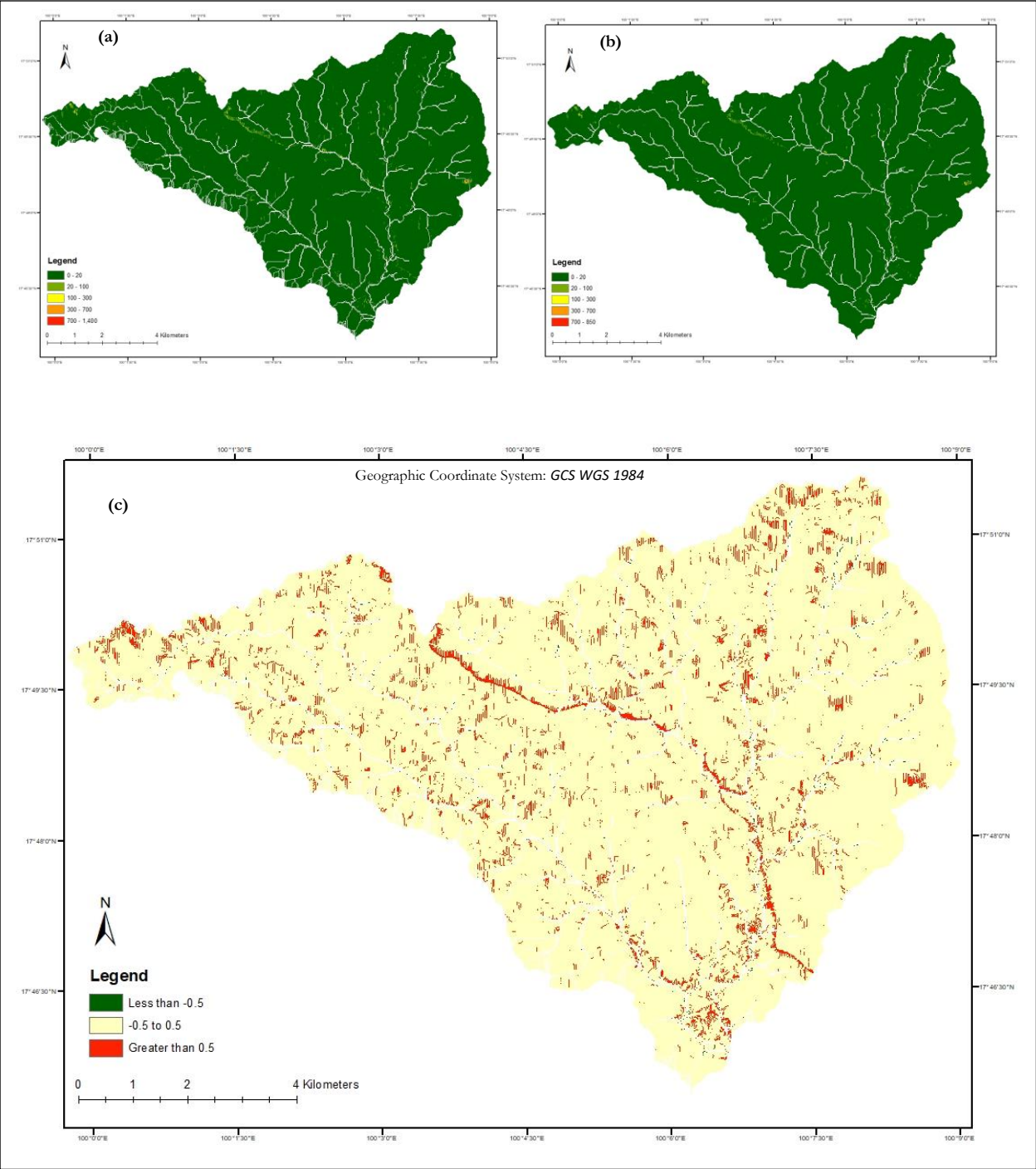
Appendix 3-5: Total soil detachment (ton/ha) map from SoilGrids250m (a), field-based data (b) and the difference map (c)

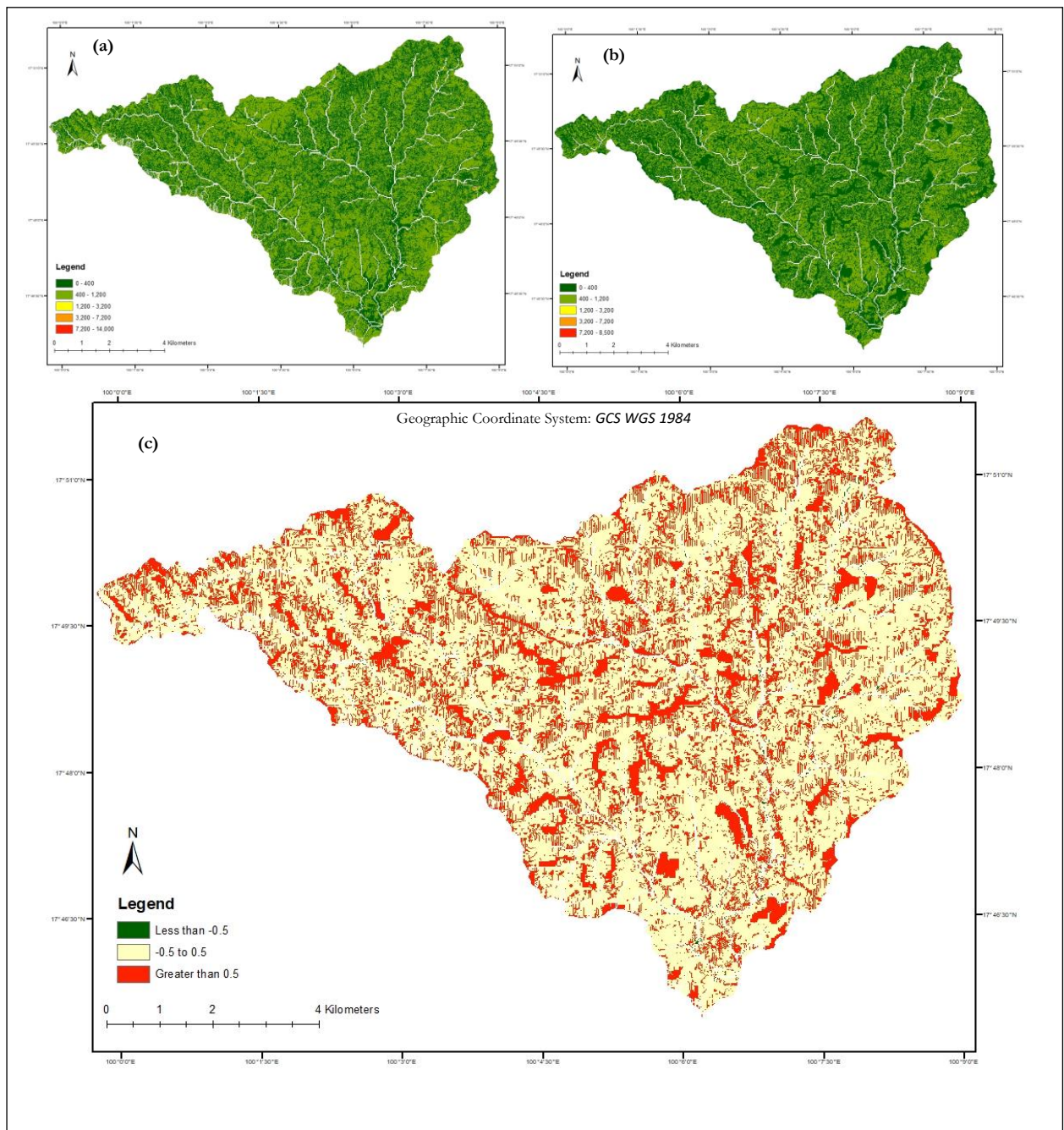**Appendix 3-6:** Runoff (mm) map from SoilGrids250m (a) and field-based data (b) and the difference map (c)
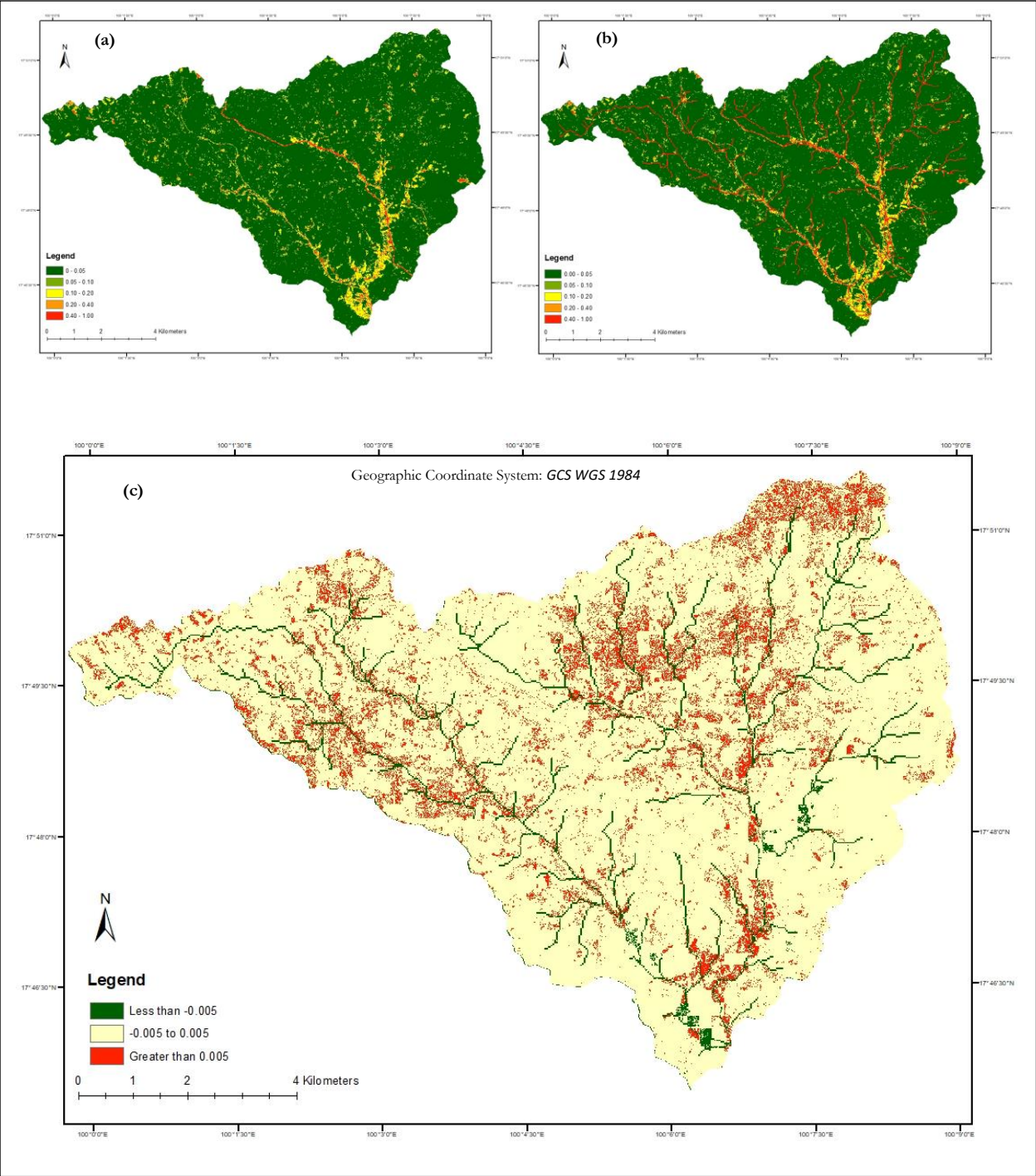
Appendix 3-7: Runoff transport capacity (kg/m²) map from SoilGrids250m (a) and field-based data (b) and the difference map (c)
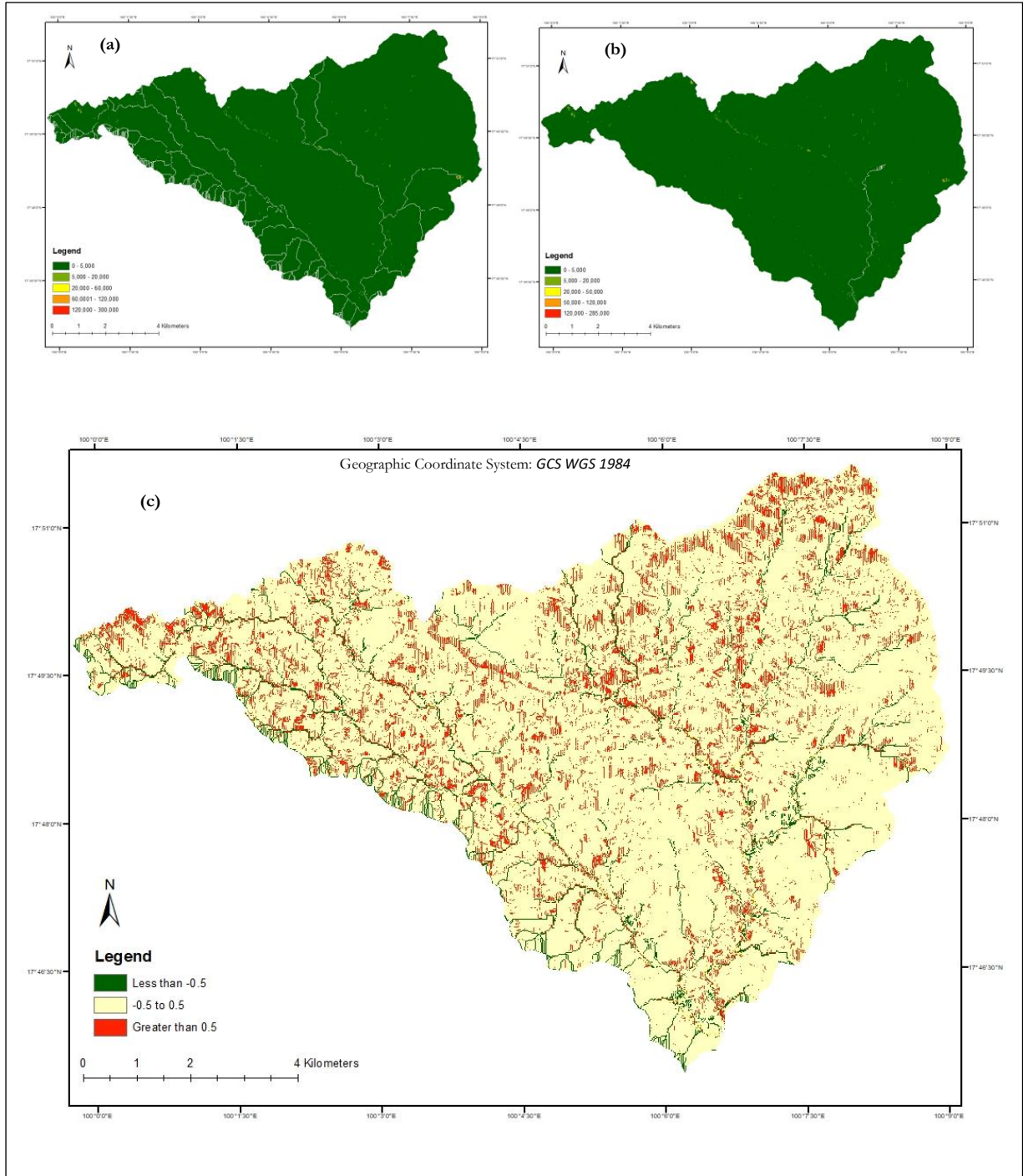
Appendix 3-8: Sediment deposition (ton/ha) map from SoilGrids250m (a), field-based data (b) and the difference map (c)
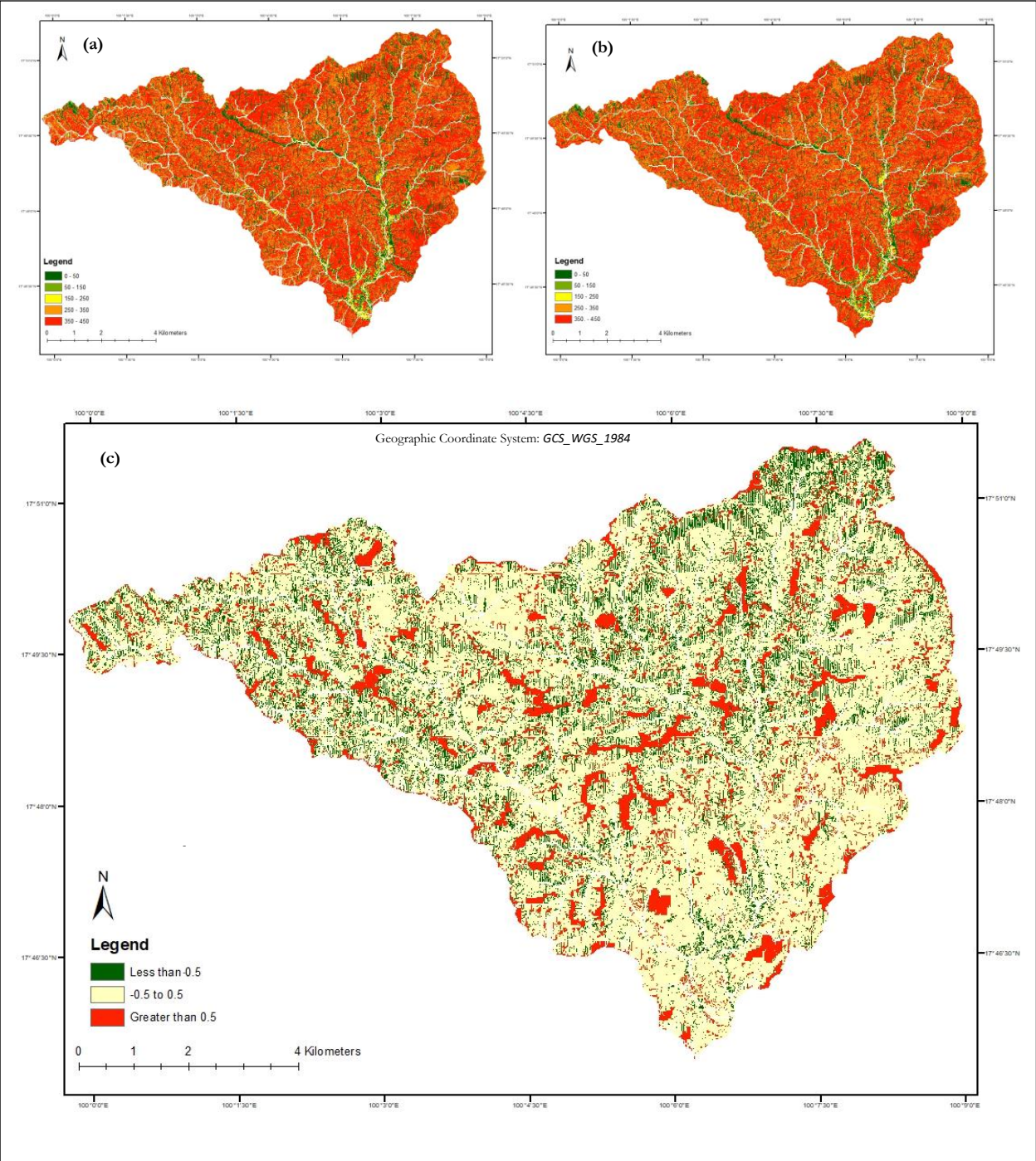
Appendix 3-9: Sensitivity of detachment by raindrops various input parameters

Factors	Parameters	Baseline	20%	40%	60%	80%	100%
Climate	RF	24.76	20.00	40.00	60.00	80.00	100.00
	RD	24.76	0.00	0.00	0.00	0.00	0.00
Soil	MS	24.76	0.00	0.00	0.00	0.00	0.00
	K	24.76	20.00	40.00	60.00	80.00	100.00
	COH	24.76	0.00	0.00	0.00	0.00	0.00
	EHD	24.76	0.00	0.00	0.00	0.00	0.00
Land Cover	Et/Eo	24.76	0.00	0.00	0.00	0.00	0.00
	C	24.76	0.00	0.00	0.00	0.00	0.00
	A	24.76	-13.47	-26.54	-39.72	-53.07	-66.15
	CC	24.76	5.53	11.42	16.90	22.79	28.32
	SC	24.76	0.00	0.00	0.00	0.00	0.00
	PH	24.76	5.92	11.37	16.43	21.19	25.70

RF = Rainfall (mm), RD = Rainy Days, MS = Field Capacity (%), K = Erodibility (kg/J), COH = Cohesion (kPa), EHD = Effective Hydrological Depth (m), Et/Eo = Ratio of Actual to Potential Evapotranspiration, C = Crop Management Factor, A = Rainfall Interception by Vegetation (mm), CC = Canopy Cover (%), SC = Surface Cover (%), PH = Plant Height (m)

Appendix 3-10: Sensitivity of detachment by runoff to various input parameters

Factors	Parameters	Baseline	20%	40%	60%	80%	100%
Climate	RF	1.153	97.27	242.99	445.14	710.26	1043.40
	RD	1.153	-34.76	-56.30	-69.23	-78.07	-83.81
Soil	MS	1.153	-33.86	-56.15	-69.32	-78.29	-83.81
	K	1.153	0.00	0.00	0.00	0.00	0.00
	COH	1.153	-16.76	-28.64	-37.55	-44.49	-50.03
	EHD	1.153	-34.51	-56.47	-69.02	-78.39	-83.81
Land Cover	Et/Eo	1.153	-34.57	-56.32	-69.23	-78.03	-83.81
	C	1.153	0.00	0.00	0.00	0.00	0.00
	A	1.153	-18.17	-30.56	-42.18	-50.90	-69.61
	CC	1.153	0.00	0.00	0.00	0.00	0.00
	SC	1.153	-10.12	-20.53	-31.33	-41.46	-51.58
	PH	1.153	0.00	0.00	0.00	0.00	0.00

RF = Rainfall (mm), RD = Rainy Days, MS = Field Capacity (%), K = Erodibility (kg/J), COH = Cohesion (kPa), EHD = Effective Hydrological Depth (m), Et/Eo = Ratio of Actual to Potential Evapotranspiration, C = Crop Management Factor, A = Rainfall Interception by Vegetation (mm), CC = Canopy Cover (%), SC = Surface Cover (%), PH = Plant Height (m)

Appendix 3-11: Sensitivity of runoff transport capacity to various input parameters

Factors	Parameters	Baseline	20%	40%	60%	80%	100%
Climate	RF	41.57	137.05	379.30	765.18	1334.64	2127.58
	RD	41.57	-40.77	-63.77	-76.46	-84.52	-89.39
Soil	MS	41.57	-39.77	-63.58	-76.58	-84.71	-89.39
	K	41.57	0.00	0.00	0.00	0.00	0.00
	COH	41.57	0.00	0.00	0.00	0.00	0.00
	EHD	41.57	-39.82	-64.13	-76.17	-84.90	-89.39
Land Cover	Et/Eo	41.57	-40.70	-63.74	-76.50	-84.46	-89.39
	C	41.57	20.83	39.91	60.09	79.17	100.00
	A	41.57	-20.62	-34.76	-47.99	-57.28	-72.82
	CC	41.57	0.00	0.00	0.00	0.00	0.00
	SC	41.57	0.00	0.00	0.00	0.00	0.00
	PH	41.57	0.00	0.00	0.00	0.00	0.00

RF = Rainfall (mm), RD = Rainy Days, MS = Field Capacity (%), K = Erodibility (kg/J), COH = Cohesion (kPa), EHD = Effective Hydrological Depth (m), Et/Eo = Ratio of Actual to Potential Evapotranspiration, C = Crop Management Factor, A = Rainfall Interception by Vegetation (mm), CC = Canopy Cover (%), SC = Surface Cover (%), PH = Plant Height (m)